[redacted]

AEC Category: HEALTH AND SAFETY

CEX-62.14

OPERATION BREN

AN EXPERIMENTAL INVESTIGATION OF THE SPATIAL DISTRIBUTION OF DOSE IN AN AIR-OVER-GROUND GEOMETRY

by:
F. F. Haywood, J. A. Auxier, and E. T. Loy

Issuance Date: October 2, 1964

CIVIL EFFECTS TEST OPERATIONS
U.S. ATOMIC ENERGY COMMISSION

LEGAL NOTICE

Printed in USA. Price $4.00. Available from the Clearinghouse for Federal Scientific and Technical Information, National Bureau of Standards, U. S. Department of Commerce, Springfield, Va.

NOTICE

This report is published in the interest of providing information which may prove of value to the reader in his study of effects data derived principally from nuclear weapons tests and from experiments designed to duplicate various characteristics of nuclear weapons.

This document is based on information available at the time of preparation which may have subsequently been expanded and re-evaluated. Also, in preparing this report for publication, some classified material may have been removed. Users are cautioned to avoid interpretations and conclusions based on unknown or incomplete data.

USAEC Division of Technical Information Extension, Oak Ridge, Tennessee

AN EXPERIMENTAL INVESTIGATION OF THE SPATIAL DISTRIBUTION OF DOSE IN AN AIR-OVER-GROUND GEOMETRY

By

F. F. Haywood
J. A. Auxier
E. T. Loy

Approved by: L. J. DEAL
Chief
Civil Effects Branch
U. S. Atomic Energy Commission

Oak Ridge National Laboratory
Oak Ridge, Tennessee
August 1964

ACKNOWLEDGEMENTS

The authors wish to express their gratitude to the following members of the Health Physics Division, Oak Ridge National Laboratory: Mr. J. H. Thorngate, Dr. R. H. Ritchie, Mr. W. H. Shinpaugh, Mr. J. S. Cheka, Mr. T. D. Jones, Mrs. J. P. Hickey, and Dr. G. S. Hurst. Their support and assistance in this study made it possible to complete the project in the most expedient fashion. Thanks are also extended to Mr. F. W. Sanders, formerly of ORNL, Mrs. I. R. Parsley of the Oak Ridge Gaseous Diffusion Plant's Central Data Processing Facility, Mr. Samuel Helf, Picatinny Arsenal, Mr. John Andrews of the General Electric Company, Mr. Jack Knight of Edgerton, Germeshausen, and Grier, and Mr. R. L. French of Radiation Research Associates.

This work was done under the auspices of the Civil Effects Test Operations, Division of Biology and Medicine, U. S. Atomic Energy Commission. Thanks are expressed to Mr. L. J. Deal and Mr. R. L. Corsbie, formerly of CETO, for their continued support and guidance in this project.

TABLE OF CONTENTS

LIST OF TABLES

LIST OF FIGURES

I. INTRODUCTION

One area of basic radiation physics which has commanded much attention in recent years is the measurement of radiation intensities at large distances from point sources of nuclear radiation. The importance of such measurements lies in the fact that several computer codes have been prepared to calculate radiation dose as a function of separation between source and detector. Results of these codes have failed to indicate a conclusive theoretical foundation for predicting neutron or gamma-ray dose as a function of distance between point source and point detector. An inherent problem associated with such a study, however, is created by the presence of the boundary between the atmosphere and the earth's surface, hereafter referred to as the air-ground interface. This problem may be stated briefly as follows: A calculation of dose as a function of distance away from a radiation source is normally performed for an infinite medium.[1] In such a calculation, it is assumed that radiation which reaches the point of interest is comprised of primary (unscattered) and scattered radiation. It is also assumed that the scattered component is isotropic. If the source is placed in a finite medium,[2] such a calculation as mentioned above is not valid. The presence of the air-ground interface clearly influences the number of collisions of source radiation in air beneath the source, and in air beneath the detector. Hence, the further a source is supported

---

[1] Infinite medium here refers to a volume of air, of infinite dimensions.

[2] Finite medium refers to a volume of air which is bounded by the earth's surface, and otherwise has infinite dimensions.

above the air-ground interface, the closer the radiation field resembles that which would be encountered in an infinite air medium. It is generally found that for a given source height above the air-ground interface, there is a certain distance from the source where the dose is the same as it would be at that distance in an infinite air medium; but at closer distances the dose is greater than, and at larger distances the dose is less than the dose in the infinite air medium.

Radiation dose as a function of distance, D(R), in an infinite air medium may be computed by:

$$D(R) = \frac{D_o\ (B)e^{-R/L}}{R^2} \qquad (1)$$

where D_o represents the dose at unit distance, B is a dose buildup factor defined as the ratio, total dose to unscattered dose, and is a function of R, $e^{-R/L}$ represents the attenuation due to the thickness of air for the distance R between source and point of interest, L is the relaxation length for the radiation considered in the formula and is defined as that distance in which there is a reduction in total dose by a factor of 1/e. One goal for this project was the determination of a series of interface factors which could be included in a computation of dose in an infinite air medium. Therefore, equation (1) may be rewritten to include a term for the air-ground interface correction:

$$D(R) = \frac{D_o\ (B)e^{-R/L}}{R^2} \cdot K(exp) \qquad (2)$$

where K(exp) represents the appropriate boundary correction factor which is a function of R, the height of the source, and the height of the detector above the air-ground interface.

The adoption of equation (2) as a means of computing dose in a finite medium is desirable from the standpoint that, as mentioned earlier, most calculations of dose as a function of distance are done without accounting for any possible effect of the interface. Ignoring this may cause estimates of dose to be low by as much as 20 percent when short distances are considered and may be high by a factor of two or more when larger distances are considered (two relaxation lengths or more).

Throughout this report, the term "measurement of neutron dose rate" is used frequently and refers to the measurement of neutron dose, independent of gamma-ray exposure. Similarly, the term "measurement of gamma-ray exposure rate"[3] is used frequently and refers to the measurement of gamma-ray exposure, independent of neutron dose. In both cases, measurements were made in air for a finite medium.

This project was designed to determine how the spatial distribution of neutron dose and gamma-ray exposure is affected by the presence of the air-ground interface. Measurements were made in the following types of radiation fields: (1) neutron field from a small bare reactor operating at steady-state power; (2) gamma-ray field from a small bare reactor operating at steady-state power (the three important components of this field are gamma rays from the fission process, from decay of fission products, and from inelastic scattering of neutrons in air); (3) gamma rays from a point gamma source. Data for

---

[3]ICRU Report 10a, NBS Handbook 84, pp. 5-6 (1962).

this project were taken at the Nevada Test Site in 1962 during Operation BREN.[4,5] The radiation sources available for the project were the ORNL Health Physics Research Reactor and a Co^{60} source whose apparent activity was 800 curies. The sources were mounted in a hoisting device on a 1527-foot tower and were supported at heights ranging from 27 to 1500 feet above the ground. Measurements of dose were made in a vertical plane which extended from a point directly beneath the center of the source hoisting device eastward for 4500 feet and from zero height to 100 feet above the interface.

The results of this study are presented in Chapter 6. The data are given in the form of graphs and tables.

Some of the experimental data are compared to theoretical models of radiation fields in a finite geometry; these comparisons are satisfactory in all cases except one.

---

[4]F. W. Sanders et al., U. S. Atomic Energy Commission Report CEX-62.02 (1962).

[5]J. A. Auxier, F. F. Haywood, and L. W. Gilley, U. S. Atomic Energy Commission Report CEX-62.03 (1963).

[6]The Co^{60} source purchased for this operation was one whose activity was reported to be 1200 curies. Measurements of gamma-ray exposure made during this project indicated that the apparent activity of this source was 800 curies.

II. BACKGROUND AND SPECIFIC EXPERIMENTAL OBJECTIVES

Most of the research efforts devoted to the air-ground interface problem to date have been of a theoretical nature. The first such case was introduced by M. J. Berger[7] in 1957. This work was directed largely at producing boundary factors[8] (K) for a geometric configuration which closely resembled that for air over ground. The boundary correction factors are given for Co^{60} source radiation for various combinations of source-detector separation. More recent publications[9-16] indicate an intense study of the air-ground interface problem as applied to monoenergetic neutrons and gamma-ray sources and neutron

---

[7] M. J. Berger, J. of Appl. Phys. 28, 1502-1508 (1957).

[8] Boundary correction factor (K) here refers to a number which for a given source-detector geometry is equal to the dose in the air-over-ground geometry divided by the dose at the same range (source-detector separation) in an infinite air medium.

[9] R. H. Ritchie, Oak Ridge National Laboratory Report ORNL-3189, 145-148 (1961).

[10] W. A. Biggers, L. J. Brown, and K. C. Kohr, Los Alamos Scientific Laboratory Report LA-2390 (1960).

[11] M. B. Wells, Health Phys. 8, 543 (1962).

[12] W. E. Kinney, Oak Ridge National Laboratory Report ORNL-3287 (1962).

[13] D. C. Kleinecke, "The Effect of an Air-Sand Interface on Gamma-Ray Transport," paper presented at NRDL-OCDM Shielding Symposium, October 31 - November 1, 1960.

[14] David Spielberg, "Neutron Fluxes from a Point Fission Source in Air; Moments Method Calculation," paper presented at NRDL-OCDM Shielding Symposium, October 31 - November 1, 1960.

[15] M. B. Wells, Radiation Research Associates, Inc. Report RRA-M33 (1963).

[16] R. L. French, Radiation Research Associates, Inc. Report RRA-M32 (1963).

sources which display a fission spectrum. In most of these reports, a calculation of the dose in the infinite medium and a calculation of the dose for source and point of interest located on the interface is given. This provides a method for computing a theoretical value for (K) for a given source-detector geometry. Ritchie[9] has computed neutron dose as a function of slant range, at the interface, for a number of source heights and, also, the neutron dose in an infinite air medium. Both of these cases were computed for a fission source as well as monoenergetic sources. Comparisons of computed values of (K) with those obtained in experiment are valid only if the measurements are made also in an infinite medium and in a finite medium. Semi-experimental boundary correction factors K(exp) may be determined by making a comparison between the experimental air-dose curve in the finite air medium, and a computed air-dose curve in the finite air medium. If the relaxation lengths of the two curves are nearly equal, data points from the experimental curve may be normalized to data points from the computed curve (see Figure 13). Therefore, these normalized data points may be used to determine K(exp) by:

$$K(exp) = \frac{\text{normalized finite medium dose (measured)}}{\text{computed infinite medium dose}}$$

This report will not present an extensive study of K(exp), but several cases will be given to illustrate the satisfactory agreement between experiment and theory.

From a purely experimental standpoint, the air-ground interface problem has been studied previously to the extent that an air-over-ground

geometry was simulated through the use of materials which were more dense than air and earth but which had relative scattering properties similar to those of air and earth. By choosing these more dense materials such that measurements in the infinite medium are possible (measurements >1 mean free path from boundaries) values of K(exp) could be determined for any given source-detector geometry. This type of experiment has included, as scatterers, steel and steel wool,[17] and concrete and polyfoam.[18] Experiments of this nature have been limited to the discrete gamma-ray energies of Co^{60}, Cs^{137}, Au^{198}, and Hg^{203}. No interface experiments have been performed and reported for neutrons. Free field measurements in the vicinity of the ORNL Tower Shielding Facility (TSR-II) have been reported,[19] but no definitive interface effects are mentioned. Data in this report[19] could be manipulated to reveal some useful information about the behavior of radiation fields in a finite medium at close source-detector distances (<1200 feet), for source heights to 175 feet, and for detector heights to 145 feet. However, the TSR-II is much larger than the HPRR and is surrounded by a coolant and hardware which probably alters the neutron energy spectrum so that it differs somewhat from that of a bare metal reactor. Additional experiments

---

[17]Frank Titus, Nuc. Sci. and Eng. 3, 609-619 (1958).

[18]C. E. Clifford, J. A. Carruthers, and J. R. Cunningham, Can. J. Phys. 38 , 504-506 (1960).

[19]F. J. Muckenthaler, L. B. Holland, and R. E. Maerker, Oak Ridge National Laboratory Report ORNL-3288 (1963).

have been conducted in order to examine the behavior of radiation fields as a function of distance from a point source[20-22] and as a function of distance from boundaries.[23-25]

Aside from the fundamental aspect of this experiment, it was important for several other reasons. The many theoretical programs which have appeared recently indicated a need for experimental verification of the conclusions which have been stated. In relation to the Ichiban Dosimetry program,[26] information was obtained whereby shielding factors for Japanese residential units may be better defined. This is possible by obtaining a general experimental relation for neutron dose or gamma-ray exposure as a function of detector height above the ground. Shielding factors for upper floors of buildings have been determined by relating the dose inside the building to the "free-field" or "in-air" dose outside the building at a given height above,

---

[20]R. E. Rexroad and M. A. Schmoke, Nuclear Defense Laboratory Report NDL-TR-2, 9 (1960).

[21]B. W. Soole, Proc. Royl. Soc. (London) 230, Series A, 343 (1955).

[22]R. L. French and C. W. Garrett, "The Angular and Energy Distribution of the Photon Flux from a Co^{60} Point Source Three Feet Above the Air-Ground Interface," talk to be presented at the meeting of the Health Physics Society, Cincinnati, Ohio, June 15-18, 1964.

[23]F. J. Davis and P. W. Reinhardt, Health Phys. 8, 233-243 (1962).

[24]K. O'Brien and J. E. McLaughlin, Jr., U. S. Atomic Energy Commission Report CEX-61.1 (preliminary) (1963).

[25]M. A. Van Dilla and G. J. Hine, Nucleonics 10, No. 7, 54-58 (1962).

[26]Cooperative venture between Oak Ridge National Laboratory and the Atomic Bomb Casualty Commission to reduce experimental error in estimates of radiation imparted to survivors of Hiroshima and Nagasaki.

but generally near, the ground. The results of this project will extend the data collected during weapons test operations[27,28] to include values of air attenuation in a finite air medium for a variety of source heights and detector heights. Most of the data collected in weapons test were for a detector located on or very near the ground, and measurements in a vertical traverse have revealed little. Hence, on the basis of the reported data from these tests, it is not possible to determine the effects of the air-ground interface except for cases where measurements of dose were made at the air-ground interface for different detonation heights.

To accomplish the goals of this experiment, it was planned to make measurements of dose at the interface as a function of source height and slant range (R), and to make measurements of dose in air above the ground (at several intervals up to 500 feet) as a function of slant range and source height. To this end, helium-filled balloons were to be used to support the instrument package. It was found, however, that winds as slow as 1 to 5 miles per hour created vibrations in the support mechanism, which were picked up by the electronics system and led to unreliable neutron dose rate data. Additional wind problems caused this part of the project to be cancelled. Instead of balloons, a small portable telescoping antenae tower, which extended to 105 feet above the ground, was used to raise the instrument package to 100 feet.

---

[27]G. S. Hurst and R. H. Ritchie, U. S. Atomic Energy Commission Report WT-1504 (Classified) (1958).

[28]J. A. Auxier, J. S. Cheka, and F. W. Sanders, U. S. Atomic Energy Commission Report WT-1725 (Classified) (1961).

The measurements taken during this project were accomplished by performing the three following experiments:

1. Measurement of neutron absorbed dose rate from a small bare reactor operating at steady-state power as a function of source height, horizontal distance from the source tower, and detector distance above the air-ground interface.
2. Measurement of gamma-ray exposure rate from a small bare reactor operating at steady-state power as a function of source height, horizontal distance from the source tower, and detector distance above the air-ground interface.
3. Measurement of gamma-ray exposure rate from an 800-curie Co^{60} source, as a function of source height, horizontal distance away from the source tower, and detector distance above the air-ground interface.

III. SITE DESCRIPTION AND SUPPORT FACILITIES

Data in this report were collected during Operation BREN, which was a large-scale field experiment conducted at the Nevada Test Site during the first half of 1962. Primarily, the purpose of this operation was the continuance of the study of penetration of nuclear weapons radiation through matter. Additional areas of investigation were spatial and angular distributions of radiation, neutron and gamma-ray dosimetry, and neutron and gamma-ray spectrometry.

Two radiation sources were utilized and, for purposes of the operation, were supported at several levels on a steel tower 1527 feet high by means of an aluminum hoist car which could be moved along one vertical face of the tower. These two sources were the Oak Ridge National Laboratory's Health Physics Research Reactor (HPRR) and a Co^{60} source whose effective activity was approximately 800 curies. Figure 1 is a general view of the BREN tower showing reactor placement in the hoist car. The HPRR core is a right circular cylinder of metal alloy, 90 wt percent uranium, which is enriched to 93.14 percent U^{235}, and 10 wt percent molybdenum. It is 8 inches outside diameter and 9 inches high. Figure 2 is a view of HPRR fully assembled and supported in a manner similar to that during Operation BREN. In Figure 3, one sees the Co^{60} source facility as it was mounted in the hoist car. Physically, the source was contained inside a stainless-steel right cylindrical annulus which was then sealed in a stainless-steel container approximately 2.5 inches in diameter and 6.4 inches long. This capsule was attached to the bottom of the shield plug of the source container by a small flexible stainless-steel cable. A mechanism mounted above

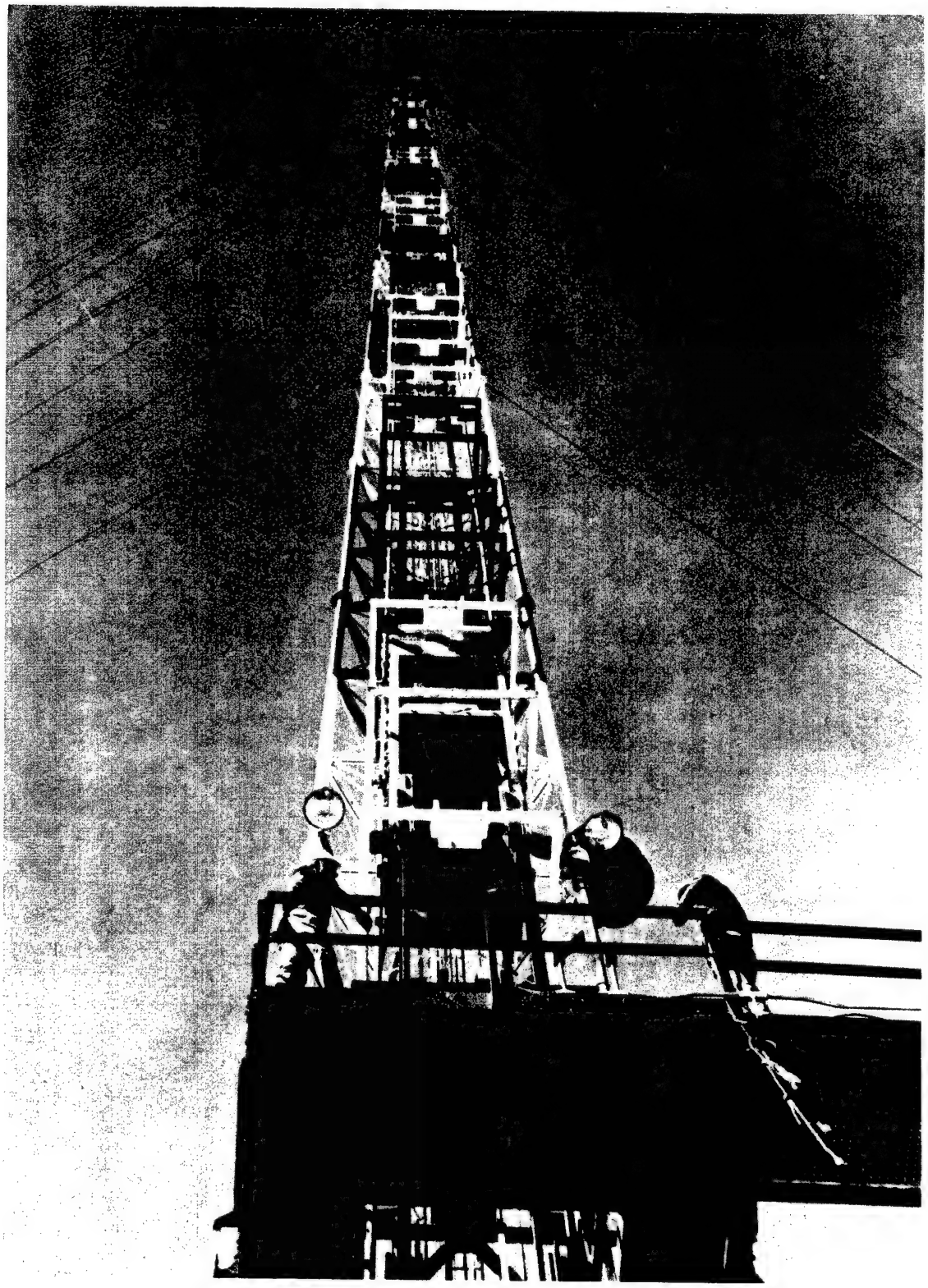

Fig. 1. View of Reactor Positioned in Hoisting Mechanism

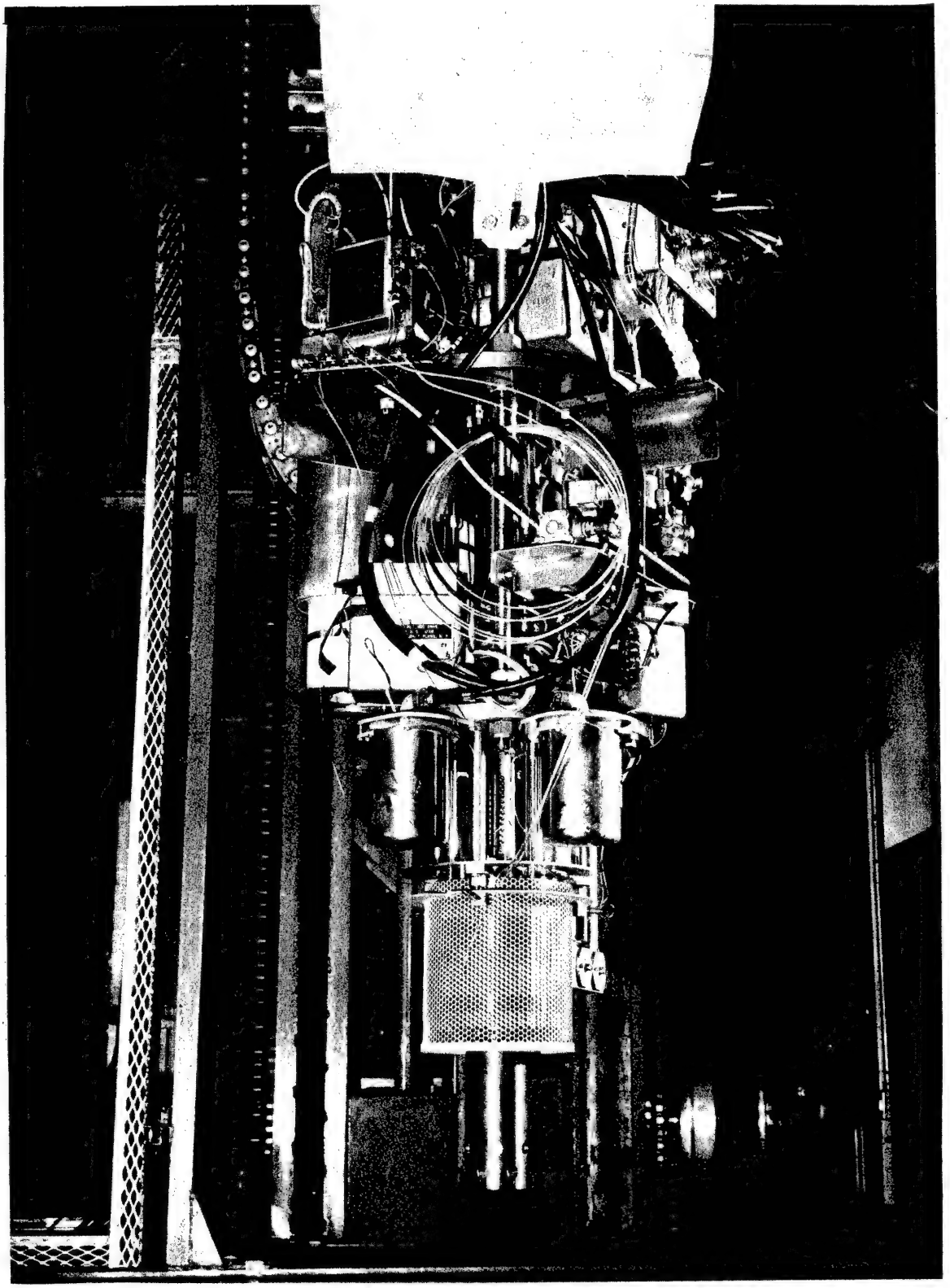

Fig. 2. Fully Assembled ORNL HPRR

Fig. 3. View of Co^{60} Facility Positioned in Hoisting Mechanism

the source container was used to raise the shield plug (see Figure 4). This raised the source to an exposed position relative to the hoist car, and this type of positioning was used throughout the operation. Both the HPRR and Co^{60} facility were operated from an underground bunker located approximately 150 feet from the base of the source tower.

The general area over which data for this project was taken is shown in Figure 5. The view presented in this figure is of the experimental area as seen at a horizontal distance of 1250 yards from the source tower.

The terrain of the Nevada desert (Yucca Flat) is relatively smooth with ground roughness limited to natural erosion normally less than 2 feet deep and at widely scattered intervals. The dirt road (arrow) in Figure 5, which served as the base of a vertical plane in which measurements of dose were made for this study, had been scraped smooth prior to the operation. This helped reduce irregularities in the ground surface near the point of measurement. There was a downhill grade of approximately 1.5 percent on the side of the tower where measurements were made. Although the primary objective of this project was to study the radiation field as a function of distance above the ground, this grade was not ignored in calculations for slant range, R (slant distance between source and detector). Measurements of dose for this study extended 4500 feet away from the east face of the source tower. Measurements of dose were made in radiation fields from both the reactor and Co^{60} source, each being supported at 27, 300, 500, 1125, and 1500 feet above the air-ground interface. The distances between source and detector ranged from about 10 feet to 4600 feet.

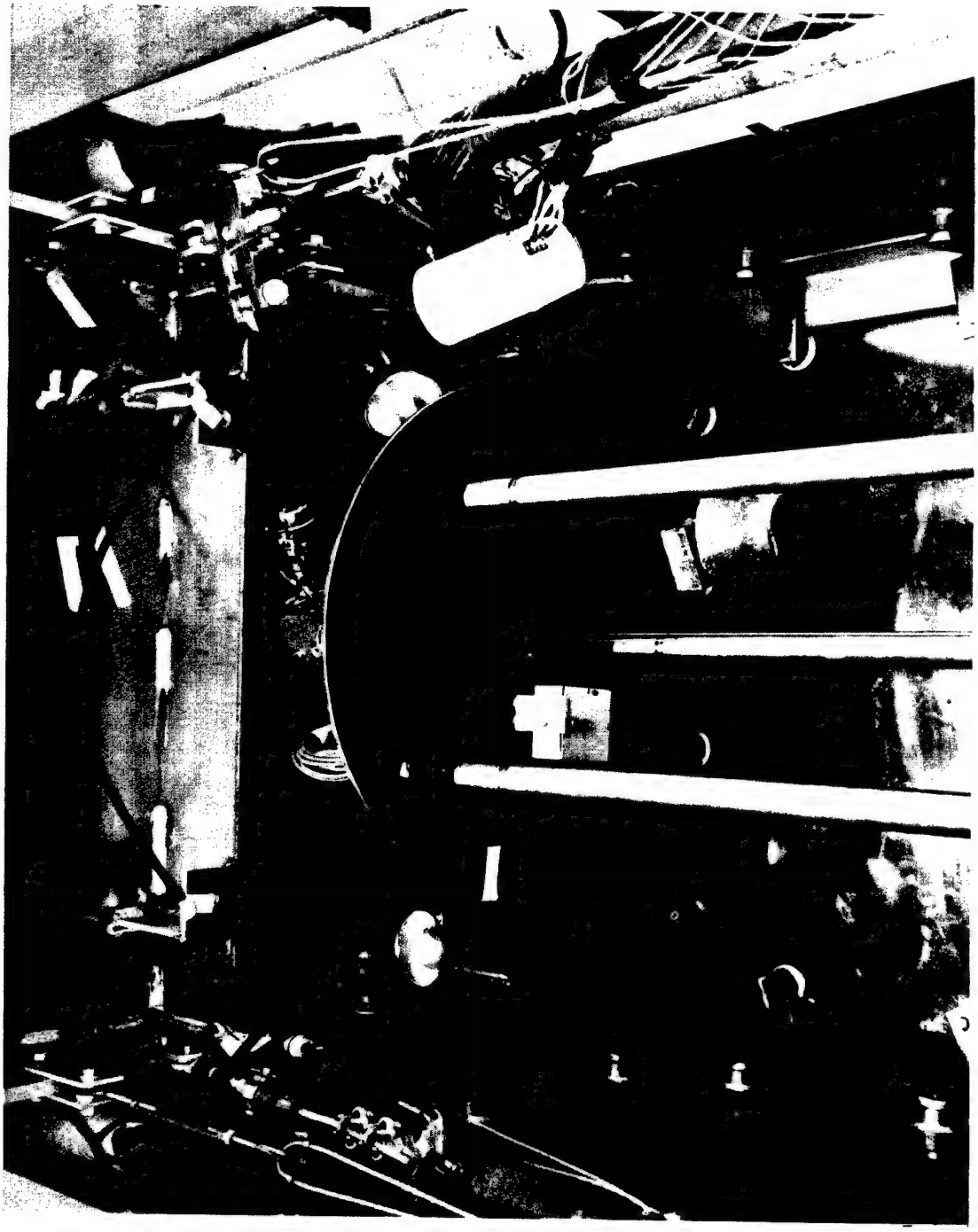

Fig. 4. Mechanism Used for Exposing Co^{60} Source

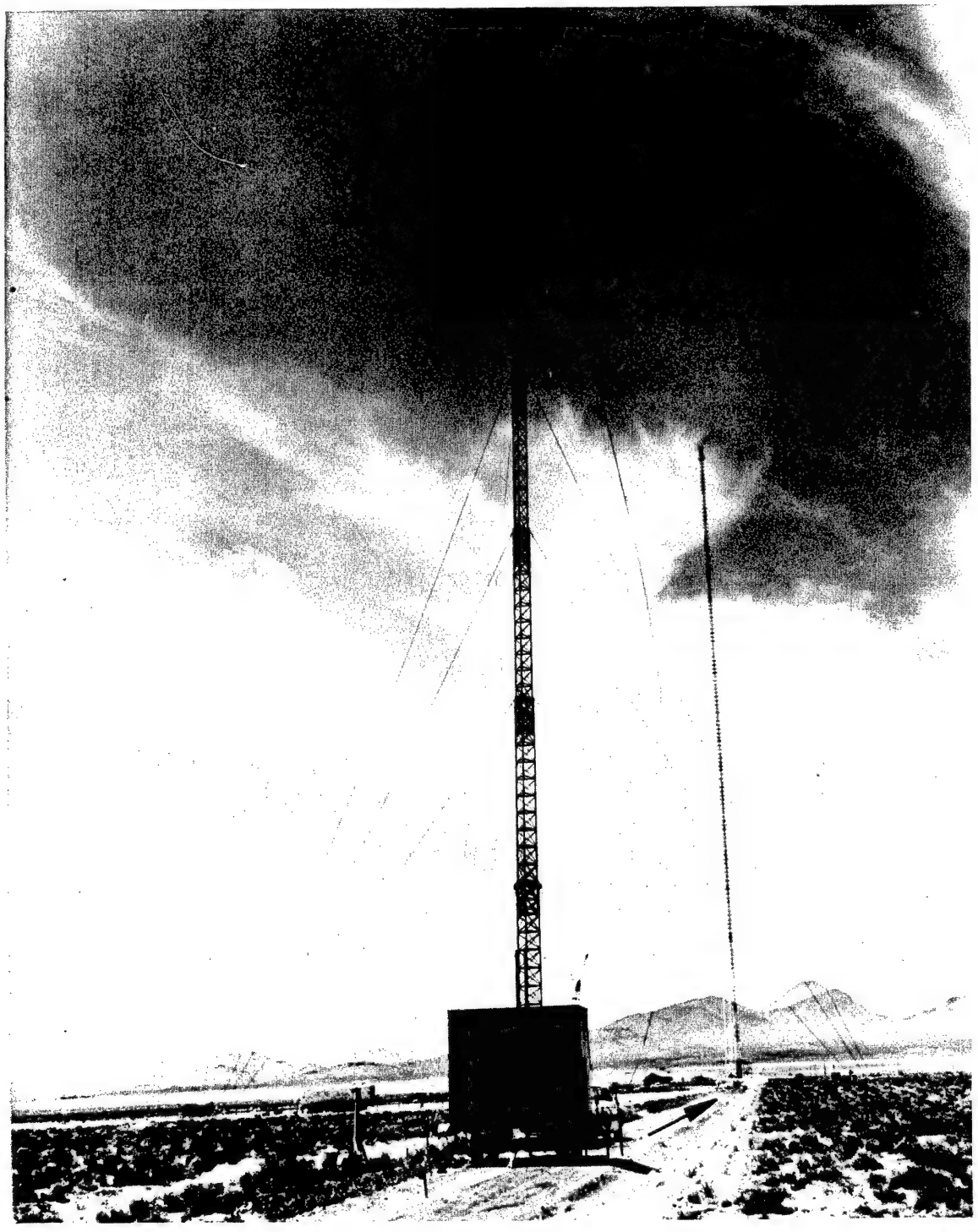

Fig. 5. General View of Experimental Area

These separations correspond to a combination of detector placements in a vertical plane which measured 4500 feet long and 100 feet high. At most of the horizontal distances, measurements of dose were made in a vertical traverse which included heights of 0, 2, 5, 16.5, 50, and 100 feet. For both sources used, a measurement of dose was made horizontally at 3 meters from the source at its lowest position on the tower (27 feet). This point is shown on several air-dose curves in Chapter 6 and was used in computing the unperturbed dose rates at "unit" distance. By using dose as measured at 3 meters, it is possible to determine experimentally the dose buildup factor for various combinations of source height and detector height and as a function of slant range, R. Such information is useful in identifying effects caused by the presence of the interface.

Instruments were positioned by utilizing light-weight laboratory ring stands, a 20-foot length of "unistrut" steel mounted on the rear of a pick-up truck, and the small telescoping antenna tower mounted on a trailer. Two of these arrangements are presented in Figures 6 and 7. The ring stand was used to make measurements of dose at 3 feet and 5 feet above the ground, the 20-foot length of steel for the 16.5-foot height, while the tower was used for heights of 50 feet and 100 feet. The instrument package was suspended approximately 3 feet away from the main structure of the small tower by means of a rope and pulley system attached to the end of a piece of channel iron which was anchored to the top of the tower. Distances were marked on the signal cables for quick detector placement above the ground, and the instrument package was raised to the desired height by hand by pulling the rope to which they were attached.

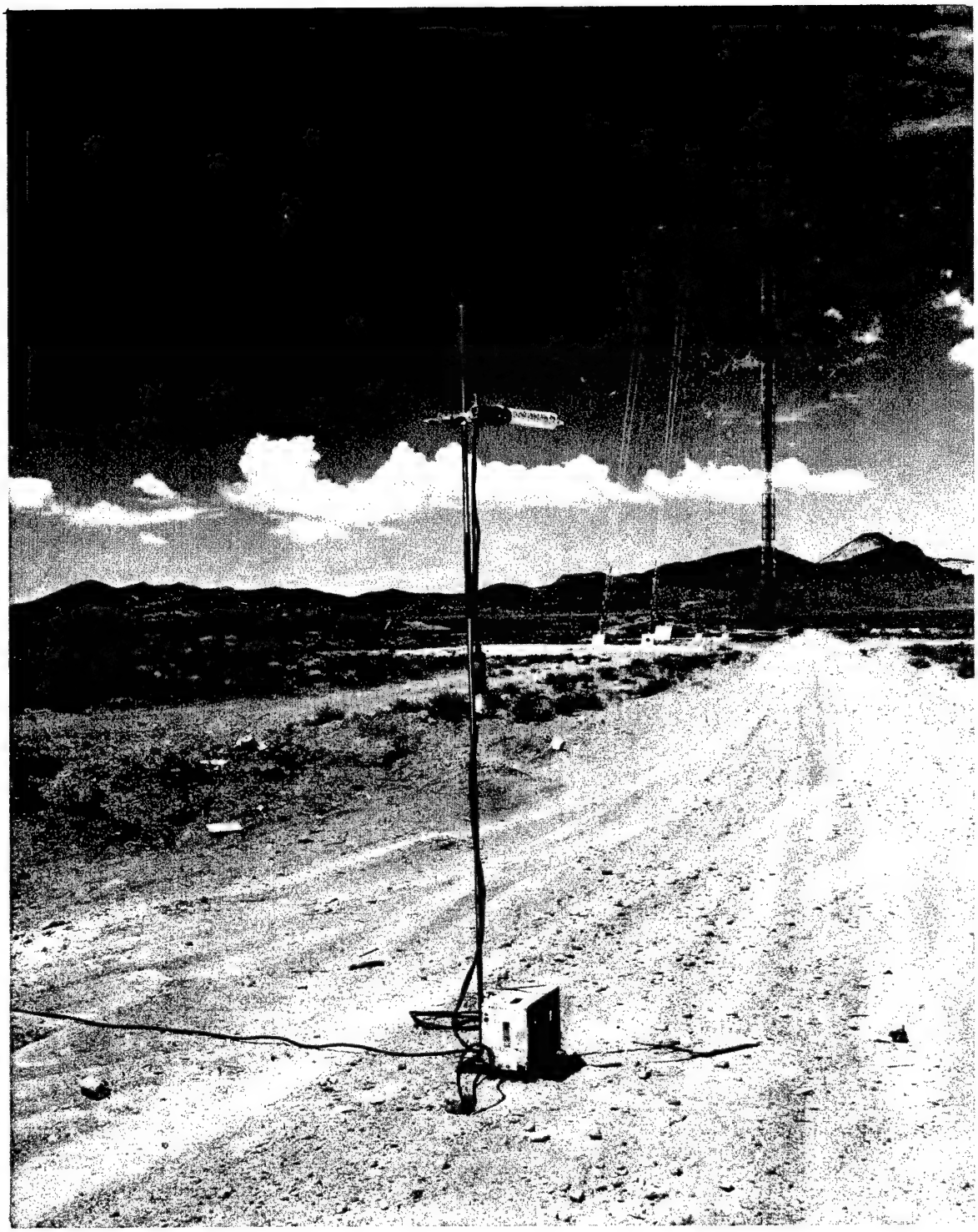

Fig. 6. Light-Weight Stand Used for Supporting Radiation Detectors Above the Air-Ground Interface

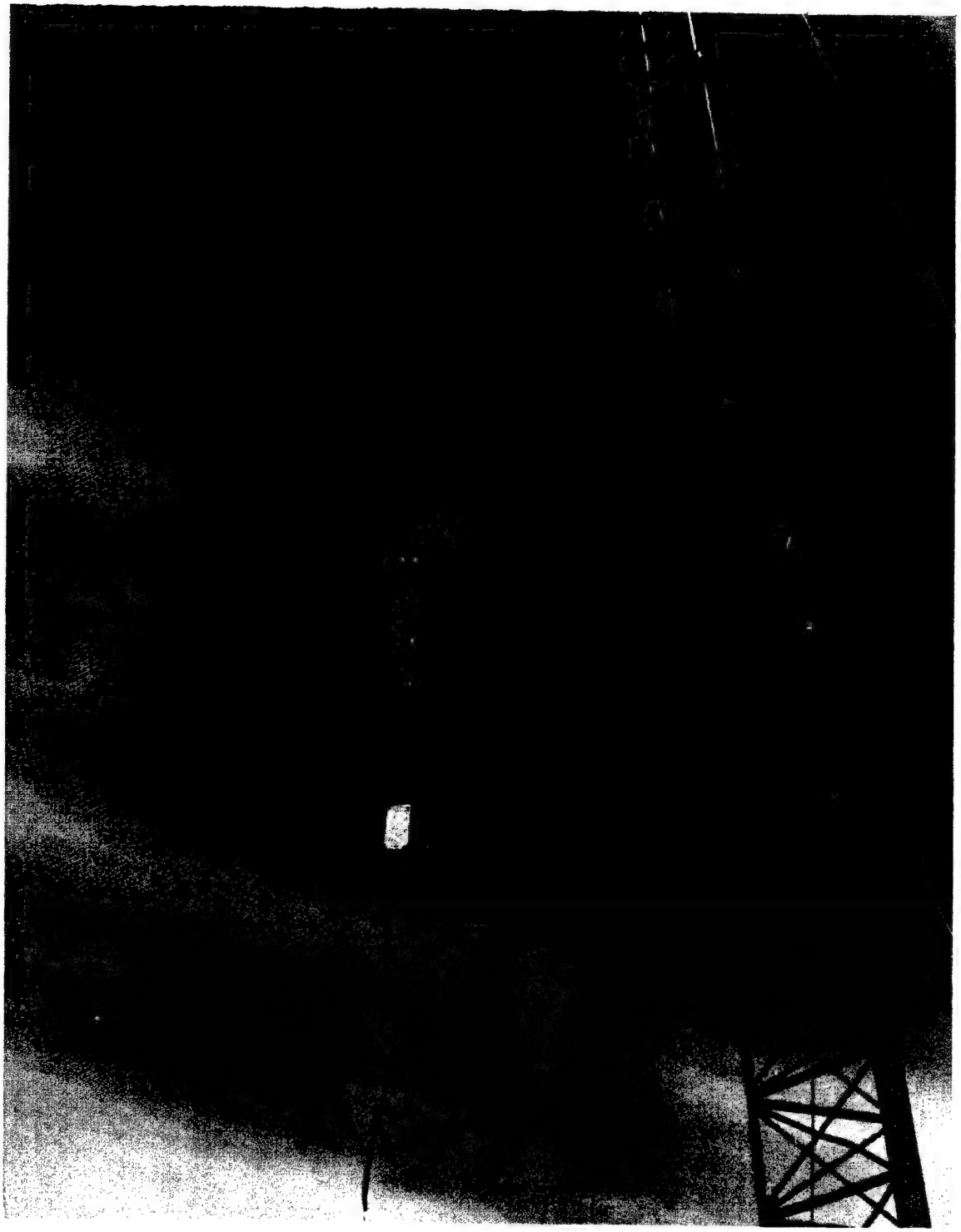

Fig. 7. Antenna Tower Used for Supporting Radiation Detectors Above the Air-Ground Interface

Electrical power was required for lights, instruments, and the motor used for raising the antenna tower. This was provided by receptacles placed every 300 feet along the dirt road which defined the experimental area. Instrument power was regulated by using a "Sola" regulating line voltage transformer.

IV. RADIATION DETECTORS AND CALIBRATION PROCEDURE

During operation of the Health Physics Research Reactor in Operation BREN, measurements of neutron dose rate were made independently of gamma-ray exposure rate using an ORNL Q-1995 "Radsan" fast neutron dosimeter[29-31] (Figure 8). This dosimeter utilizes a recoil proton proportional counter lined with polyethylene (C_nH_{2n}) and filled with cyclopropane (also C_nH_{2n}) and operates at approximately 1400 volts. Protons are produced both in the proportional counter wall material and in the counter gas by neutrons which undergo elastic collisions in these media. Protons which recoil through the active volume of the counter cause ionization, in the cyclopropane, which produces pulses proportional to the energy deposited in the cavity. Pulses from ionizing events which occur in the counter are amplified by a transistorized preamplifier and passed to the main amplifier through 500 feet of cable. Here the random pulses are sorted, "weighed", and added by a four-stage binary integrator. The uniform output pulses from the integrator are numerically proportional to the energy deposited in the chamber and are passed to a decade scaler. Dose rates may be read directly in millirad per hour by adjusting the length of count while calibrating the counter with a neutron source of known strength.

---

[29]G. S. Hurst, Brit. J. of Radiol. 27, No. 318, 353-357 (1954).

[30]E. B. Wagner and G. S. Hurst, Rev. Sci. Instrum. 29, No. 2, 153-158 (1958).

[31]E. B. Wagner and G. S. Hurst, Health Phys. 2, 57-61 (1959).

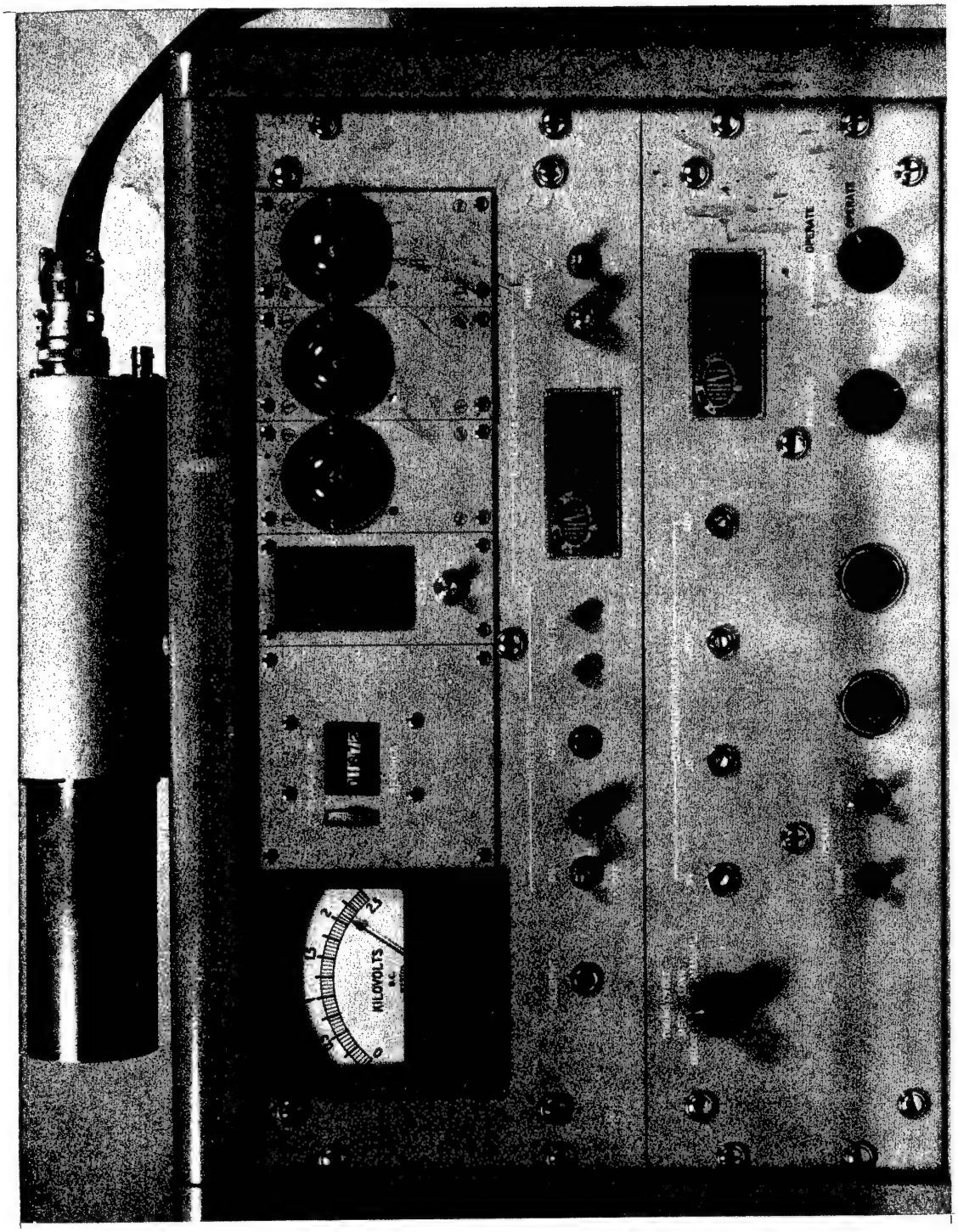

Fig. 8. Radsan, Fast Neutron Dosimeter

Independent experiments[30] indicate that the response of the Radsan to gamma radiation is significant for exposure rates greater than 2 R/hr. It was found that 2 R/hr of gamma radiation would give the same reading as a fast neutron dose rate of 0.4 millirad per hour and gamma-ray exposure rate of 20 R/hr would give the same reading as 80 millirad/hr of fast neutrons. The maximum gamma-ray field during the course of this study corresponded to an exposure rate of approximately 60 mR/hr. This exposure rate was encountered while making a close-in reference measurement (source-detector separation = 3m). During a routine calibration of the Radsan using a one-curie Pu-Be source, the sensitivity of the counter to gamma rays was checked by introducing a Co^{60} source in such a way as to expose the counter to an exposure rate of >60 mR/hr. This resulted in no significant increase in response. Therefore, no compensations for gamma-ray contribution to dose were necessary.

The response of the Radsan as a function of angle of incidence between source and detector has been determined to be within 5 percent over the front end and sides when exposed to Pu-Be neutrons at one meter. At angles greater than 150° from the forward direction, the response is reduced significantly by absorption in the preamplifier and its housing located at the rear of the proportional counter. For an isotropic neutron field, the reading on the Radsan would be low by approximately 2.5 percent due to this decrease in response over the rear 60° acceptance angle. However, in the case for neutrons emitted from the reactor operating at steady-state power, the field was found to be peaked in the forward direction. Because most of the

radiation incident on the detector is from the forward direction, only a small fraction of the total field is not measured due to the decreased response over the rear 60° acceptance angle of the detector.

Calibration of the Radsan Fast Neutron Dosimeter

In order to obtain reliable values of fast neutron dose rate through measurements made with the Radsan fast neutron dosimeter, it was necessary to achieve precision in calibration procedures. This precision is required, especially when it is necessary to substitute proportional counters.

The component of the Radsan which translates pulse information to dose information is the binary integrator circuit. This component integrates amplifier pulses and, in turn, produces one output pulse for approximately every 80 volts of integrated amplifier pulse. This one output pulse is equivalent to approximately 5.85×10^{-4} millirad. There are four discriminator stages which must be set accurately for the integrator to operate properly. These four stages are biased at 5 volts, 10 volts, 20 volts, and 40 volts. The output pulse of each discriminator is, in turn, used to operate conventional binary stages of the integrator.

An alpha source is built into the proportional counter and is intended as a device for determining the energy response of the counter. The α source is exposed to the active volume of the chamber by activating a solenoid-operated shutter. A standard procedure given in the test procedure for this instrument calls for setting each discriminator so that the count rate is one-half the maximum

possible count rate from the α source; however, the 5-volt discriminator has to be set using an oscilloscope and pulser. A more satisfactory method[32] of setting the discriminators has been found to be as follows:

1. Feed into the amplifier, 60-cycle pulses from a precision pulser (ORNL Q-1212) and monitor the output of the binary discriminator stage with an oscilloscope (Tektronix Model No. 515A) which has a rise time at least as good as that of the amplifier.
2. Adjust the input pulse height until the pulse, as measured on the scope, through the amplifier has the value which corresponds to the discriminator stage.
3. Adjust the threshold of the discriminator stage until a count rate of 30 c/sec is indicated on the Radsan scaler.

When the above procedure has been extended to all four discriminator stages of the integrator, the instrument should respond in a way so that one pulse from the binary integrator in 21 seconds corresponds to 0.1 mrad/hr.[33] For the duration of this experiment, the amplifier gain was set at the beginning of each operating day. Throughout any given operational period, the α source was routinely used to monitor the amplifier gain. If a gain shift had occurred, the detailed calibration procedure was repeated.

In addition to the careful calibration of the Radsan electronics, a one-curie, sealed, plutonium-beryllium neutron source, whose emission was 1.84×10^6 n/sec, was used to obtain a calibration factor for the

---

[32] J. H. Thorngate, private communication.

[33] $5.85 \times 10^{-4} \frac{\text{mrad}}{\text{pulse}} \times \frac{1 \text{ pulse}}{21 \text{ sec}} \times \frac{3600 \text{ sec}}{1 \text{ hour}} = \frac{0.1 \text{ mrad}}{\text{hour}}$

proportional counter. This procedure was necessary because counters were replaced occasionally due to malfunctions. The proportional counter and source were placed at a fixed separation and at a fixed height above the ground for all determinations of the calibration factor throughout the operational period. The computed dose rate from a Pu-Be neutron source[30] at a distance r, in cm, from the center of the source is given by:

$$\text{dose rate (mrad/hr)} = \frac{1.27 \times 10^{-3}\ S_o B}{r^2} \qquad (3)$$

where

S_o = source strength in n/sec.

B = dose buildup factor = 1

r = distance in cm from center of source to center of counter.

The calibration factor for the counter is given as:

$$F_c = \frac{\text{calculated dose rate}}{\text{measured dose rate}}$$

Three counters were used for this project, and the calibration factors were in the range 1.14 to 1.44.

Gamma-ray exposure rates for experiments two and three, listed in Chapter 2, were measured using the "Phil"[34] gamma-ray dosimeter (Figure 9). The Phil was used at all detector locations during reactor operation, and, with the exception of one detector station, it was used exclusively during work using the 800-curie Co^{60} source. Metaphosphate glass rods[35] were utilized for a "close-in" reference

---

[34]E. B. Wagner and G. S. Hurst, Health Phys. 5, 20-26 (1961).

[35]J. S. Cheka, private communication.

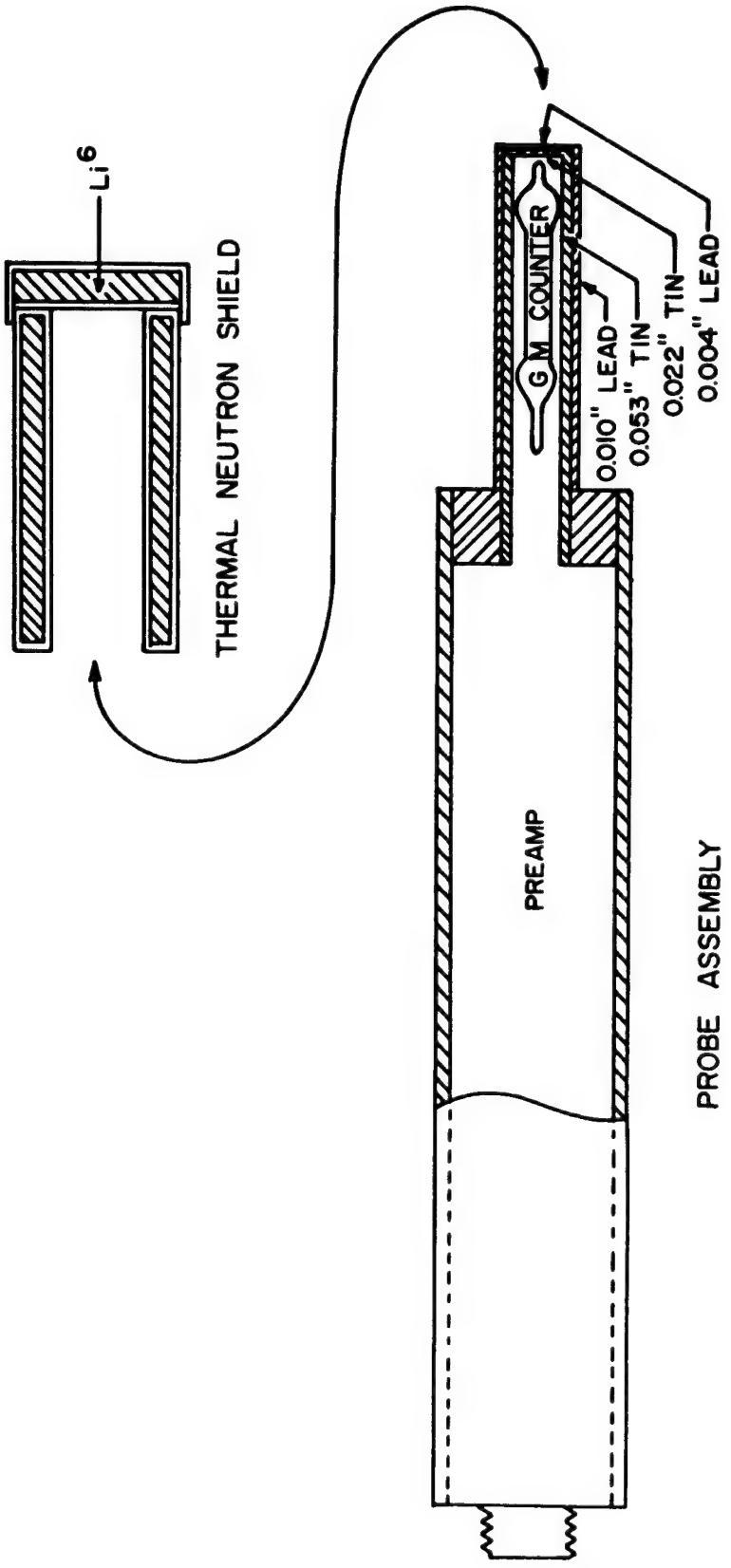

Fig. 9. Diagram of Geiger-Mueller Gamma-Ray Dosimeter

point at about 3m from the 800-curie Co^{60} source because the exposure rate at this distance was 120 R/hr, and coincidence (scaling) losses in the scaler and dead-time losses in the GM counter would have been prohibitively high.

The Phil dosimeter utilizes a Philips No. 18509 Geiger-Mueller tube filled with neon, argon, and a halogen-quenching agent. By adding a shield of 0.053 inches of tin plus 0.010 inches of lead over the tube, the response of the counter was made to be proportional to exposure in roentgens for photon energies in the range 0.15 Mev to 3 Mev.

The gamma-ray field resulting from a fission source is made up of three major components, namely gamma rays from the fission process (prompt gamma rays) gamma rays due to the decay of fission products inside the core of the reactor, and gamma rays resulting from the inelastic scattering of neutrons in the atmosphere between the source and detector. These latter gamma rays are primarily those from N^{16} (6.13 and 7.10 Mev). The response of the Phil to gamma rays in this energy region has been measured and has been found to increase linearly with photon energy.[36] This response is not precisely equal to "exposure", but the error in the total exposure due to the photons of energy greater than 3 Mev is less than 5 percent.

The neutron sensitivity of the Phil has been determined experimentally.[34] An integrated thermal neutron flux of 5×10^9 n/cm^2 was found to give approximately the same reading as an exposure of one roentgen of gamma radiation. By placing a shield of 1/8-inch Li^6 over

---

[36] J. H. Thorngate, private communication.

the counter, the response to thermal neutrons is reduced by a factor of 300; or an integrated thermal flux of 1.5×10^{12} is required to produce the same reading as an exposure of one roentgen of gamma radiation. The results of independent experiments have shown that the response of the Phil to fast neutrons is less than 0.5 percent than that for gamma rays.[34]

The Phil was determined to have an angular response of ±9 percent over the front end and sides. Some attenuation in the preamplifier located on the rear end of the counter assembly was responsible in reducing the over-all response. A procedure similar to that used for the Radsan fast neutron dosimeter indicates that a reading made with the Phil in an isotropic gamma-ray field would be low by approximately one percent. In both of the gamma-ray experiments of this project, the gamma-ray field was peaked in the forward direction so that the decrease in total Phil response due to attenuation in the preamplifier was insignificant. The Co^{60} angular distribution at a horizontal distance of 2250 feet is shown in Figure 10.[37] The counter was placed (during measurement and calibration) so that the angle between the counter axis and line of sight to source was 0°.

Pulses from the counter were passed to a pulse scaler by a transistorized preamplifier through 500 feet of cable. Measurements of gamma-ray exposure rate were made by taking counts over timed intervals, and the measurement was recorded in units of counts/minute.

---

[37] J. H. Thorngate et al., U. S. Atomic Energy Commission Report CEX-62.12 (to be published).

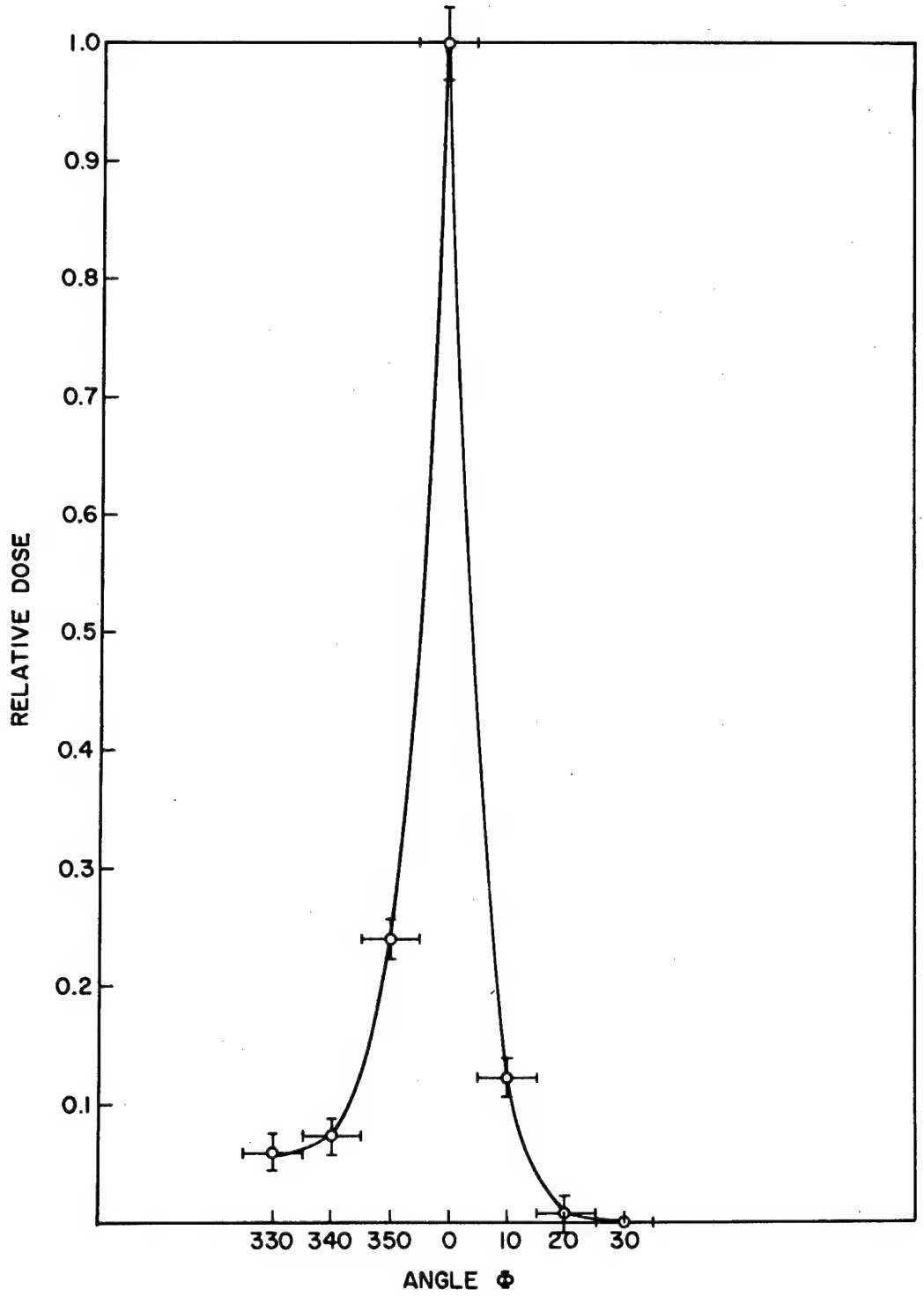

Fig. 10. Angular Exposure Distribution: Co^{60} Gamma-Ray Exposure as a Function of Polar Angle

Calibration of Phil Gamma-Ray Dosimeter

The calibration procedure of the Phil is less complicated than that of the Radsan because a pulse height integrator circuit and amplifier is not required for readings of exposure. Because the Phil is essentially independent of incident photon energy in the range of 0.15 Mev to 3.0 Mev, random pulses are recorded on a digital scaler, and this reading is converted to exposure rate by applying an appropriate calibration factor. When the net counts per minute is multiplied by the counter calibration factor, the measurement reading is in units of mR/hr. The following procedure was used:

1. Counter background was determined by counting for 30 minutes.
2. Source[38] and detector placed at fixed separation (one meter) and height above the ground (one meter).
3. Count interval regulated to allow one percent statistical accuracy.
4. Determine the net counts per minute.
5. Determine the calibration factor by:

$$\frac{\text{mk/hr}}{\text{c/m}} = \frac{1}{\text{net c/m}} \cdot \left[S_o\right]\left[e^{-\lambda t}\right] \qquad (4)$$

where

S_o = exposure rate (mR/hr) at calibration date.

λ = decay constant for Co^{60} (day^{-1}).

t = length of time (days) since calibration.

---

[38] Co^{60} source whose activity was about 6 mc and was calibrated by the National Bureau of Standards on June 8, 1960, to have an exposure rate of 8.11 mR/hr at one meter.

Associated Electronics

Because the detectors were initially planned to be suspended at heights above the ground to 500 feet, it was desirable to keep the weight of the instrument package at a minimum. Therefore, battery-operated, transistorized, high-voltage supplies and preamplifier power supplies were built and placed in a small unit supported approximately 6 feet below the Radsan and Phil counters. This eliminated the heavy, cumbersome cables which would have been required if the power supplies had been located on the ground.

V. NORMALIZATION AND DATA ADJUSTMENT CRITERIA

In order that systematic measurements of dose rate have meaning, they must be normalized to standard values of parameters such as reactor power, source activity, and air density.

When measurements of dose are made in radiation fields in air, careful attention must be given to the mass of air between the source and detector as the separation between them increases. This is extremely important if there has been a significant change in the density of this air mass during the period measurements are made. Observations of the changes in air density during this study revealed a maximum fluctuation of 9 percent. For a fixed reactor power level, this change in air density would correspond to a difference of 43 percent in neutron dose at a slant range (R) of 1000 yards. Similarly, there would be a difference of 35 percent in gamma-ray exposure at 1000 yards (gamma-ray exposure relaxation length is greater than that for neutron dose). By the nature of this phenomenon, it was necessary to develop procedures and techniques whereby values of dose could be derived in terms of reactor power level for a "standard" air density. This chapter is devoted to a description of these procedures and techniques.

Unlike a sealed Co^{60} source, whose activity remains fixed except for radioactive decay (5.3 years), a reactor's power level is influenced by parameters such as calibration of the electronics, control-rod settings, ambient temperature, etc. For data taken during operation of the reactor, it was necessary to take careful measures for determining the flux leaving the reactor. Therefore, a neutron-sensitive instrument, which was capable of monitoring slight changes in reactor power, was

placed at a stationary position to provide both integral and differential counting data during all reactor runs.

Reactor Power Level Monitors

A neutron-sensitive count-rate channel[5,39] was set up at a horizontal distance (X_L) of 790 yards, and later at 1000 yards, from the center of the base of the 1527-foot tower which was used to support the reactor. This counter was of the cylindrical, boron tri-fluoride type and, except for the ends of the counter, the surface was covered with 9.4 cm of paraffin. This configuration was sufficient to render the counter relatively insensitive to small changes in the neutron energy spectrum (Figure 11). By mounting the counter so its longitudinal axis was parallel to the ground and perpendicular to a line between it and the reactor, serious changes in geometry were avoided.

The counter was standardized prior to and just after each reactor run. For this purpose, a one-curie, plutonium-beryllium neutron source (1.84×10^6 n/sec) was positioned at a fixed distance from the counter and at a fixed height above the ground. The counter pulse rate was amplified and fed to a linear count-rate meter, and was displayed both on a scaler and on a strip-chart recorder. Hence, both differential and integral counting information was available for normalizing experimental data to reactor power.

---

[39]This count-rate channel was a modified Hanson-McKibben long counter. Many references must be made in this chapter to parameters associated with this detector. For this reason, the following symbols will be referred to frequently: X_L = horizontal distance between center of the base of source tower and center of the counter; R_L = slant distance between center of reactor and center of the counter; C_L = standard normalization channel count rate which is the number of thousands of counts per 10-minute interval (C_L = cts/10 min $\times 10^{-3}$). This unit was chosen for convenience because 10 minutes corresponds to the length of counting time for most individual data points.

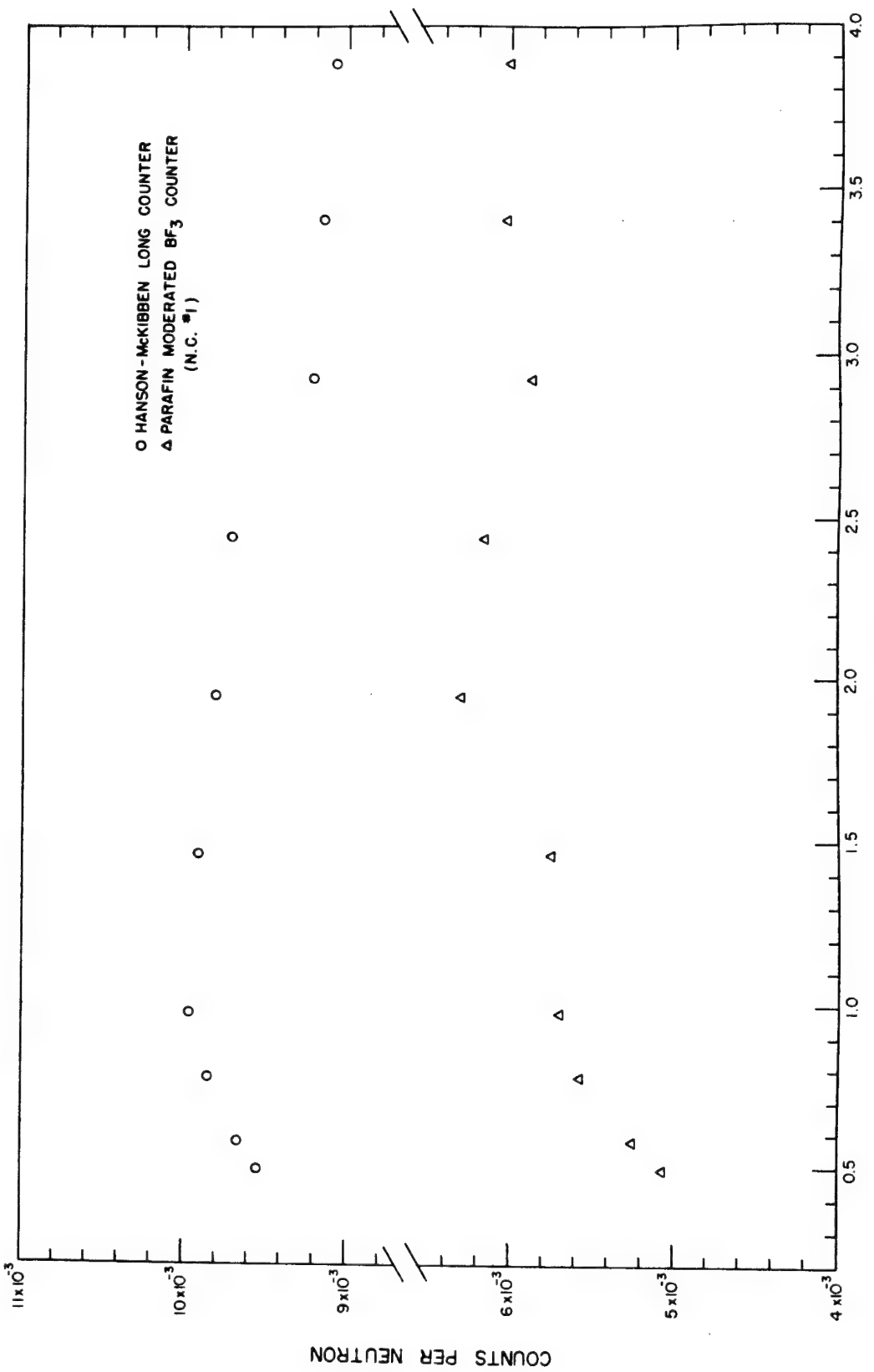

Fig. 11. BF_3 Normalization Channel Response as a Function of Neutron Energy

In addition to the above-mentioned count-rate channel, a secondary device consisting of a sulfur pellet[5] (1.5 inches in diameter and 0.375 inches thick), was placed in a fixed position on the outside of the source hoisting mechanism (aluminum car which housed the reactor) during each reactor run. It was then possible to monitor integrated reactor power by measuring P^{32} activity which was induced in the pellet through the reaction S^{32} (n,p) P^{32}, which is observed for neutron energies >2.5 Mev. The P^{32} activity is measured by counting the sample in a beta scintillation counter. Counts from this instrument were converted to a value of fluence at the pellet by:

$$\phi_s = \frac{(N)(C)}{e^{-\lambda t}} \text{ n/cm}^2 \qquad (5)$$

where

N = constant which is dependent on the count interval, counting geometry and sample size.

C = net counts per unit time.

λ = P^{32} decay constant = 2.03×10^{-3} hr^{-1}.

t = elapsed time (hr) from the mean of the exposure time.

When this number (ϕ_s) for neutron fluence (nvt) was obtained for individual runs, it was then related to reactor power by comparing it to an absolute reactor power calibration. Such a calibration was made by operating the reactor for 5.8 hours at a steady-state nominal power level of 1000 watts.[40] During this period, a sample of reactor fuel

---

[40]Prior to absolute power calibration, power levels were referred to as nominal power.

(90 percent U and 10 percent Mo) was irradiated in the "glory hole" (sample irradiation facility) in the reactor core. During the initial critical experiments with the reactor, an experiment was conducted to determine the vertical and radial fission density in the reactor.[41] Through a chemical analysis of fission products in the sample, the total number of fissions in the sample was determined. Hence, by knowing the total number of fissions in the irradiated fuel sample, and the radial and vertical fission density in the reactor core, it was possible to compute a value for the total number of fissions in the core. The reactor power level was then obtained by:

$$\text{power (watts)} = \frac{\text{total fissions in core}}{\text{time (seconds)}} \times \frac{1 \text{ watt}}{3.1 \times 10^{10} \frac{\text{fissions}}{\text{sec}}} \qquad (6)$$

To find the neutron fluence rate at the sulfur pellet, the fluence (nvt) obtained from measurements of P^{32} activity in the sulfur pellet, located in a standard position, was related to reactor power by:

$$F = \frac{\phi_s \ (n \cdot cm^{-2})}{\text{time (sec)}} \times \frac{1}{\text{power (kw)}} \qquad (7)$$

The value of F, which is given in terms of fast neutron fluence rate per unit reactor power, was determined to be 1.23×10^8 $n \cdot cm^{-2} \cdot sec^{-1} \cdot kw^{-1}$ and is used later in connection with measurements of dose rate which were normalized to reactor power by using count rates (C_L) from the BF_3 proportional counter which was used as the primary normalization channel for reactor power.

---

[41] J. T. Mihalczo, Oak Ridge National Laboratory Report ORNL-TM-189 (1962).

Determination of Standard Conditions

If individual points of measured dose rate times R^2 are plotted as a function of R, a curve through these points will be a straight line for R greater than L if the measurements are made at one air density (ρ). If there are changes in (ρ) while the measurements of dose are in progress, the points on the graph will not fall on a straight line. Hence, it was necessary to make air density corrections for measurements of dose rate if these measurements were made for some value of ρ other than ρ_o. To make these corrections, it was necessary to determine a set of "standard conditions" whereby all the experimental data could be presented in terms of these "standard conditions".

The relaxation lengths, which are considered for the purpose of this study as standard values, were determined experimentally. With the reactor supported at 1125 feet, a horizontal traverse of measurements of neutron dose rate and gamma-ray exposure rate was made between slant ranges of 1875 feet and 3200 feet. For this traverse, the instruments were lying on the interface. The air density was found to be fixed during the period of these measurements with a value of 1.02 g/l (P_o = 25.32 inches Hg and T_o = 291.2°K); therefore, the standard air density was chosen as ρ_o = 1.02 g/l. The standard relaxation length for neutron dose and that for gamma-ray exposure was found to be L_{n_o} = 248 yards and L_{γ_o} = 320 yards, respectively. Therefore, in the final data analysis, these values were used for normalization of dose measurements to ρ_o.

Neutron dose rate or gamma-ray exposure rate as a function of source-detector slant range (R) may be given by the following relation:

$$D(R) = \frac{D_o\ (B)e^{-R/L}}{R^2} \cdot K(exp) \qquad (2)$$

where

D_o = dose rate at unit distance from source.

L = relaxation length (under poor geometry conditions, this is the distance in which there is a reduction in total dose rate by a factor of 1/e).

B = dose buildup factor.

R = slant range (slant separation between source and detector).

K(exp) = boundary correction factor.

From the above relation, it is seen that neutron dose rates and gamma-ray exposure rates are dependent on the parameter, L, which is directly proportional to air density:

$$L = \frac{\rho_o}{\rho} L_o \qquad (8)$$ [42]

where

L_o = a standard relaxation length for radiation in question for standard air density (ρ_o).

ρ_o = an air density chosen as standard (1.02 g/liter).

ρ = air density at the time of measurement.

L = relaxation length for radiation in question for an air density (ρ).

Values for relaxation length may also be computed without first computing the density of the air:

---

[42] R. H. Ritchie and G. S. Hurst, Health Phys. 1, 390-404 (1959).

$$L = \left(\frac{P_o}{T_o} \cdot \frac{T}{P}\right) L_o \qquad (9)$$

where

P_o = atmospheric pressure in inches of Hg at the air density chosen as standard (ρ_o= 1.02 g/liter).

T_o = absolute temperature at the standard air density.

T = absolute temperature at time of measurement.

P = atmospheric pressure in inches of Hg at time of measurement.

Equation (9) follows from one in which the density of dry air is computed by $\rho = \rho_o [T_o/P_o \cdot P/T]$,[43] or $\rho_o/\rho = [P_o/T_o \cdot T/P]$. Values for P in the area where reactor operations were conducted were not recorded there during operation. Therefore, it was necessary to compute values for P using hourly readings which were obtained from a U. S. Weather Bureau station located nearby. If the atmospheric pressure P is known at one elevation, it may be computed at another elevation by the following formula if the difference in elevation is not greater than 1000 meters:

$$P = P_1 \left(\frac{A(1+Bt)-H}{A(1+Bt)+H}\right)^{44} \qquad (10)$$

where

P = atmospheric pressure in inches of Hg at $\frac{H_R}{2}$ (H_R = reactor height).

P_1 = atmospheric pressure in inches of Hg at U. S. weather station.

t = mean of the ordinary temperatures at the two elevations (°C).

$B = 4 \times 10^{-3}$.

---

[43] C. D. Hodgman, ed., Handbook of Chemistry and Physics (Chemical Rubber Publishing Co., Cleveland, Ohio, 1963) p. 2200.

[44] Ibid., p. 3204.

$$A = 5.249 \times 10^4$$

$$H = \left(316 + \frac{H_R}{2}\right) \text{ feet}$$

The mean sea level elevation of the U. S. Weather Bureau station is 316 feet less than the elevation of the experimental area.

Normalization of Data

Neutron and gamma-ray data were initially recorded according to the following relations:

$$\text{neutron dose rate} = D_n \ (\text{mrad}.\text{hr}^{-1}.C_L^{-1}) \tag{11}$$

$$\text{gamma exposure rate} = D_\gamma \ (\text{mR}.\text{hr}^{-1}.C_L^{-1}) \tag{12}$$

This practice consisted of recording a measurement from both the neutron and gamma-ray dosimeters and then dividing these measurements by (C_L), which was the number of thousand normalization channel counts in thousands during the counting interval. Hence, the dose measurements are recorded in units proportional to reactor power at an air density ρ, which corresponds to the air density at the time the dose measurement was made. Because this type of normalization was done, it was necessary to calibrate the normalization channel count rate. This procedure was complicated because the normalization channel was positioned at a horizontal distance $(X_L)^{39}$ = 790 yards part of the time and at (X_L) = 1000 yards the remainder of the time. For most groups of data at a fixed reactor height, some of the dosimeter readings are normalized to reactor power by using values of (C_L) at 790 yards and others are normalized by using values of (C_L) at 1000 yards. It then became apparent that air density corrections would be necessary for both the dosimeter and the normalization channel, and corrections would be necessary to account for the difference in horizontal positioning of the normalization channel.

Because the dosimeter readings were divided by the term C_L, it was necessary, in the final analysis of data, to multiply all dosimeter readings by a function which would adjust the dosimeter reading to dose rate per unit reactor power ($mrad.hr^{-1}.kw^{-1}$), and would at the same time make an adjustment for the fact that the normalization channel was located at two horizontal positions. This function was labeled $G(H_R,X_L)$, thus indicating it to be a function of reactor height and horizontal distance between a point beneath the center of the normalization channel and a point beneath the center of the reactor. It was observed that, for a fixed reactor power, the normalization channel count rate with the reactor supported at 27 feet was less than the count rate with the reactor supported at 300 feet. Therefore, for each position at which the reactor was operated, at least three individual reactor runs were chosen at random in order to determine the function $G(H_R,X_L)$. Because of the fact that the normalization channel was positioned at two horizontal locations, the response of this instrument, in determining $G(H_R,X_L)$, was adjusted to the response at unit distance. The following procedure is offered as an example for reactor run No. 51A.

$$G(H_R,X_L) = \frac{C_L}{\phi_s/t} \times e^{R_L/L_n} \times R_L^2 \times F \qquad (13)$$

where

H_R = 27 feet.

X_L = 3000 feet.

R_L = 3000 feet.

$C_L = 67.8 \frac{cts}{10\ min} \times 10^{-3}$.

$\frac{\phi_s}{t}$ = fast neutron fluence rate at the sulfur pellet during this particular reactor run (1.81×10^8 n.cm^{-2}.sec^{-1}).

F = calibrated fast neutron fluence rate per unit reactor power (1.23×10^8 n.cm^{-2}.sec^{-1}.kw^{-1}).

$L_n = L_{n_o} \frac{P_o}{T_o} \cdot \frac{T}{P} = 747$ feet.

$e^{R_L/L_n} = e^{3000/747} = e^{4.016}$.

Therefore

$$G(H_R,X_L) = \frac{67.8 \text{ (cts/10 min} \times 10^{-3})}{1.81 \times 10^8 \text{ (n.cm}^{-2}\text{.sec}^{-1})} \times e^{4.016} \times 9 \times 10^6 \text{ ft}^2 \times 1.23 \times 10^8 \text{ n.cm}^{-2}\text{.sec}^{-1}\text{.kw}^{-1}$$

$$= 2.30 \times 10^{10} \frac{\text{(cts/10 min} \times 10^{-3})}{\text{kw}} \times \text{ft}^2$$

The above procedure was extended to all reactor heights, and the results are given in Table 1, which presents the mean value and standard deviation of $G(H_R,X_L)$ for the individual reactor runs at each height. Figure 12 graphically represents the normalization channel count rate dependence on reactor height. At 1500 feet reactor height, the value of $G(H_R,X_L)$ is taken from a curve which is asymptotically approaching a limiting value.

Air Density Correction for Measurements From the Reactor

When measurements of dose rate are made at an air density (ρ) other than the standard air density (ρ_o), the measurement may be corrected to what it would be at ρ_o in the following manner. By multiplying the measured dose rate by the square of the source-detector separation (R^2) and by the exponential $e^{R/L}$, where L is the relaxation length for an air density ρ, the measured dose is extended to what it would be at unit distance from the source. If this dose at unit

Table 1

$G(H_R, X_L)$ AS A FUNCTION OF REACTOR HEIGHT

H_R (feet)	$G(H_R, X_L) \frac{\text{counts} \times 10^{-3}}{10 \text{ min-kw}} \times \text{ft}^2$
27	$2.25 \pm .14 \times 10^{10}$
300	$3.46 \pm .09 \times 10^{10}$
500	$3.91 \pm .29 \times 10^{10}$
1125	$5.32 \pm .12 \times 10^{10}$
1500	$5.72 \pm .44 \times 10^{10}$

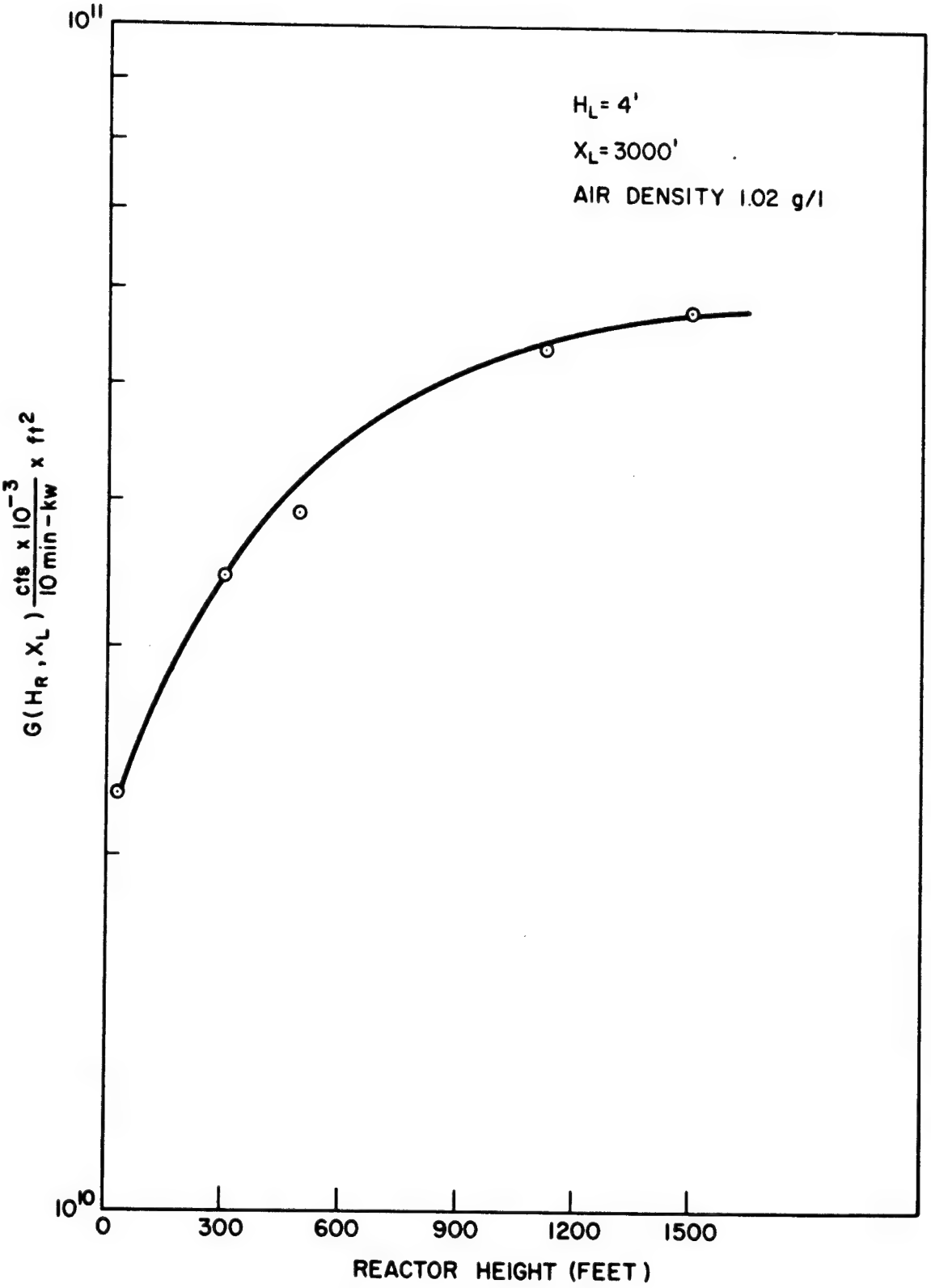

Fig. 12. BF_3 Normalization Channel Response as a Function of Reactor Height

distance is then multiplied by $1/R^2$ and e^{-R/L_o}, it is corrected to what it would be at the source-detector separation R for an air density of ρ_o. Hence

$$D_1 = D \cdot R^2 \cdot e^{R/L} \cdot 1/R^2 \cdot e^{-R/L_o}$$

$$D_1 = D \cdot e^{R/L} \cdot e^{-R/L_o}$$

$$D_1 = D \exp [-R (1/L_o - 1/L)] \qquad (14)$$

Where L is computed by equation (10),

D_1 = dose for an air density ρ_o, and

D = measured dose for an air density ρ.

It was mentioned earlier in this chapter that raw data for neutron dose rate and gamma-ray exposure rate were recorded in units of $mrad.hr^{-1}.C_L^{-1}$ and $mR.hr^{-1}.C_L^{-1}$, respectively.

In order to reduce this data to a useful form, it was necessary to correct all instrument readings to their value at the standard air density. It was also necessary to apply the normalization channel interface function[45] $G(H_R,X_L)$ so that C_L would be in terms of reactor power. These manipulations are accomplished in the following formulae:

For neutrons,

$$D_{n_1} = D_n \left(\frac{mrad}{hr\text{-}C_L}\right) \times \frac{G(H_R,X_L)}{R_L^2 \, (e^{-R_L/L_{n_o}})} \frac{C_L \times ft^2}{kw\text{-}ft^2} \times \frac{\exp [-R_D \, (1/L_{n_o} - 1/L_{n_1})]}{\exp [-R_L \, (1/L_{n_o} - 1/L_{n_1})]}$$

$$D_{n_1} = D_n \times \frac{G(H_R,X_L)}{R_L^2 \, (e^{-R_L/L_{n_o}})} \times \exp [-(R_D - R_L)(1/L_{n_o} - 1/L_{n_1})] \frac{mrad}{hr\text{-}kw} \qquad (15)$$

---

[45]Interface corrections were necessary for the normalization channel only since it was being used for reactor power normalization.

where

D_n = raw neutron dose rate.

$G(H_R, X_L)$ = interface factor at unit distance.

R_L = slant distance between center of reactor and center of normalization channel (feet).

L_{n_o} = standard condition relaxation length for neutron dose = 744 feet.

R_D = slant distance between center of reactor and center of fast neutron dosimeter (feet).

L_{n_1} = relaxation length for neutron dose, for an air density of ρ_1, at the time the raw data were collected.

For gamma rays,

$$D_{\gamma 1} = D_\gamma \left(\frac{mR}{hr\text{-}C_L}\right) \times \frac{G(H_R, X_L)}{R_L^2 \, (e^{-R_L/L_{n_o}})} \frac{C_L \times ft^2}{kw\text{-}ft^2} \times \frac{\exp\left[-R_D \, (1/L_{\gamma_o} - 1/L_{\gamma_1})\right]}{\exp\left[-R_L \, (1/L_{n_o} - 1/L_{n_1})\right]}$$

$$D_{\gamma 1} = D_\gamma \times \frac{G(H_R, X_L)}{R_L^2 \, (e^{-R_L/L_{n_o}})} \times \frac{\exp\left[-R_D \, (1/L_{\gamma_o} - 1/L_{\gamma_1})\right]}{\exp\left[-R_L \, (1/L_{n_o} - 1/L_{n_1})\right]} \frac{mR}{hr\text{-}kw} \qquad (16)$$

where

D_γ = raw gamma-ray exposure rate.

R_L, L_{n_o}, and L_{n_1} remain the same as in the previous case.

R_D = slant distance between center of reactor and center of gamma-ray dosimeter (feet).

L_{γ_o} = standard condition relaxation length for gamma-ray exposure = 960 feet.

L_{γ_1} = relaxation length for gamma-ray exposure at ρ, at the time the raw data were collected.

The use of these formulae serves two purposes; the raw data are now presented as dose rate per kilowatt reactor power, and the error introduced by fluctuations in air density is reduced. Comparisons to other experimental data may be accomplished with a minimum of manipulation.

Air Density Corrections for Measurements from Co^{60}

Measurements of gamma-ray exposure rate were made in the radiation field from an 800-curie Co^{60} source which was supported on the 1527-foot tower after operations involving the HPRR had ceased. Except for source-detector slant separation less than 400 feet and greater than 2500 feet, measurements of exposure rate were made in approximately the same places as the case of reactor operation.

Three weeks were required to complete the Co^{60} gamma-ray measurements. Due to the 5.3 year half-life of Co^{60}, it was necessary to make corrections for changes in air density only. An air density correction for this case is conducted in the same manner as that in the previous section.

A standard relaxation length for exposure rate from Co^{60} was determined experimentally by making measurements along a line horizontally away from the 1527-foot tower and for a fixed source height and fixed detector height. The air density was found to be 1.01 g/l = ρ_o, and the relaxation length was L_o = 690 feet. Hence, all data were corrected to the air density ρ_o by the following:

$$D_1 = D \times e^{-R_D (1/L_o - 1/L_1)}$$

where

D = exposure rate in mR/hr.

R_D = slant distance between source and detector (feet).

L_o = standard relaxation length = 690 feet.

L = relaxation length (feet) for an air density of ρ_1 [computed according to equation (10)].

and the multiplier $e^{-R_D (1/L_o - 1/L_1)}$ simply corrects the exposure rate reading to what it should be for an air density of ρ_o = 1.01 g/l. It is not necessary to include an interface factor in these corrections because no normalization channel was needed for changes in source activity.

Method for Making Corrections

The number of individual corrections for data points for the three cases (reactor neutrons, reactor gamma rays, and Co^{60} gamma rays) of measurements represented a tremendous task if undertaken by hand. Therefore, a Fortran program was written to make all corrections due to changes in air density, and to make the many determinations of pressure, relaxation length (L_1) at ρ_1, and slant range, all of which were used in the air density correction formulae. The program was run on an IBM-7090 computer.

VI. EXPERIMENTAL RESULTS

At each dosimeter position throughout the course of this study, values of neutron dose or gamma-ray exposure were derived from digital information which was collected during carefully measured time intervals. This digital information was transferred to dose by applying calibration factors as outlined in Chapter IV. The accuracy of individual data points is dependent upon the spread of values about an average measurement of dose. This spread of values is subject to statistical fluctuations due to the random manner in which radiation was emitted from the reactor and the Co^{60} source. Therefore, in assessing the accuracy of data, the standard deviation,[46] (σ), in the number of counts per unit time (also dose rate) is computed by:

$$\sigma = \left(\frac{n_1}{t_1} + \frac{n_2}{t_2}\right)^{\frac{1}{2}} \tag{18}$$

where

σ = standard deviation

n_1 = average total count rate in c/m (source plus background).

t_1 = time of observation of total count rate.

n_2 = background count rate.

t_2 = time of observation of background count rate.

Further, the fractional standard deviation of the count rate (also dose rate) is given by:

$$S_n = \frac{\sigma}{n} \% \tag{19}$$

---

[46] Y. Beers, Introduction to the Theory of Error (Addison-Wesley Publishing Co., Inc., Reading, Massachusetts, 1957) P. 48.

where

n = average net count rate in c/m = $(n_1 - n_2)$.

As an example, the following gamma-ray data were taken at a slant range of 4635 feet from the reactor which was operating at steady state and was supported 1125 feet above the interface. The background of the gamma-ray dosimeter was observed for 36.6 minutes and was 2.4 c/min. Three individual counts (35.5 minutes each which was the typical counting time at this separation) were made at this position while the reactor was operating. These count rates were 5.55, 5.80, and 5.50 counts per minute, respectively. The standard deviation for this data point is determined by equation (18):

$$\sigma = \left(\frac{5.61}{35.5} + \frac{2.40}{36.6}\right)^{\frac{1}{2}}$$

$$\sigma = (.228)^{\frac{1}{2}} = 0.48$$

The average net count rate is 3.21 c/min; therefore, the fractional standard deviation for this data point is:

$$S_n = \frac{\pm 0.48}{3.21} = \pm 14\%$$

Because the dose rate is determined by a simple multiplication of count rate by a calibration factor, S_n for the count rate is the same for dose rate. Through the procedure described above, it is estimated that S_n at slant ranges closer than 750 yards to the reactor for neutron and gamma-ray dose rates was generally within ±4 percent. The accuracy decreased as the slant range increased so that at 1000 yards values of dose rate were accurate within approximately ±10 percent, and at 1500 yards S_n had increased to ±15 percent. By the same procedure, it is estimated that during use of the Co^{60} source, values of gamma-ray

exposure rate for slant ranges less than 500 yards were accurate within ±3 percent. At a slant range of 750 yards, S_n had increased to ±10 percent.

Extreme care was taken during the experimental part of this study to keep the systematic errors from being large enough to influence appreciably the accuracy of the measurements of dose. This was accomplished by making careful measurements of distance, by calibrating detectors in a fixed geometry using sources which had been calibrated by the National Bureau of Standards, and by making corrections in dose readings, as outlined in Chapter V, for changes in air density. The adequacy of these air density corrections may be attested by the following argument. It was shown in Chapter V that errors in neutron dose rate at 1000 yards could be as large as 43 percent due to the air density fluctuation of 9 percent which was observed during this study. It has been stated elsewhere[42] that a semi-log plot of $D \times R^2$ as a function of R results in a straight line through the data points for slant ranges greater than about one relaxation length. Several graphs of $D \times R^2$ vs R are presented in this chapter. It is readily seen that the maximum deviation of data points from the "smooth curve" is approximately 15 percent. Deviations of this magnitude were not observed often.

All data which were collected in this study are given in Tables 2 through 21.

Neutron Data from HPRR Operation

Figure 13 presents neutron dose times slant range squared vs slant range (R). Curve (A) represents Ritchie's[9] computed neutron dose data for the fission source and detector located in an infinite air medium

Table 2

NEUTRON DOSE RATE VALUES FOR DETECTOR LYING ON THE AIR-GROUND INTERFACE AS A FUNCTION OF REACTOR HEIGHT (H_R) AND SLANT RANGE (R)

Reactor Height H_R (feet)	Horizontal Separation X_D (feet)	Slant Range R (feet)	$D_{nl} \times R^2$ mrad·ft^2·hr^{-1}·kw^{-1}
27	100	104	5.833×10^7
27	200	202	4.882×10^7
27	300	302	3.799×10^7
27	400	401	3.655×10^7
27	700	701	2.713×10^7
27	1500	1501	1.022×10^7
27	2250	2251	3.791×10^6
27	3000	3001	1.558×10^6
300	100	319	3.855×10^7
300	1500	1535	1.403×10^7
300	2250	2275	5.374×10^6
300	3000	3020	1.790×10^6
500	3000	3049	2.126×10^6
1125	1500	1890	1.396×10^7
1125	2200	2487	5.077×10^6
1125	2250	2532	5.480×10^6
1125	3000	3220	2.130×10^6
1125	3750	3930	8.321×10^5
1125	4500	4653	3.249×10^5
1500	3000	3374	2.315×10^6

Table 3

NEUTRON DOSE RATE VALUES FOR DETECTOR
SUPPORTED 2 FEET ABOVE THE AIR-GROUND INTERFACE
AS A FUNCTION OF REACTOR HEIGHT (H_R) AND SLANT RANGE (R)

Reactor Height H_R (feet)	Horizontal Separation X_D (feet)	Slant Range R (feet)	$D_{n_1} \times R^2$ $mrad.ft^2.hr^{-1}.kw^{-1}$
27	100	104	6.061×10^7
27	200	202	4.757×10^7
27	300	302	3.941×10^7
27	400	401	4.050×10^7
27	700	701	2.740×10^7
27	1500	1501	1.326×10^7
27	2250	2251	3.749×10^6
27	3000	3001	1.558×10^6

Table 4

NEUTRON DOSE RATE VALUES FOR DETECTOR
SUPPORTED 3 FEET ABOVE THE AIR-GROUND INTERFACE
AS A FUNCTION OF REACTOR HEIGHT (H_R) AND SLANT RANGE (R)

Reactor Height H_R (feet)	Horizontal Separation X_D (feet)	Slant Range R (feet)	$D_{n_1} \times R^2$ mrad.ft^2.hr^{-1}.kw^{-1}
300	2250	2274	5.688×10^6
300	3000	3019	1.869×10^6
500	3000	3048	2.006×10^6
1125	2200	2486	5.572×10^6
1125	2250	2530	5.223×10^6
1125	3000	3219	1.893×10^6
1125	3750	3929	7.313×10^5
1500	3000	3373	2.156×10^6

Table 5

NEUTRON DOSE RATE VALUES FOR DETECTOR
SUPPORTED 5 FEET ABOVE THE AIR-GROUND INTERFACE
AS A FUNCTION OF REACTOR HEIGHT (H_R) AND SLANT RANGE (R)

Reactor Height H_R (feet)	Horizontal Separation X_D (feet)	Slant Range R (feet)	$D_{n_1} \times R^2$ mrad.ft^2.hr^{-1}.kw^{-1}
27	100	103	5.918×10^7
27	200	202	4.519×10^7
27	300	301	4.027×10^7
27	400	401	4.404×10^7
27	700	701	2.835×10^7
27	1500	1501	1.079×10^7
27	2250	2251	3.825×10^6
27	3000	3001	1.430×10^6
300	2250	2274	5.340×10^6
300	3000	3019	2.126×10^6
500	3000	3048	2.140×10^6
1125	1500	1887	1.291×10^7
1125	2200	2485	5.615×10^6
1125	2250	2529	5.244×10^6
1125	3000	3218	1.659×10^6
1125	3750	3929	9.143×10^5
1125	4500	4652	2.624×10^5
1500	3000	3372	1.921×10^6

Table 6

NEUTRON DOSE RATE VALUES FOR DETECTOR
SUPPORTED 16.5 FEET ABOVE THE AIR-GROUND INTERFACE
AS A FUNCTION OF REACTOR HEIGHT (H_R) AND SLANT RANGE (R)

Reactor Height H_R (feet)	Horizontal Separation X_D (feet)	Slant Range R (feet)	$D_{n_1} \times R^2$ mrad.ft^2.hr^{-1}.kw^{-1}
27	100	101	4.630×10^7
27	200	201	4.573×10^7
27	300	300	4.144×10^7
27	400	400	3.850×10^7
27	700	700	2.806×10^7
27	1500	1500	1.035×10^7
27	2250	2250	3.962×10^6
27	3000	3000	1.505×10^6
300	100	303	3.510×10^7
300	200	350	4.124×10^7
300	300	417	4.456×10^7
300	400	495	4.656×10^7
300	700	760	3.693×10^7
300	1500	1531	1.405×10^7
300	2250	2273	5.580×10^6
300	3000	3018	2.112×10^6
500	3000	3046	2.154×10^6
1125	1500	1880	1.202×10^7
1125	2250	2524	5.223×10^6
1125	3000	3214	1.670×10^6
1125	3750	3925	7.099×10^5
1125	4500	4649	2.387×10^5
1500	3000	3366	2.009×10^6

Table 7

NEUTRON DOSE RATE VALUES FOR DETECTOR
SUPPORTED 50 FEET ABOVE THE AIR-GROUND INTERFACE
AS A FUNCTION OF REACTOR HEIGHT (H_R) AND SLANT RANGE (R)

Reactor Height H_R (feet)	Horizontal Separation X_D (feet)	Slant Range R (feet)	$D_{n_1} \times R^2$ mrad·ft^2·hr^{-1}·kw^{-1}
27	2250	2250	3.864×10^6
27	3000	3000	1.535×10^6
300	1500	1525	1.578×10^7
300	2250	2268	5.988×10^6
300	3000	3014	2.303×10^6
500	3000	3040	2.351×10^6
1125	2250	2509	5.461×10^6
1125	3000	3202	1.845×10^6
1125	3750	3916	7.883×10^5
1500	3000	3351	2.131×10^6

Table 8

NEUTRON DOSE RATE VALUES FOR DETECTOR
SUPPORTED 100 FEET ABOVE THE AIR-GROUND INTERFACE
AS A FUNCTION OF REACTOR HEIGHT (H_R) AND SLANT RANGE (R)

Reactor Height H_R (feet)	Horizontal Separation X_D (feet)	Slant Range R (feet)	$D_{n_1} \times R^2$ mrad·ft^2·hr^{-1}·kw^{-1}
27	2250	2250	4.108×10^6
27	3000	3000	1.654×10^6
300	100	226	3.328×10^7
300	200	286	3.978×10^7
300	400	451	4.091×10^7
300	700	732	3.758×10^7
300	1500	1517	1.573×10^7
300	2250	2262	6.346×10^6
300	3000	3010	2.210×10^6
500	3000	3033	2.336×10^6
1125	1500	1831	1.292×10^7
1125	2250	2485	5.911×10^6
1125	3000	3185	1.920×10^6
1125	3750	3901	8.157×10^5
1500	3000	3329	2.028×10^6

Table 9

GAMMA EXPOSURE RATE VALUES FOR DETECTOR LYING ON THE AIR-GROUND INTERFACE AS A FUNCTION OF REACTOR HEIGHT (H_R) AND SLANT RANGE (R)

Reactor Height H_R (feet)	Horizontal Separation X_D (feet)	Slant Range R (feet)	$D_{\gamma 1} \times R^2$ $mR \cdot ft^2 \cdot hr^{-1} \cdot kw^{-1}$
27	100	104	8.684×10^6
27	200	202	8.869×10^6
27	300	302	7.720×10^6
27	400	401	8.655×10^6
27	700	701	8.171×10^6
27	1500	1501	4.771×10^6
27	2250	2251	2.297×10^6
27	3000	3001	1.179×10^6
300	100	319	8.909×10^6
300	1500	1535	5.786×10^6
300	2250	2275	3.217×10^6
300	3000	3020	1.581×10^6
500	3000	3049	1.698×10^6
1125	1500	1890	6.981×10^6
1125	2200	2487	3.989×10^6
1125	2250	2532	3.565×10^6
1125	3000	3220	1.603×10^6
1125	3750	3930	8.683×10^5
1125	4500	4653	4.763×10^5
1500	3000	3374	1.771×10^6

Table 10

GAMMA EXPOSURE RATE VALUES FOR DETECTOR
SUPPORTED 2 FEET ABOVE THE AIR-GROUND INTERFACE
AS A FUNCTION OF REACTOR HEIGHT (H_R) AND SLANT RANGE (R)

Reactor Height H_R (feet)	Horizontal Separation X_D (feet)	Slant Range R (feet)	$D_{\gamma_1} \times R^2$ $mR \cdot ft^2 \cdot hr^{-1} \cdot kw^{-1}$
27	100	104	8.739×10^6
27	200	202	7.933×10^6
27	300	302	7.682×10^6
27	400	401	9.421×10^6
27	700	701	8.160×10^6
27	1500	1501	4.409×10^6
27	2250	2251	2.300×10^6
27	3000	3001	1.037×10^6

Table 11

GAMMA EXPOSURE RATE VALUES FOR DETECTOR
SUPPORTED 3 FEET ABOVE THE AIR-GROUND INTERFACE
AS A FUNCTION OF REACTOR HEIGHT (H_R) AND SLANT RANGE (R)

Reactor Height H_R (feet)	Horizontal Separation X_D (feet)	Slant Range R (feet)	$D_{\gamma_1} \times R^2$ $mR \cdot ft^2 \cdot hr^{-1} \cdot kw^{-1}$
300	2250	2274	3.207×10^6
300	3000	3019	1.756×10^6
500	3000	3048	1.447×10^6
1125	2200	2486	3.797×10^6
1125	2250	2530	3.719×10^6
1125	3000	3219	1.786×10^6
1125	3750	3929	8.283×10^5
1500	3000	3373	1.564×10^6

Table 12

GAMMA EXPOSURE RATE VALUES FOR DETECTOR SUPPORTED 5 FEET ABOVE THE AIR-GROUND INTERFACE AS A FUNCTION OF REACTOR HEIGHT (H_R) AND SLANT RANGE (R)

Reactor Height H_R (feet)	Horizontal Separation X_D (feet)	Slant Range R (feet)	$D_{\gamma 1} \times R^2$ $mR \cdot ft^2 \cdot hr^{-1} \cdot kw^{-1}$
27	100	103	7.913×10^6
27	200	202	7.773×10^6
27	300	301	7.924×10^6
27	400	401	9.544×10^6
27	700	701	8.561×10^6
27	1500	1501	4.466×10^6
27	2250	2251	2.375×10^6
27	3000	3001	1.267×10^6
300	2250	2274	3.200×10^6
300	3000	3019	1.421×10^6
500	3000	3048	1.612×10^6
1125	1500	1887	6.616×10^6
1125	2200	2485	3.559×10^6
1125	2250	2529	3.826×10^6
1125	3000	3218	1.241×10^6
1125	3750	3929	7.833×10^5
1125	4500	4652	5.066×10^5
1500	3000	3372	1.662×10^6

Table 13

GAMMA EXPOSURE RATE VALUES FOR DETECTOR
SUPPORTED 16.5 FEET ABOVE THE AIR GROUND INTERFACE
AS A FUNCTION OF REACTOR HEIGHT (H_R) AND SLANT RANGE (R)

Reactor Height H_R (feet)	Horizontal Separation X_D (feet)	Slant Range R (feet)	$D_{\gamma_1} \times R$ $mR \cdot ft^2 \cdot hr^{-1} \cdot kw^{-1}$
27	100	101	6.856×10^6
27	200	201	7.310×10^6
27	300	300	7.881×10^6
27	400	400	8.453×10^6
27	700	700	7.595×10^6
27	1500	1500	4.494×10^6
27	2250	2250	2.473×10^6
27	3000	3000	1.112×10^6
300	100	303	7.431×10^6
300	200	350	8.489×10^6
300	400	495	1.042×10^7
300	700	760	9.707×10^6
300	1500	1531	5.958×10^6
300	2250	2273	2.851×10^6
300	3000	3018	1.583×10^6
500	3000	3046	1.509×10^6
1125	1500	1880	6.347×10^6
1125	2250	2524	3.849×10^6
1125	3000	3214	1.367×10^6
1125	3750	3925	7.448×10^5
1125	4500	4649	4.394×10^5
1500	3000	3366	1.675×10^6

Table 14

GAMMA EXPOSURE RATE VALUES FOR DETECTOR
SUPPORTED 50 FEET ABOVE THE AIR-GROUND INTERFACE
AS A FUNCTION OF REACTOR HEIGHT (H_R) AND SLANT RANGE (R)

Reactor Height H_R (feet)	Horizontal Separation X_D (feet)	Slant Range R (feet)	$D_{\gamma_1} \times R^2$ $mR \cdot ft^2 \cdot hr^{-1} \cdot kw^{-1}$
27	2250	2250	2.299×10^6
27	3000	3000	1.146×10^6
300	1500	1525	5.123×10^6
300	2250	2268	2.851×10^6
300	3000	3014	1.380×10^6
500	3000	3040	1.507×10^6
1125	2250	2509	3.644×10^6
1125	3000	3202	1.366×10^6
1125	3750	3916	7.706×10^5
1500	3000	3351	1.581×10^6

Table 15

GAMMA EXPOSURE RATE VALUES FOR DETECTOR
SUPPORTED 100 FEET ABOVE THE AIR-GROUND INTERFACE
AS A FUNCTION OF REACTOR HEIGHT (H_R) AND SLANT RANGE (R)

Reactor Height H_R (feet)	Horizontal Separation X_D (feet)	Slant Range R (feet)	$D_{\gamma 1} \times R^2$ $mR \cdot ft^2 \cdot hr^{-1} \cdot kw^{-1}$
27	2250	2250	2.316×10^6
27	3000	3000	1.104×10^6
300	100	226	4.326×10^6
300	200	286	6.102×10^6
300	400	451	7.466×10^6
300	700	732	7.709×10^6
300	1500	1517	5.657×10^6
300	2250	2262	2.991×10^6
300	3000	3010	1.442×10^6
500	3000	3033	1.575×10^6
1125	1500	1831	5.395×10^6
1125	2250	2487	3.362×10^6
1125	3000	3185	1.350×10^6
1125	3750	3901	8.515×10^5
1500	3000	3329	1.511×10^6

Table 16

Co^{60} GAMMA EXPOSURE RATE VALUES FOR DETECTOR LYING ON THE AIR-GROUND INTERFACE AS A FUNCTION OF SOURCE HEIGHT (H_S) AND SLANT RANGE (R)

Source Height H_S (feet)	Horizontal Separation X_D (feet)	Slant Range R (feet)	$D_{\gamma_1} \times R^2$ $mR \cdot ft^2 \cdot hr^{-1}$
27	400	401	1.14×10^7
27	700	701	6.79×10^6
27	1200	1201	3.36×10^6
27	1500	1501	2.34×10^6
27	2250	2251	7.68×10^5
300	400	505	1.09×10^7
300	700	767	7.58×10^6
300	1200	1242	4.03×10^6
300	1500	1535	2.98×10^6
300	2250	2275	1.09×10^6
1125	700	1336	3.62×10^6
1125	1100	1587	2.98×10^6
1125	1200	1659	2.79×10^6
1125	1300	1734	2.58×10^6
1125	1400	1811	2.31×10^6
1125	1500	1890	2.10×10^6
1125	1600	1971	1.80×10^6
1125	1700	2054	1.65×10^6
1125	1800	2138	1.47×10^6
1125	2250	2531	9.02×10^5
1500	2250	2723	7.35×10^5

Table 17

Co^{60} GAMMA EXPOSURE RATE VALUES FOR DETECTOR SUPPORTED 2 FEET ABOVE THE AIR-GROUND INTERFACE AS A FUNCTION OF SOURCE HEIGHT (H_S) AND SLANT RANGE (R)

Source Height H_S (feet)	Horizontal Separation X_D (feet)	Slant Range R (feet)	$D_{\gamma_1} \times R^2$ $mR.ft^2.hr^{-1}$
27	400	401	1.08×10^7
27	700	701	6.47×10^6
27	1200	1201	3.39×10^6
27	1500	1501	2.19×10^6
27	2250	2251	8.66×10^5
300	400	503	1.05×10^7
300	700	766	7.66×10^6
300	1200	1242	5.00×10^6
300	1500	1534	2.89×10^6
300	2250	2274	1.07×10^6
1125	700	1334	3.56×10^6
1125	1200	1658	2.71×10^6
1125	1500	1889	2.10×10^6
1125	2250	2530	8.66×10^5
1125	2370	2638	8.25×10^5
1500	2250	2722	8.82×10^5

Table 18

Co^{60} GAMMA EXPOSURE RATE VALUES FOR DETECTOR SUPPORTED 5 FEET ABOVE THE AIR-GROUND INTERFACE AS A FUNCTION OF SOURCE HEIGHT (H_S) AND SLANT RANGE (R)

Source Height H_S (feet)	Horizontal Separation X_D (feet)	Slant Range R (feet)	$D_{\gamma_1} \times R^2$ $mR \cdot ft^2 \cdot hr^{-1}$
27	400	401	1.12×10^7
27	700	701	6.52×10^6
27	1200	1201	3.45×10^6
27	1500	1501	2.19×10^6
27	2250	2251	8.02×10^5
300	400	502	1.07×10^7
300	700	765	7.55×10^6
300	1200	1241	4.14×10^6
300	1500	1534	3.00×10^6
300	2250	2274	1.06×10^6
1125	700	1331	3.37×10^6
1125	1100	1583	3.78×10^6
1125	1200	1656	2.69×10^6
1125	1300	1730	2.47×10^6
1125	1400	1808	2.14×10^6
1125	1500	1887	2.12×10^6
1125	1600	1968	1.85×10^6
1125	1700	2051	1.84×10^6
1125	1800	2135	1.35×10^6
1125	2250	2529	8.59×10^5
1500	2250	2721	7.08×10^5

Table 19

Co^{60} GAMMA EXPOSURE RATE VALUES FOR DETECTOR SUPPORTED 16.5 FEET ABOVE THE AIR-GROUND INTERFACE AS A FUNCTION OF SOURCE HEIGHT (H_S) AND SLANT RANGE (R)

Source Height H_S (feet)	Horizontal Separation X_D (feet)	Slant Range R (feet)	$D_{\gamma 1} \times R^2$ $mR \cdot ft^2 \cdot hr^{-1}$
27	400	400	1.26×10^7
27	700	700	6.74×10^6
27	1200	1200	3.43×10^6
27	1500	1500	2.13×10^6
27	2250	2250	7.91×10^5
300	400	495	1.31×10^7
300	700	760	8.41×10^6
300	1200	1238	4.39×10^6
300	1500	1531	3.21×10^6
300	2250	2272	1.22×10^6
1125	700	1322	3.53×10^6
1125	1200	1648	2.56×10^6
1125	1500	1880	2.01×10^6
1125	2250	2524	9.42×10^5
1500	2250	2714	7.51×10^5

Table 20

Co^{60} GAMMA EXPOSURE RATE VALUES FOR DETECTOR SUPPORTED 50 FEET ABOVE THE AIR-GROUND INTERFACE AS A FUNCTION OF SOURCE HEIGHT (H_S) AND SLANT RANGE (R)

Source Height H_S (feet)	Horizontal Separation X_D (feet)	Slant Range R (feet)	$D_{\gamma_1} \times R^2$ $mR.ft^2.hr^{-1}$
27	400	400	1.26×10^7
27	700	700	7.54×10^6
27	1200	1200	3.69×10^6
27	1500	1500	2.34×10^6
27	2250	2250	8.63×10^5
300	400	476	1.12×10^7
300	700	748	8.50×10^6
300	1200	1230	4.71×10^6
300	1500	1525	3.21×10^6
300	2250	2268	1.30×10^6
1125	700	1293	3.79×10^6
1125	1200	1625	2.84×10^6
1125	1500	1860	2.09×10^6
1125	2250	2509	8.54×10^5
1500	2250	2696	6.67×10^5

Table 21

Co^{60} GAMMA EXPOSURE RATE VALUES FOR DETECTOR SUPPORTED 100 FEET ABOVE THE AIR-GROUND INTERFACE AS A FUNCTION OF SOURCE HEIGHT (H_S) AND SLANT RANGE (R)

Source Height H_S (feet)	Horizontal Separation X_D (feet)	Slant Range R (feet)	$D_{\gamma_1} \times R^2$ $mR.ft^2.hr^{-1}$
27	400	405	1.10×10^7
27	700	703	8.41×10^6
27	1200	1201	3.70×10^6
27	1500	1501	2.59×10^6
27	2250	2250	9.90×10^5
300	400	451	1.18×10^7
300	700	732	7.99×10^6
300	1200	1220	4.87×10^6
300	1500	1517	3.18×10^6
300	2250	2262	1.27×10^6
1125	700	1252	3.97×10^6
1125	1200	1592	2.90×10^6
1125	1500	1831	2.14×10^6
1125	2250	2487	1.03×10^6
1500	2250	2668	6.36×10^5

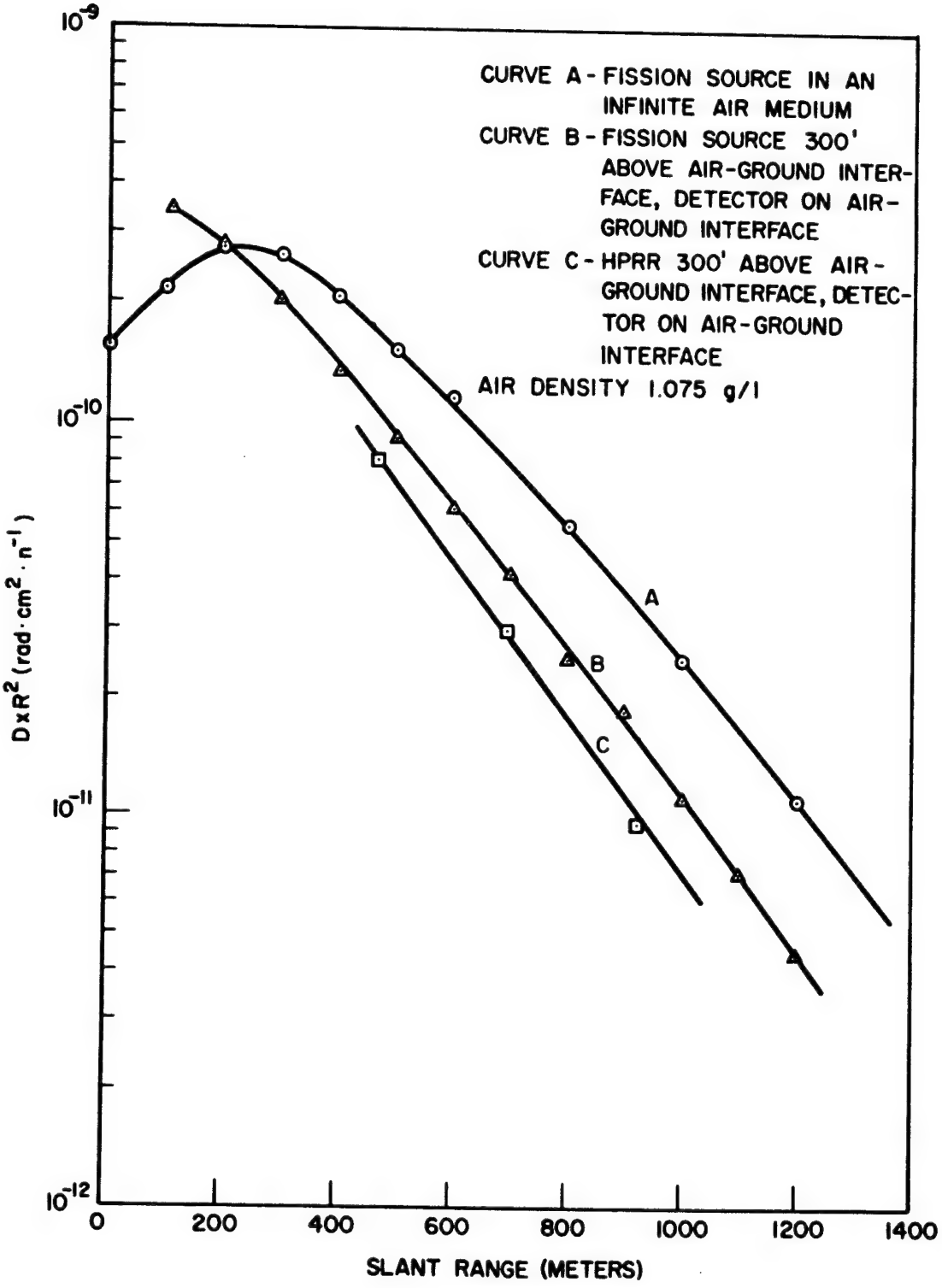

Fig. 13. Comparison of Measured Neutron Dose to Computed Neutron Dose in a Finite Medium as a Function of Slant Range (R)

(1.075 g/l). Curve (B) represents computed neutron data for the fission source at 300 feet above the air-ground interface and detector lying on the interface. Curve (C) represents experimental data collected during this project for a source detector geometry identical to that in curve (B). The computed neutron dose data, in curves (A) and (B), are for neutron energies in the spatial dose distribution greater than 150 kev. This represents approximately the lower energy threshold of response for the Radsan fast neutron dosimeter. By normalizing the experimental values to the computed values of neutron dose in the finite geometry, and air density of 1.075 g/l, [normalize curve (C) to curve (B)], a semi-experimental determination of the boundary correction factor K(exp) as a function of slant range may be determined. To perform this task, one simply divides the values in a typical $D \times R^2$ vs R curve, normalized to the computed Radsan response, by values of neutron dose at the same slant range from curve (A). This procedure is valid only if the experimental data is for the same air density as curve (A), namely 1.075 g/l. The results of this are shown in Figure 14, where the computed boundary correction factor (K) is represented by the solid line and where the semi-experimental boundary correction factor K(exp) is represented by a dashed line through the data points. The experimental curve is representative of the boundary correction factor for a source supported at 27 feet above the ground while the computed boundary correction factor is for a source supported at 10 meters (32.8 feet). It should be noted in Figure 14 that for slant ranges between 100 meters and 1000 meters, the agreement between K and K(exp) lies within approximately 20 percent even for the worst case. Some of this difference undoubtedly

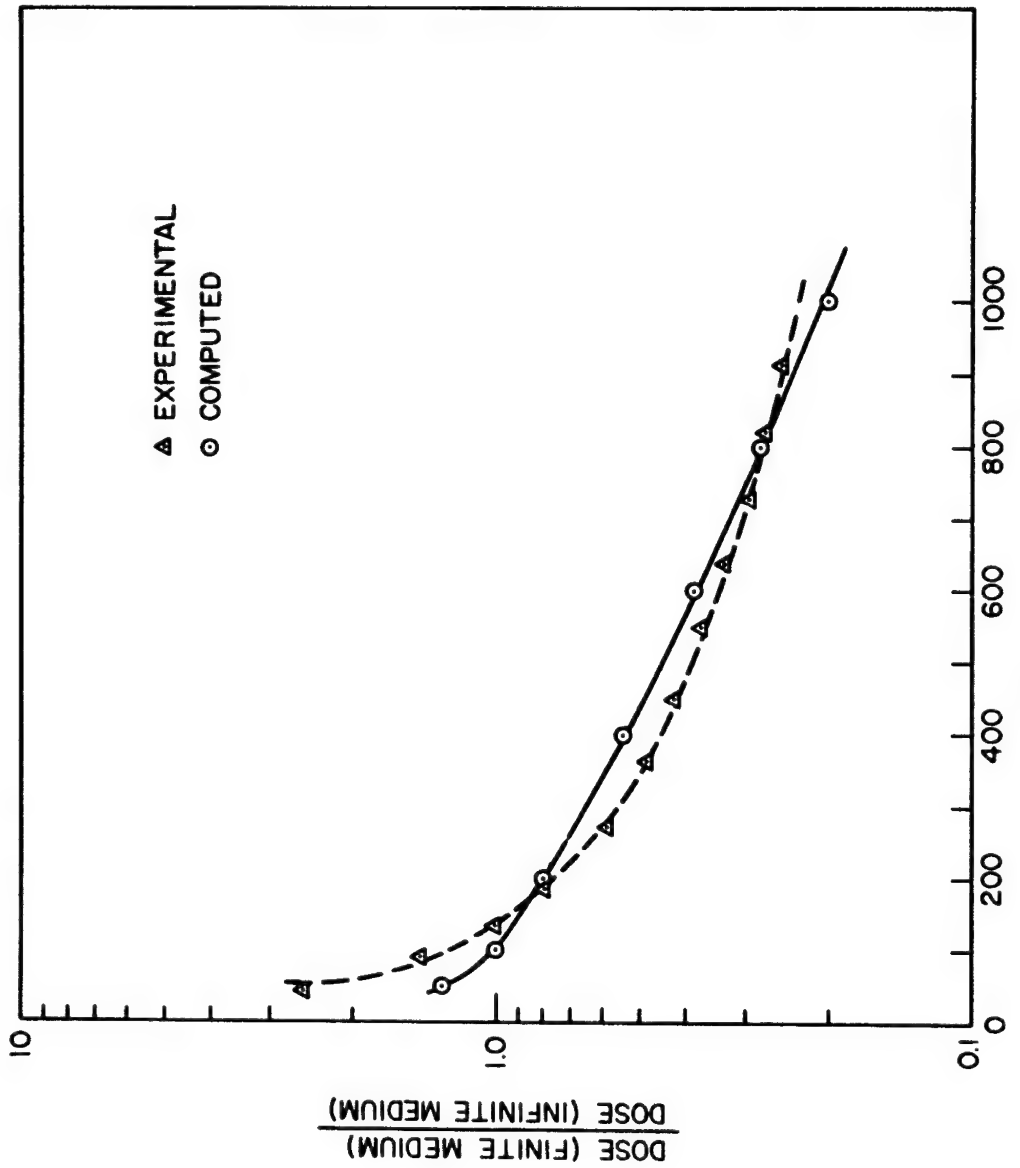

Fig. 14. Comparison of Experimental Boundary Correction Factor K(exp) to Computed Boundary Correction Factor for Neutron Dose as a Function of Slant Range (R)

lies in the fact that values for K are for 3 Mev neutrons which are more energetic than the mean neutron energy in this neutron energy spectrum, and the source height for K was larger than in the experimental case. Further treatment of neutron data in this fashion is not presented here because boundary correction factors cannot be considered reliable unless measurements of dose are made both in a finite and in an infinite air medium. For this project, the reactor was supported high enough above the ground so that the source could be considered in the infinite medium (to be shown later in this chapter), but the dosimeter was never employed successfully at heights greater than 100 feet.

It has been stated earlier that the presence of the ground increases the dose at points near the source and decreases it at distant points. This relation may be seen in Figures 15 and 16. Neutron dose rate multiplied by slant range squared is plotted as a function of slant range (R) in these figures for an air density of 1.02 g/l. In Figure 15, the reactor was supported 27 feet above the ground, and the two curves represent measurements of neutron dose rate with the detector placed on the interface and at 16.5 feet above the ground. It is readily seen that the values, in the curve for detector lying on the interface, are larger near the source, but no definite statement can be made for large separations. In general, the same relationship is shown in Figure 16 where the source is supported 300 feet above the air-ground interface and the detectors are placed at 16.5 feet and 100 feet above the interface. At source detector separations less than about 600 feet, the values of dose increase as the dosimeter is brought closer to the ground, and at separations greater than 600 feet the values of dose increase as the dosimeter is raised above the ground.

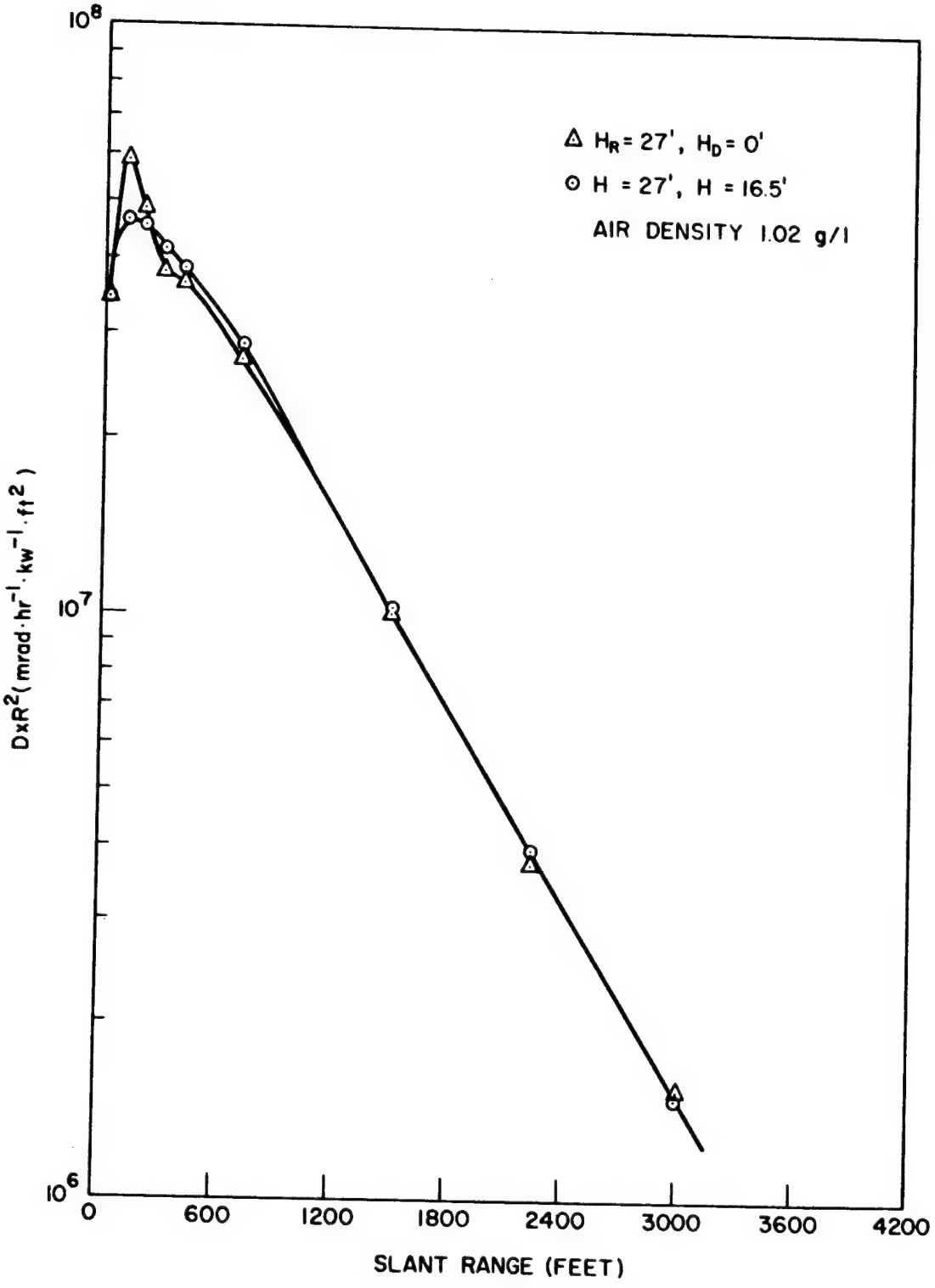

Fig. 15. Neutron D x R^2 as a Function of Slant Range (R) for a Reactor Height of 27 Feet and Detector Heights of 0 Feet and 16.5 Feet

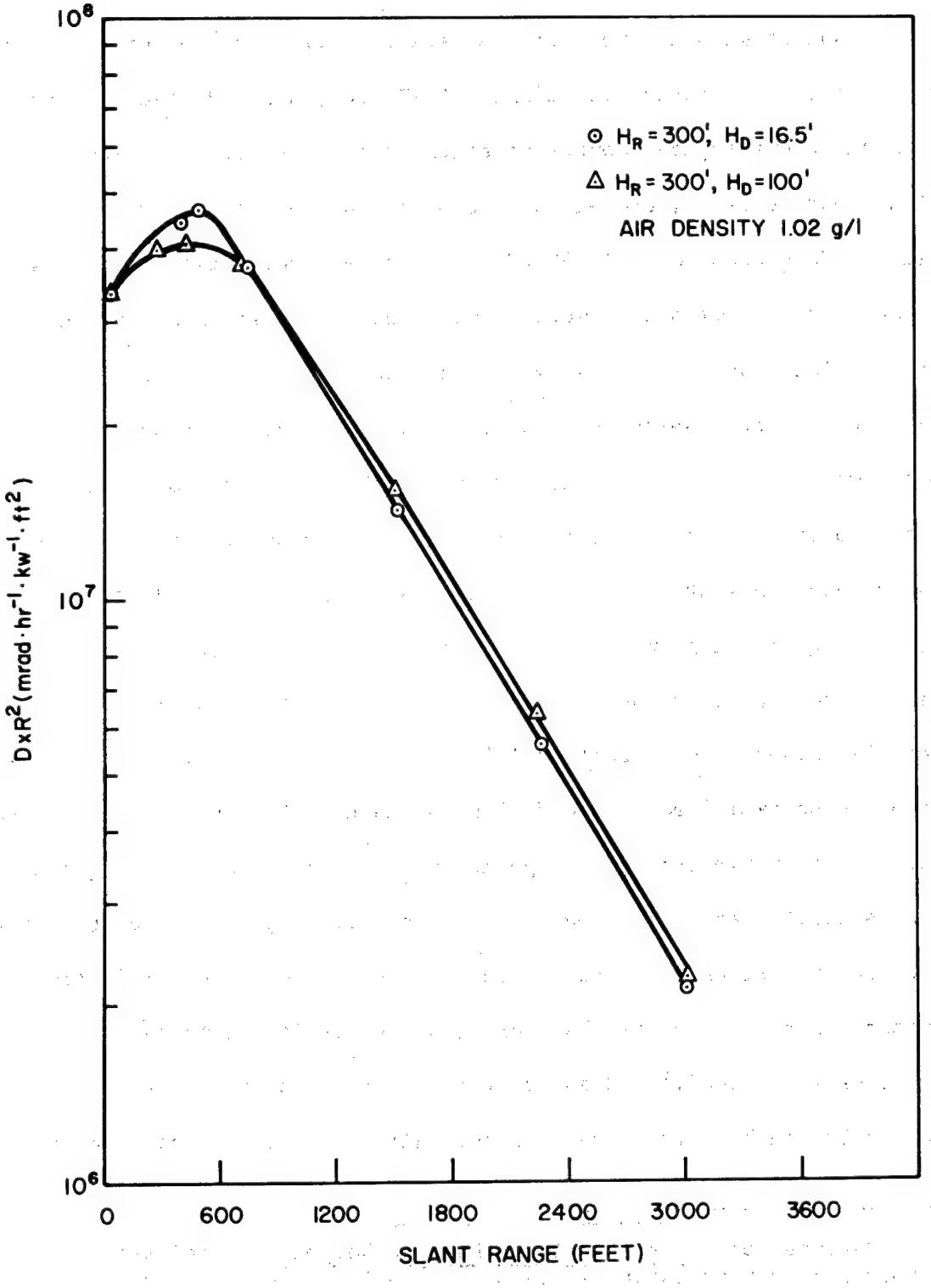

Fig. 16. Neutron D x R^2 as a Function of Slant Range (R) for a Reactor Height of 300 Feet and Detector Heights of 16.5 Feet and 100 Feet

In Figure 17, values for neutron dose rate times slant range squared versus slant range are given for the detector lying on the interface and for the reactor supported at heights of 27, 300, and 1125 feet. These curves represent typical source-detector geometry employed during nuclear weapons tests, and all have been normalized to 1.02 g/l air density. When reduced to 1.293 g/l, the average relaxation length is 195 yards, which compares favorably with data reported from weapons tests.[47] The peak which is shown in the dose rate versus distance curve for a reactor height (H_R) of 27 feet occurs at a horizontal separation (X) of approximately 100 feet. This peak is assumed to be due to albedo scattering, as it compares satisfactorily with previous data for neutron scattering from thick slabs ($H_R/X = 0.27$).[48,49]

For a given slant range greater than 1500 feet, there is an increase in dose rate at the interface by a factor of 2.1 as the fission source is raised from 27 feet to 1125 feet. The mechanism for this increase may be explained in the following manner. For an isotropic source supported in an air-over-ground geometry, the radiations reaching a point, which is located at a slant range R from the source, are direct (unscattered) radiation, radiation scattered in the air above the source, radiation scattered in the air below the source, and radiation scattered from the surface of the ground.[16] Clearly, these latter two components are influenced by the heights of the source. Although there is some reflection

---

[47]S. Glasstone, ed., The Effects of Nuclear Weapons (United States Atomic Energy Commission, 1962) pp. 369-413.

[48]J. W. Cure and G. S. Hurst, Nucleonics 12, No. 8, 36-38 (1954).

[49]T. D. Strickler, H. E. Gilbert, and J. A. Auxier, Nuc. Sci. and Eng. 3, 11-18 (1957).

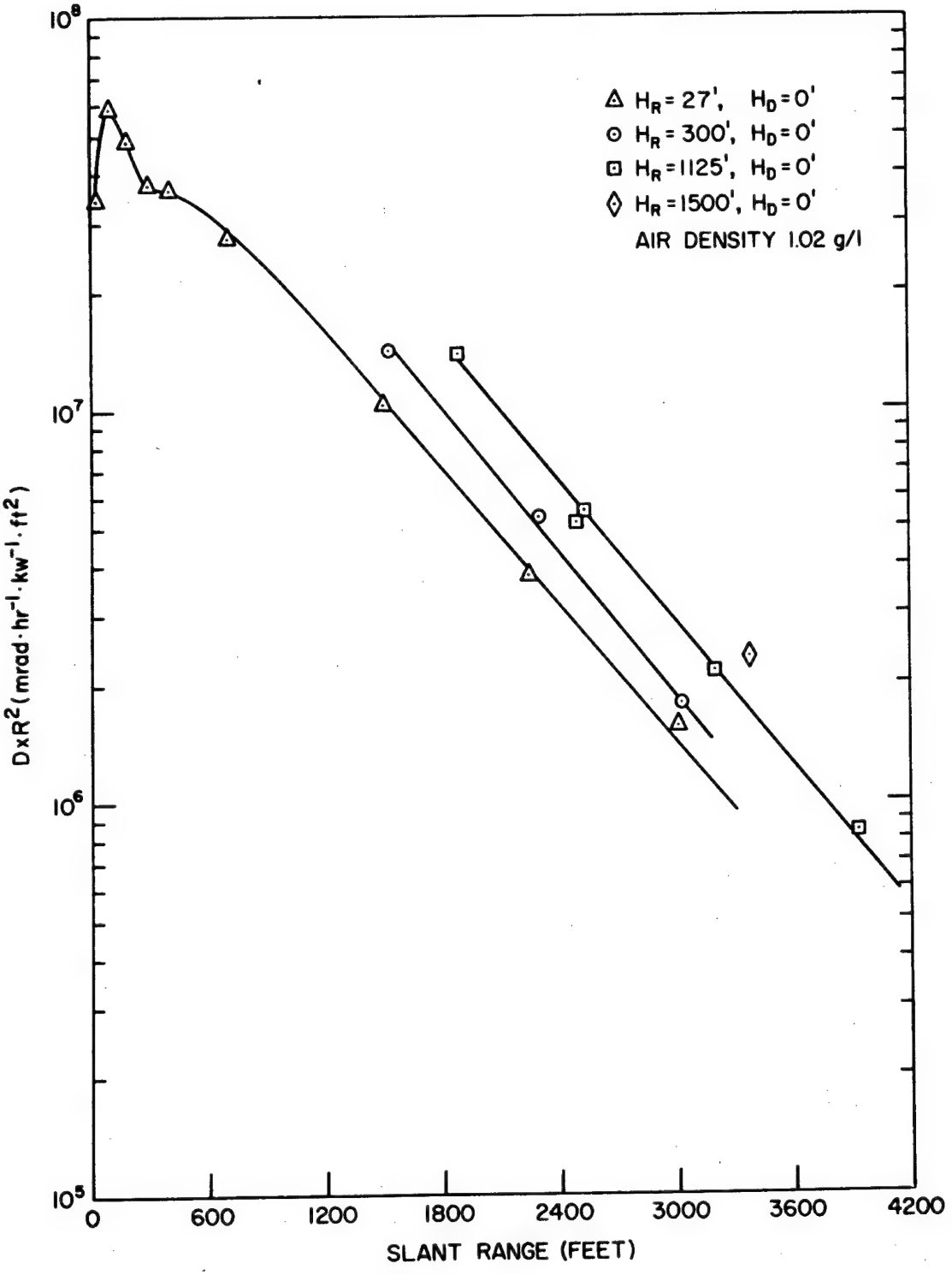

Fig. 17. Neutron D x R^2 as a Function of Slant Range (R) for a Detector Height of 0 Feet and Reactor Heights of 27, 300, and 1125 Feet

of radiation from the ground, a percentage of that striking the ground enters the ground and is absorbed. It follows then that as the source is raised above the ground, there should be a general increase in dose delivered to the point of interest, and at some height, the increase will show an asymptotic approach to a limiting value. Such behavior is shown in Figure 18, where the ordinate represents neutron dose rate (arbitrary units) for distance (X) of 1000 yards, which has been corrected for inverse square attenuation, and which has been corrected for attenuation caused by the mass of air between source and point of interest (these corrections are necessary due to different source-detector separations). The height of the source above the air-ground interface is given along the abscissa. Two sets of computed data[9,16] are given in this figure along with two sets of experimentsl data. Of the latter two cases, the values collected during this project are represented by ⊖. The two points represented by Δ are for values collected at the Nevada Test Site during one of the weapons test operations.[27] The data from weapons tests and the two sets of computed data are normalized to the data of this project at the greatest source height. The comparison between the two experimental cases indicates agreement to approximately one percent. A comparison of the two experimental cases to computed data does not show satisfactory agreement. However, choosing a different normalization point for the data would obviously change the apparent poor agreement seen in Figure 18.

A situation analogous to that just discussed is found in the case where the detector height is varied. According to French,[16] scattered radiation in the vicinity of the detector has a significant bearing on

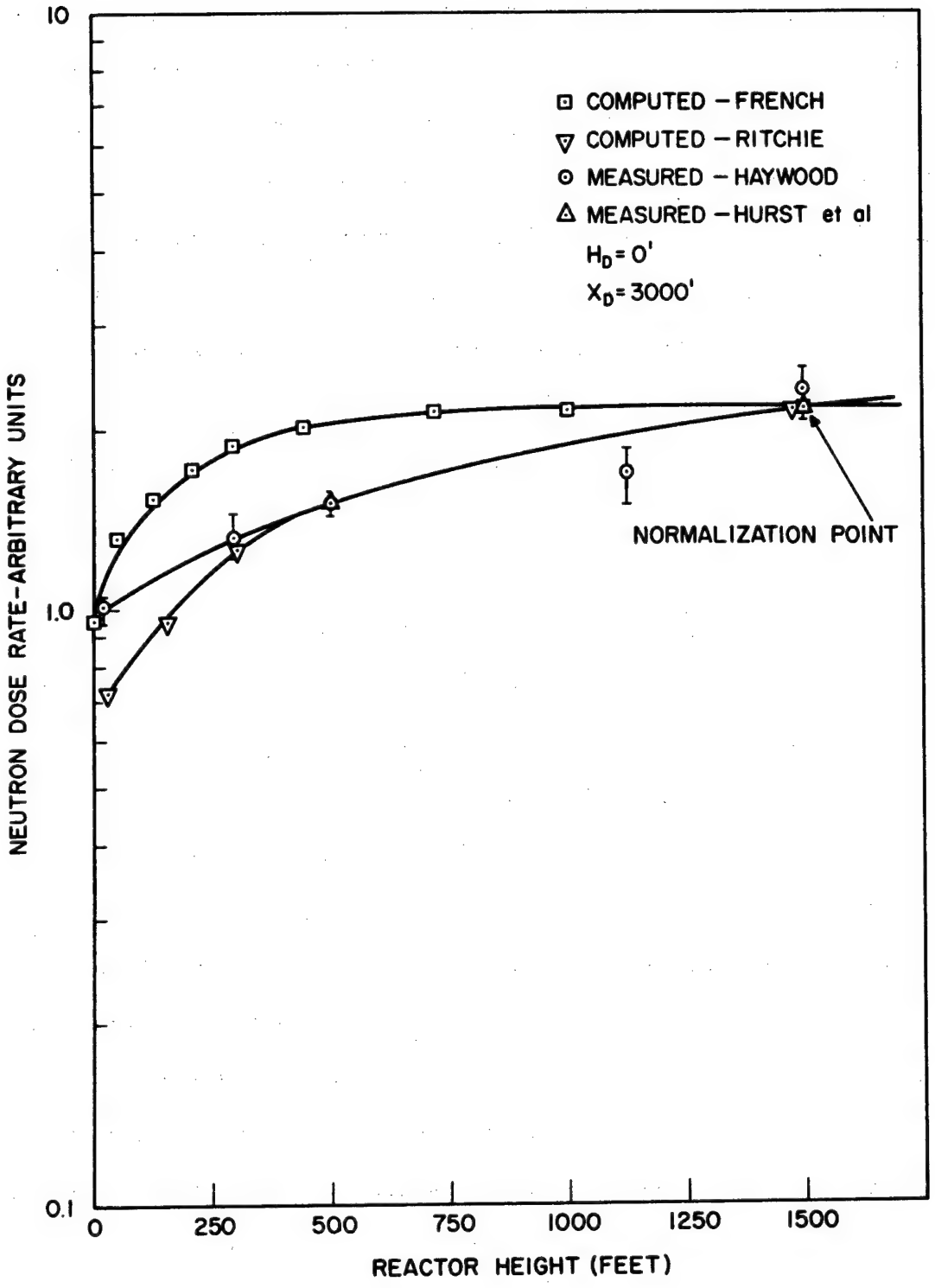

Fig. 18. Comparison of Measured Neutron Dose to Computed Neutron Dose as a Function of Reactor Height (H_R) and for a Detector Height of 0 Feet

the detector's response as it is raised above the interface. In Figure 19, values of neutron dose rate as a function of detector height above the interface are compared to the response predicted by French. Values of neutron dose rate with corrections for inverse square of distance and attenuation due to the air mass between source and detector are given in arbitrary units on the ordinate. These values are plotted as a function of detector height. The results of French's calculation are normalized to the measured value at 100 feet. The point on the interface is the worst case in this comparison, but the agreement here is within 12 percent.

The dependence of the ratio of neutron dose rate to gamma-ray exposure rate on detector height and slant range is presented in Figure 20. The lower curve represents the neutron to gamma ratio of dose for a detector height of 16.5 feet above the interface for source heights of 27, 300, and 1125 feet. The upper curve represents the neutron to gamma ratio for a detector height of 100 feet above the interface and for reactor heights of 300 feet and 1125 feet. For a given detector height, the values on each curve vary little regardless of the reactor height. Measurements of dose for other reactor heights, not given in Figure 20, indicate a similar behavior. Hence, the statement may be made that for a given detector height above the air-ground interface, the ratio of neutron dose rate to gamma-ray exposure rate is independent of the height of the reactor, whether the reactor is positioned between the limits of infinite air medium or finite air medium, or positioned at either of these limits.

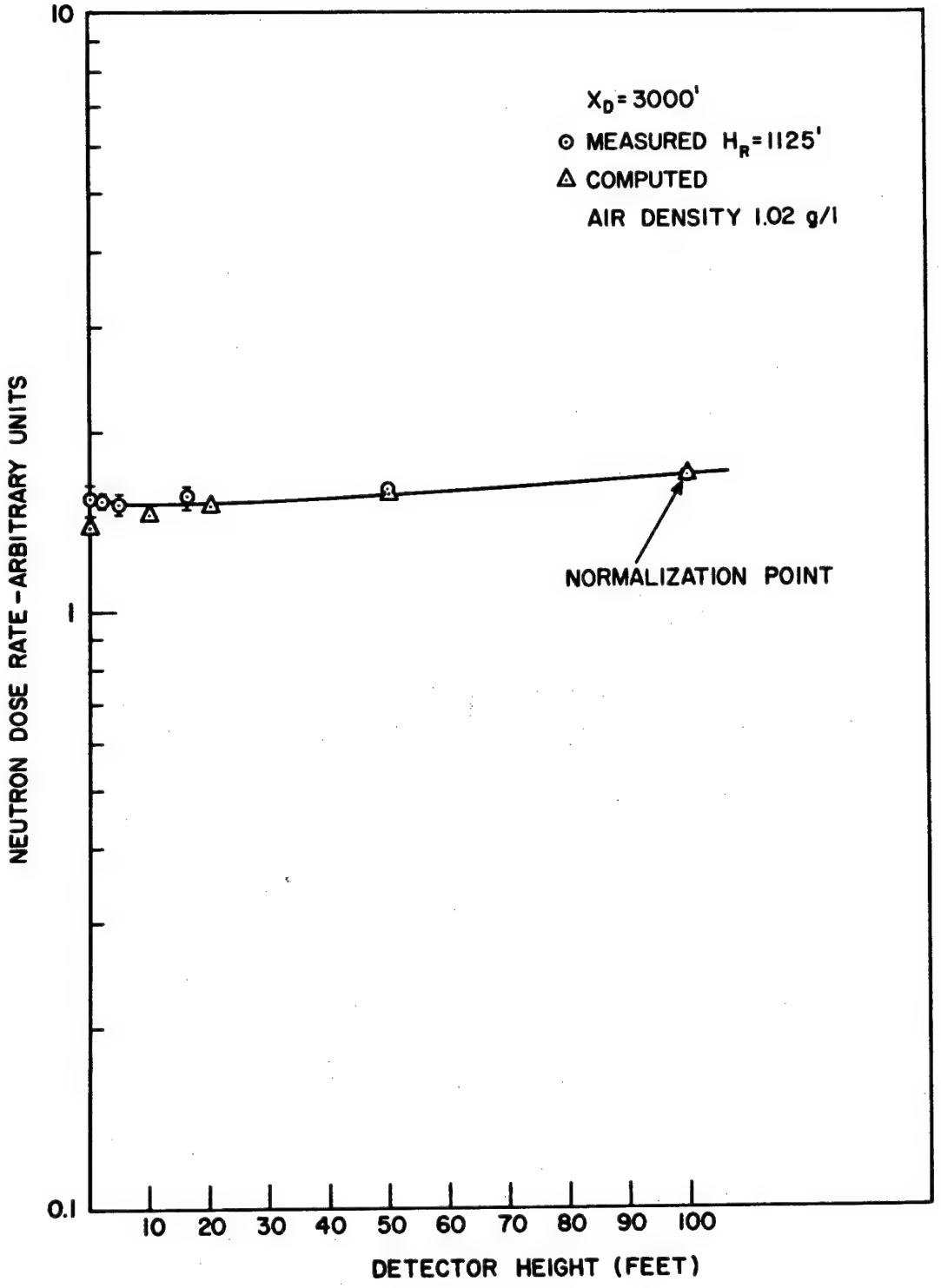

Fig. 19. Comparison of Measured Neutron Dose to Computed Neutron Dose as a Function of Detector Height (H_D) for a Reactor Height of 1125 Feet

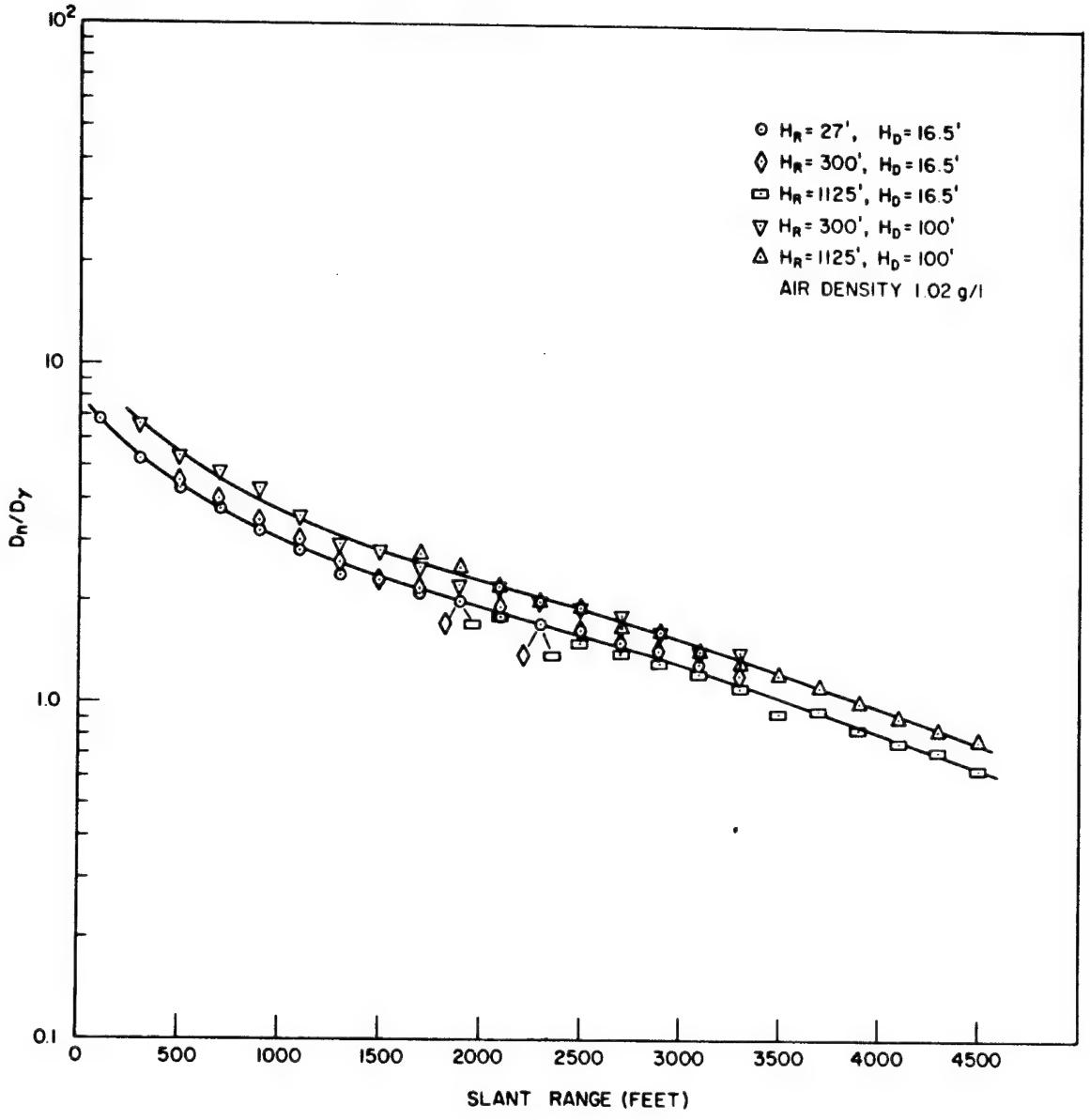

Fig. 20. Ratio, Neutron Dose to Gamma-Ray Exposure as a Function of Slant Range (R)

Gamma-Ray Data From HPRR Operation

The data presented in this and the following section are treated similarly to the neutron data in the preceding section. In Figure 21, gamma-ray exposure rate times slant range squared is plotted as a function of slant range for a reactor height of 27 feet and for the detector positioned both on the interface and at 16.5 feet above the interface. At slant ranges to approximately 250 feet, the values for the detector lying on the interface are significantly higher (25 percent) than for the case where the detector is positioned at 16.5 feet; but at slant ranges greater than 750 feet, the difference in exposure rate is only 7 to 12 percent.

Similar values of exposure rate are plotted in Figure 22, but for a reactor height of 300 feet and detector heights of 16.5 feet and 100 feet. When these two curves are compared to neutron data at the same reactor-detector geometry (Figure 16), a similarity is seen in shape, but there is no place in Figure 22 where the exposure rate, for a detector height of 100 feet, is greater than it is in the case for a detector positioned at 16.5 feet. Although measurements of thermal neutron dose were not made during this study, the population of thermal neutrons, for a given slant range, probably increases as the detector approaches the interface. This would create more gamma rays through inelastic collision of neutrons in the air and the ground, hence apparently accounting for the behavior of the two curves in Figure 22.

For a detector lying on the interface and for reactor heights of 27, 300, and 1125 feet, gamma-ray exposure rate times slant range squared as a function of slant range is presented in Figure 23.

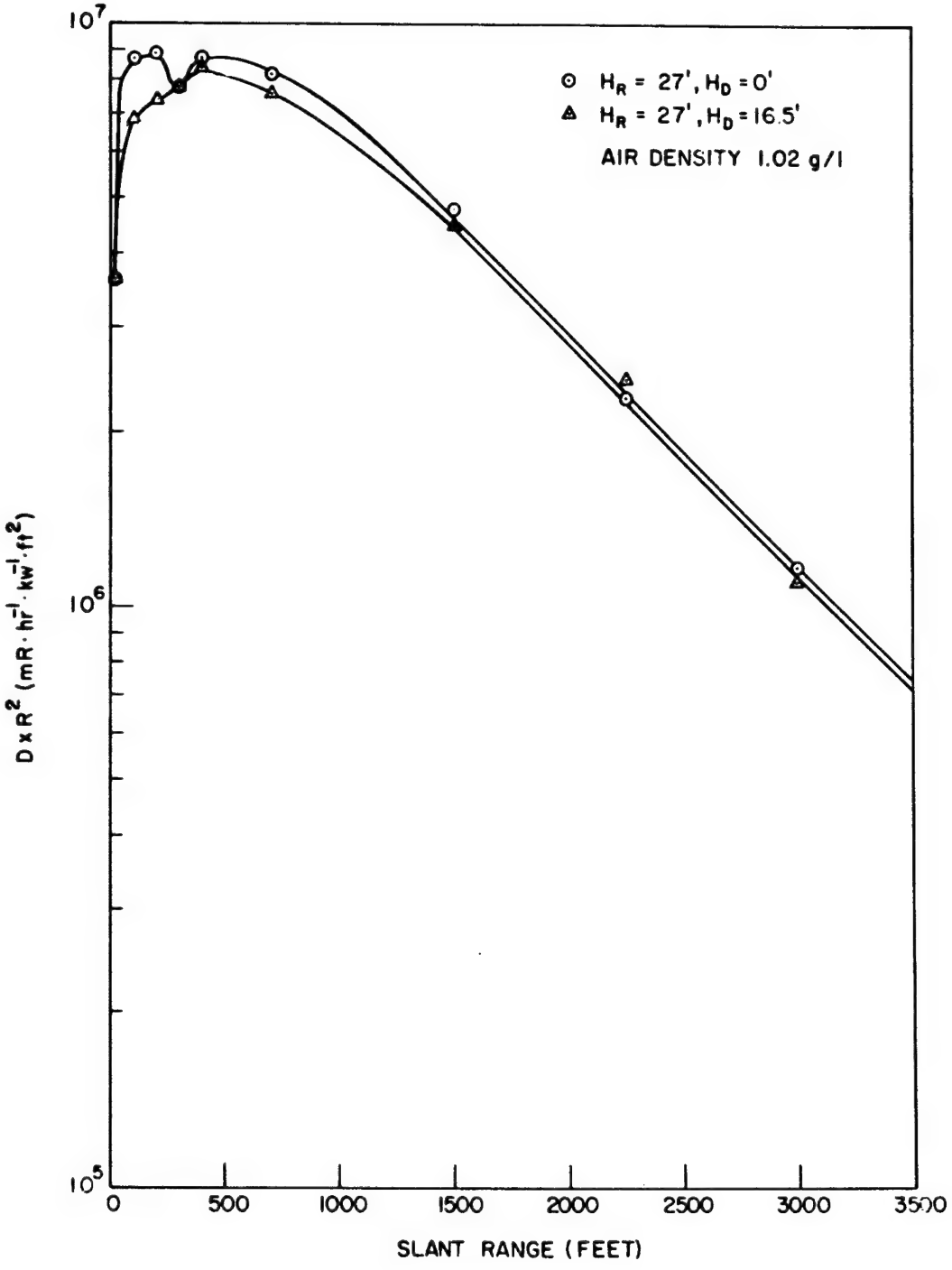

Fig. 21. Gamma-Ray D x R^2 as a Function of Slant Range (R) for a Reactor Height of 27 Feet and for Detector Heights of 0 Feet and 16.5 Feet

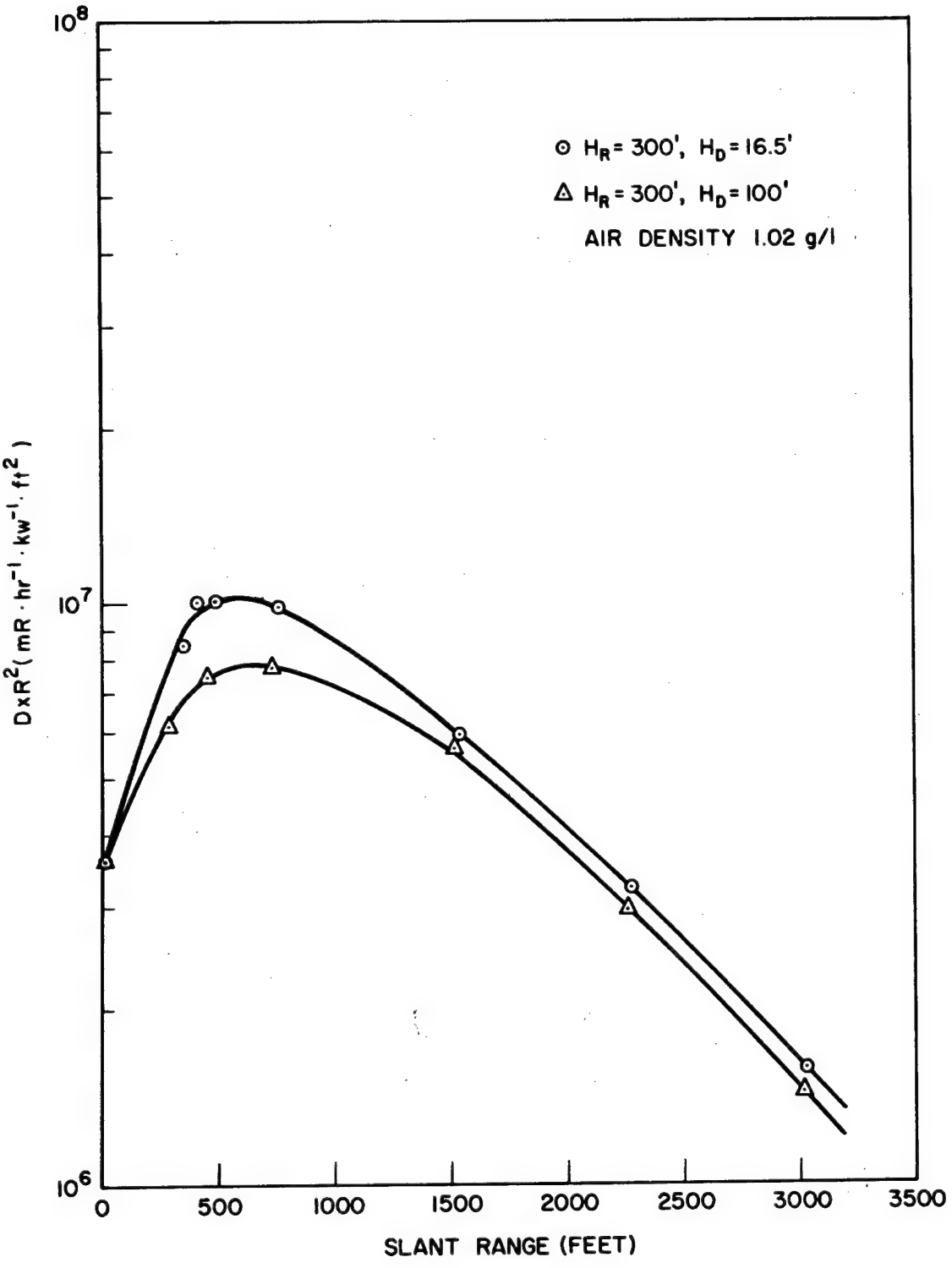

Fig. 22. Gamma-Ray D x R^2 as a Function of Slant Range (R) for a Reactor Height of 300 Feet and for Detector Heights of 16.5 Feet and 100 Feet

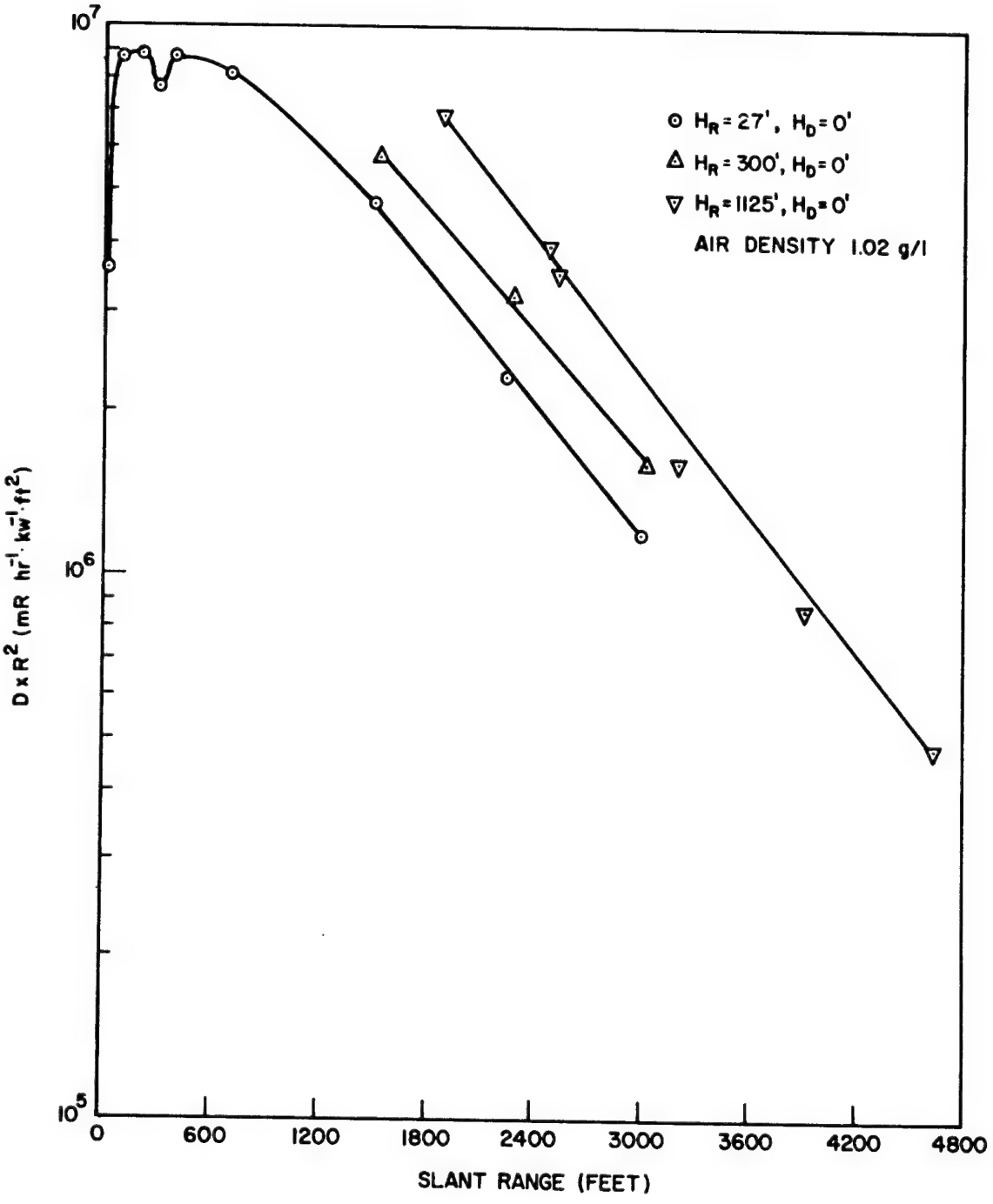

Fig. 23. Gamma-Ray D x R^2 as a Function of Slant Range (R) for a Detector Height of 0 Feet and for Reactor Heights of 27, 300, and 1125 Feet

When reduced to 1.293 g/l, the average relaxation length is 271 yards. An albedo peak was observed for gamma rays, in the curve for a reactor height of 27 feet, at a slant range of approximately 100 feet. It is seen that for R > 500 yards, the increase in exposure rate at the interface is 1.9 as the reactor is raised from 27 feet to 1125 feet. This statement is further supported by the information presented in Figure 24 where the increase in exposure rate is seen to be approximately 1.9 as the reactor is raised from 27 feet to 1125 feet. The data presented in Figure 24 cannot be validated by a comparison to computed data at this time; however, two points are given which were measured during the series of weapons tests in 1957.[27]

For a fixed reactor height, the gamma-ray exposure rate as a function of detector height above the interface is given in Figure 25. The exposure rate is seen to decrease by 15 percent at 100 feet above the interface as compared to the exposure rate at the ground. This decrease could be explained by a decrease in the number of inelastic collisions of thermal neutrons in air, assuming that the thermal neutron population increases near the interface.

Gamma-Ray Data for Co^{60}

The data given in this section were collected during the use of a Co^{60} source whose effective activity was 800 curies. After operations with the HPRR had terminated, the Co^{60} source facility (see Figure 3) was placed in the same hoisting mechanism and was supported at the same heights above the interface as the reactor. In this section, emphasis will be placed on comparisons between the measured boundary correction factors K(exp) and boundary correction factors K which were computed by

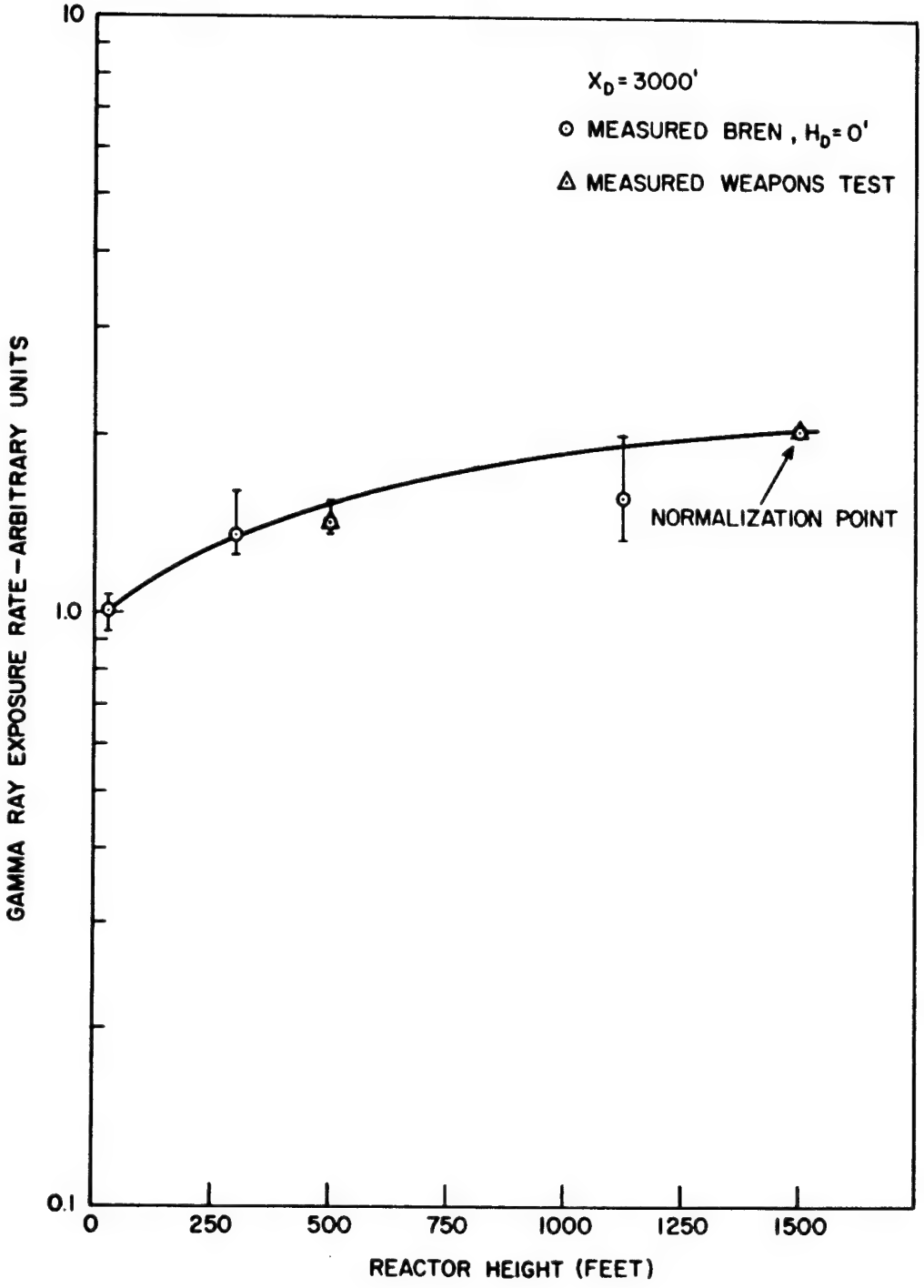

Fig. 24. Gamma-Ray Exposure Rate as a Function of Reactor Height for a Detector Height of 0 Feet

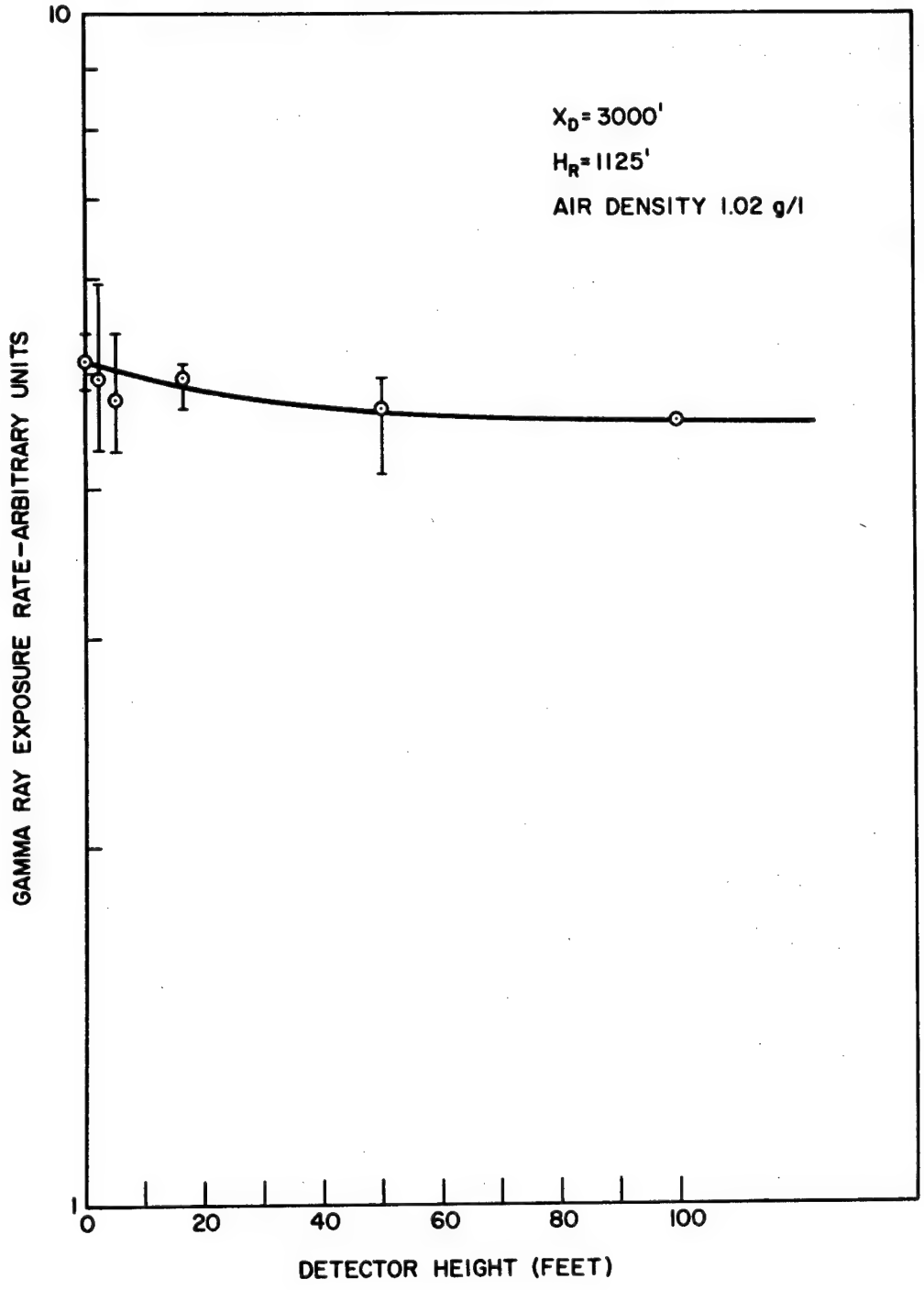

Fig. 25. Gamma-Ray Exposure Rate as a Function of Detector Height for a Reactor Height of 1125 Feet

M. J. Berger.[7] However, experimental results will also be presented in a manner similar to that of the two preceding sections.

Gamma-ray exposure rates from Co^{60} as a function of slant range are presented in Figure 26 for three source heights with detectors lying on the interface. The average relaxation length for an air density of 1.293 g/l is 193 yards. A similar plot is given in Figure 27 for a source height of 300 feet and detectors placed at 0 and 100 feet above the interface. It is seen in this figure that the values of exposure rate for the detector lying on the interface is lower than that at 100 feet for R > 500 feet.

Values of exposure rate (arbitrary units) as a function of source height, for a slant range of 750 to 900 yards, are given in Figure 28. At a source height of 1500 feet, the exposure rate is approaching its limiting value and is approximately a factor of 2.0 greater than the value for a source height of 27 feet. Berger's computed values are normalized to the experimental data at a source height of 283 feet which for an air density of 1.01 g/l corresponds to one-half mean free path. The other point from Berger's data is for the source at the interface. By extrapolating the experimental curve to a source height $H_s = 0$, one sees that this intercept is in good agreement with the computed point.

Values of exposure rate as a function of detector height are given in Figure 29 for a source height of 300 feet. There is an initial decrease in exposure rate at approximately 5 feet above the interface and an increase of 19 percent from that point to 100 feet above the interface.

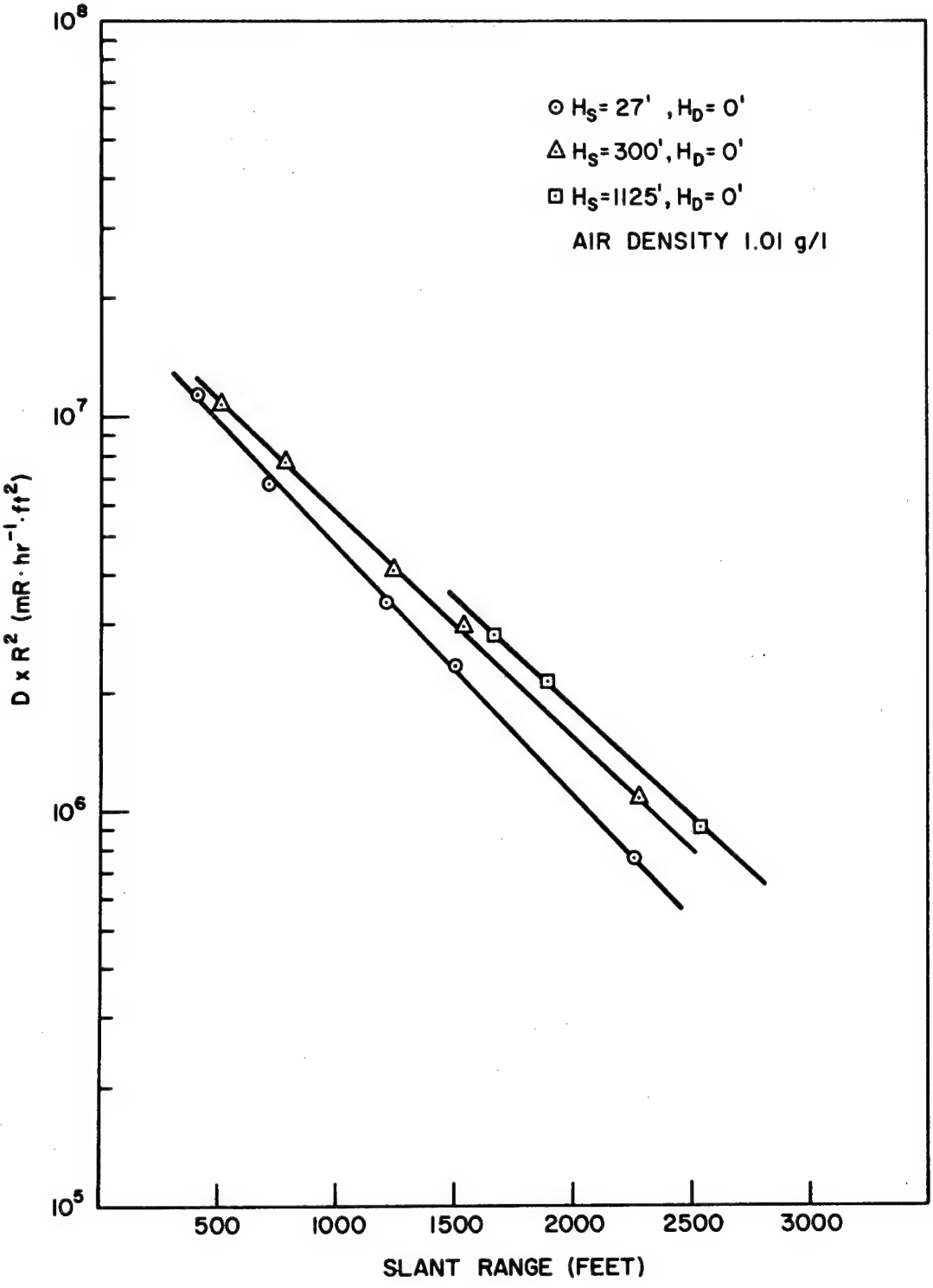

Fig. 26. Gamma-Ray D x R^2 as a Function of Slant Range (R) for a Detector Height of 0 Feet and Co^{60} Source Heights of 27, 300, and 1125 Feet

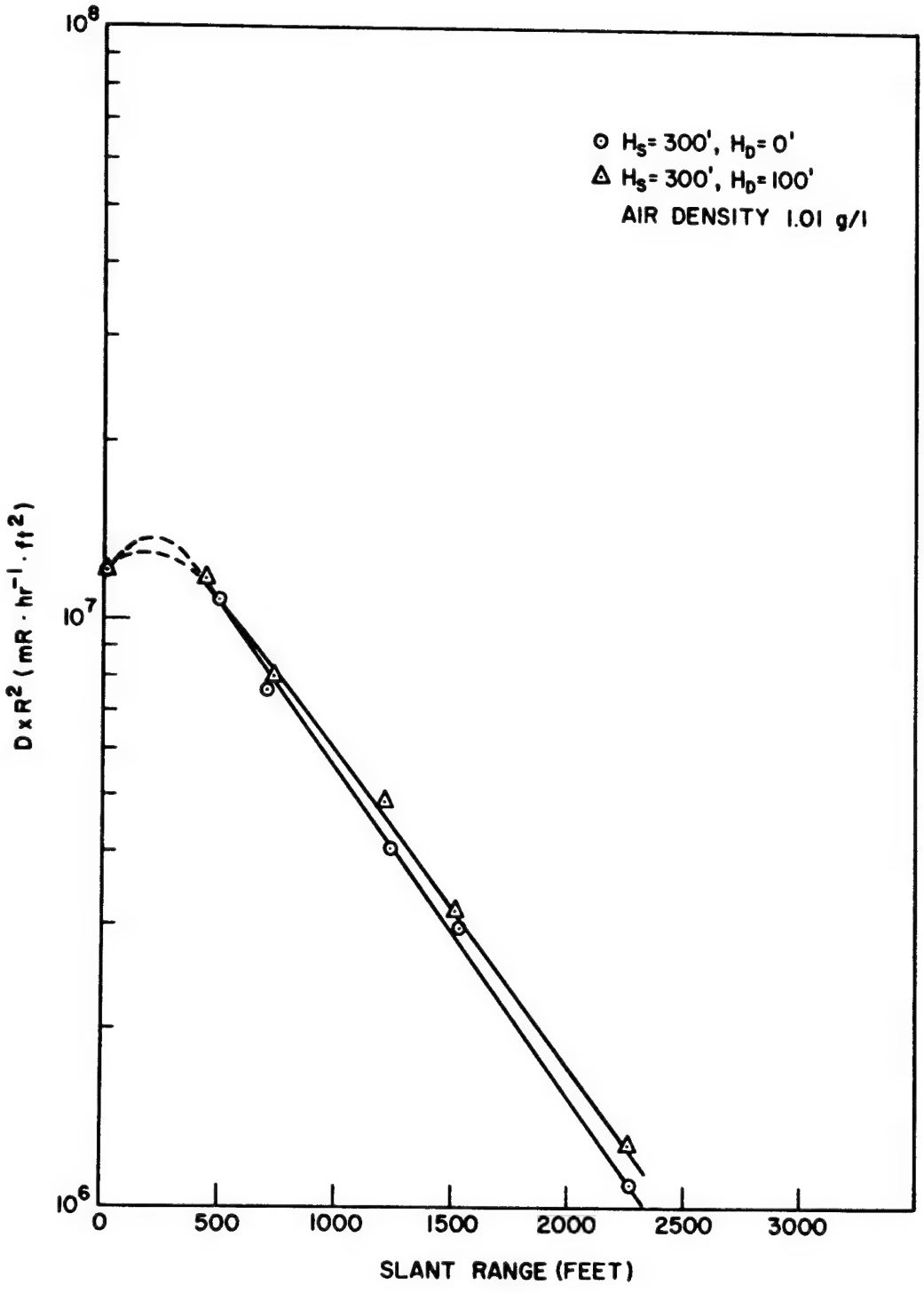

Fig. 27. Gamma-Ray D x R^2 as a Function of Slant Range (R) for a Co^{60} Source Height of 300 Feet and Detector Heights of 0 Feet and 100 Feet

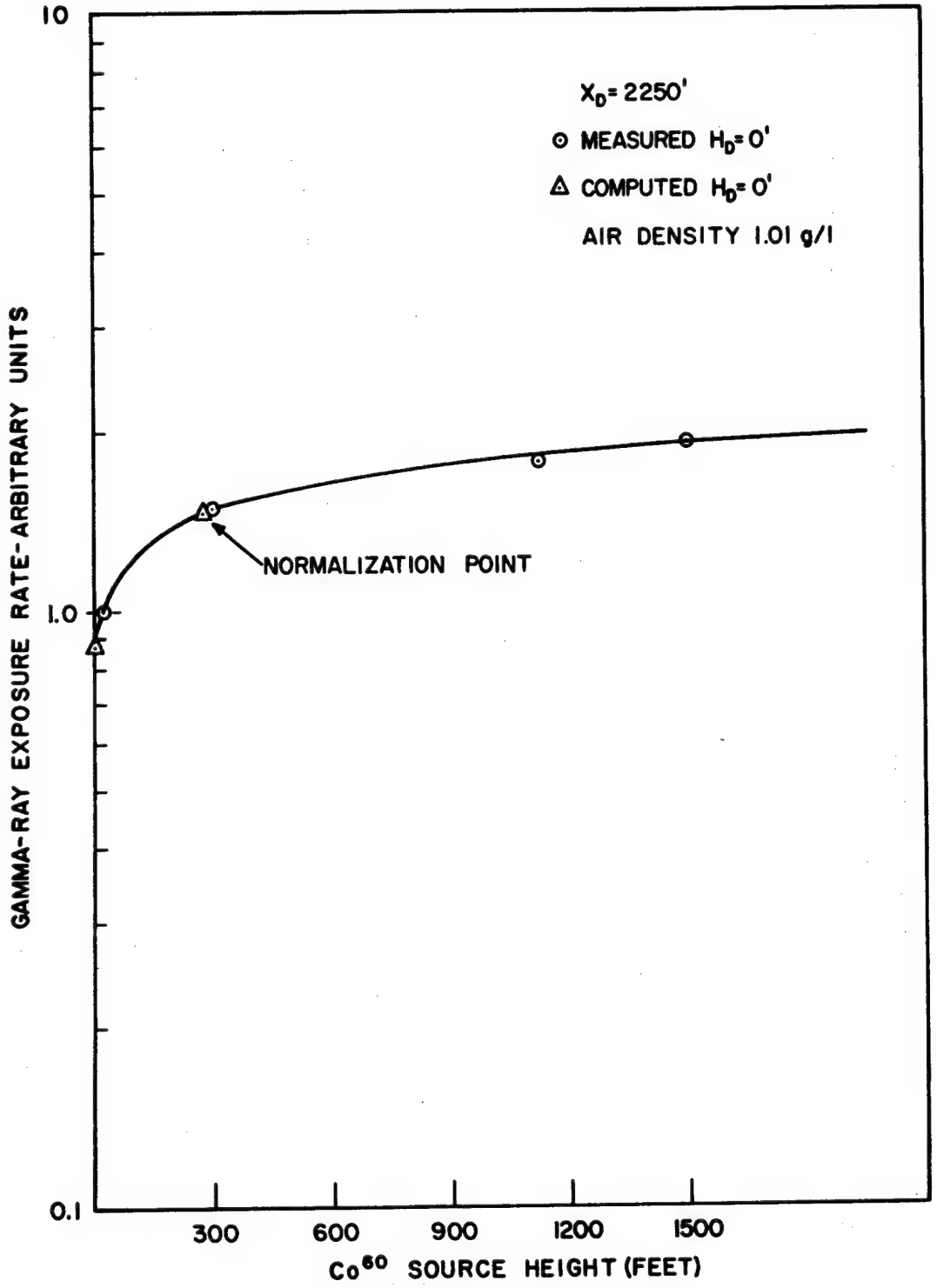

Fig. 28. Comparison of Measured Gamma-Ray Exposure to Computed Gamma-Ray Exposure as a Function of Co^{60} Source Height for a Detector Height of 0 Feet

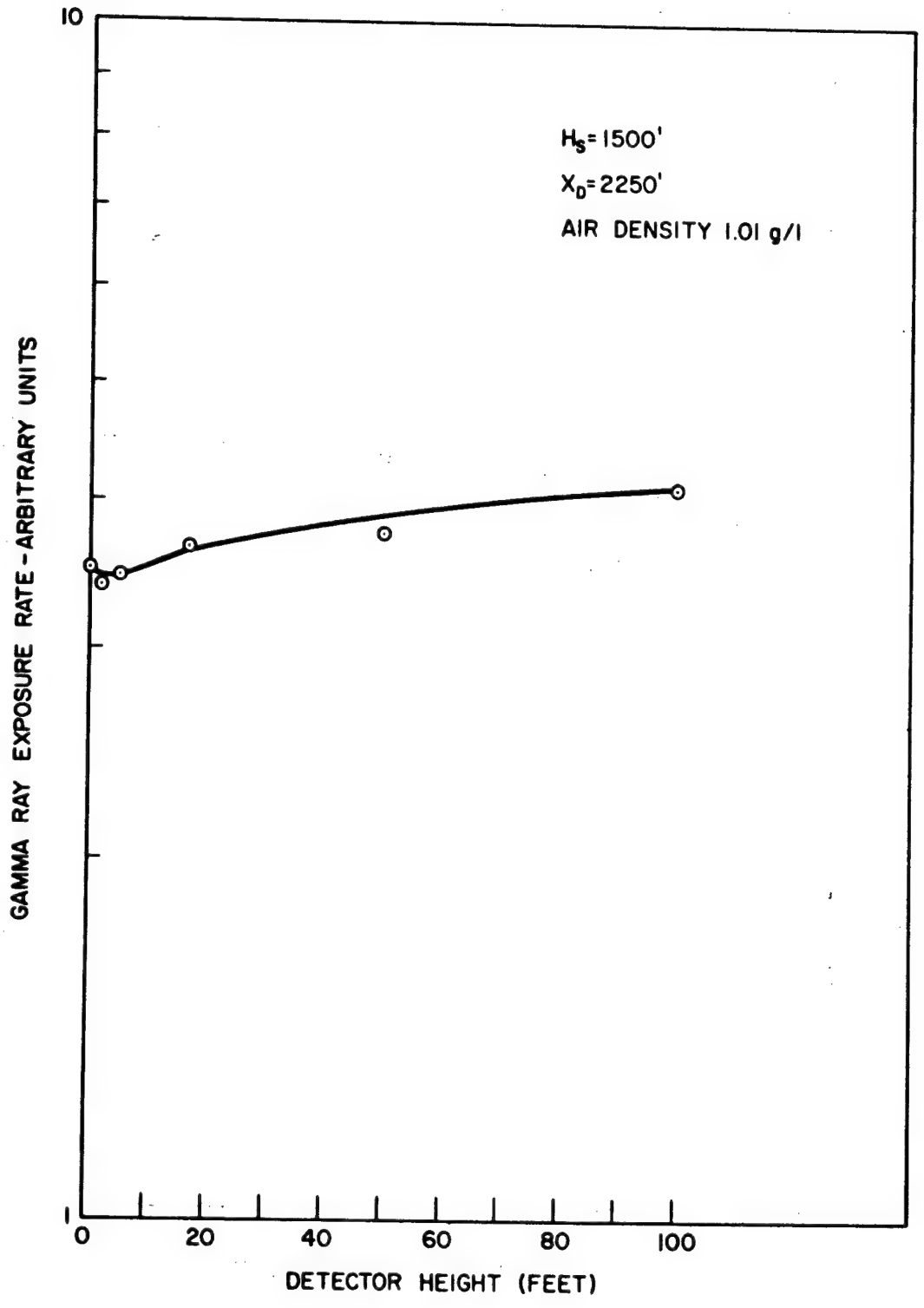

Fig. 29. Gamma-Ray Exposure Rate as a Function of Detector Height for a Co^{60} Source Height of 1500 Feet

For purposes of this section, a gamma-ray exposure buildup factor, for a given slant range, is defined as the ratio of the total exposure rate to the exposure rate due to primary beam radiation alone. In Figure 30, computed values[50] and measured values of the exposure buildup factor are presented as a function of mean free path. This figure lends support to the generalized statement that the presence of the air-ground interface enhances the exposure rate near the source and decreases the exposure rate elsewhere. It is seen here that for a given slant range the experimental values increase in magnitude as the source height increases, and the experimental curve for each source height intercepts the computed curve at a different point. Hence, the slant range at which K(exp) = 1 varies directly as the height of the source above the interface.

In order to compare experimental values of boundary correction factors K(exp) to computed values (K), it was necessary to calculate the infinite air medium exposure rate as a function of slant range for ρ = 1.01 g/l. Gamma-ray exposure was calculated according to the formula:

$$(D \cdot R^2) = SBD_1 R^2 e^{-\mu R} \qquad (20)$$

where

S = source activity in curies.

B = exposure buildup factor.

D_1 = exposure rate per curie at one foot.

---

[50] H. Goldstein and J. E. Wilkins, Jr., U. S. Atomic Energy Commission Report NYO-3075 (1954).

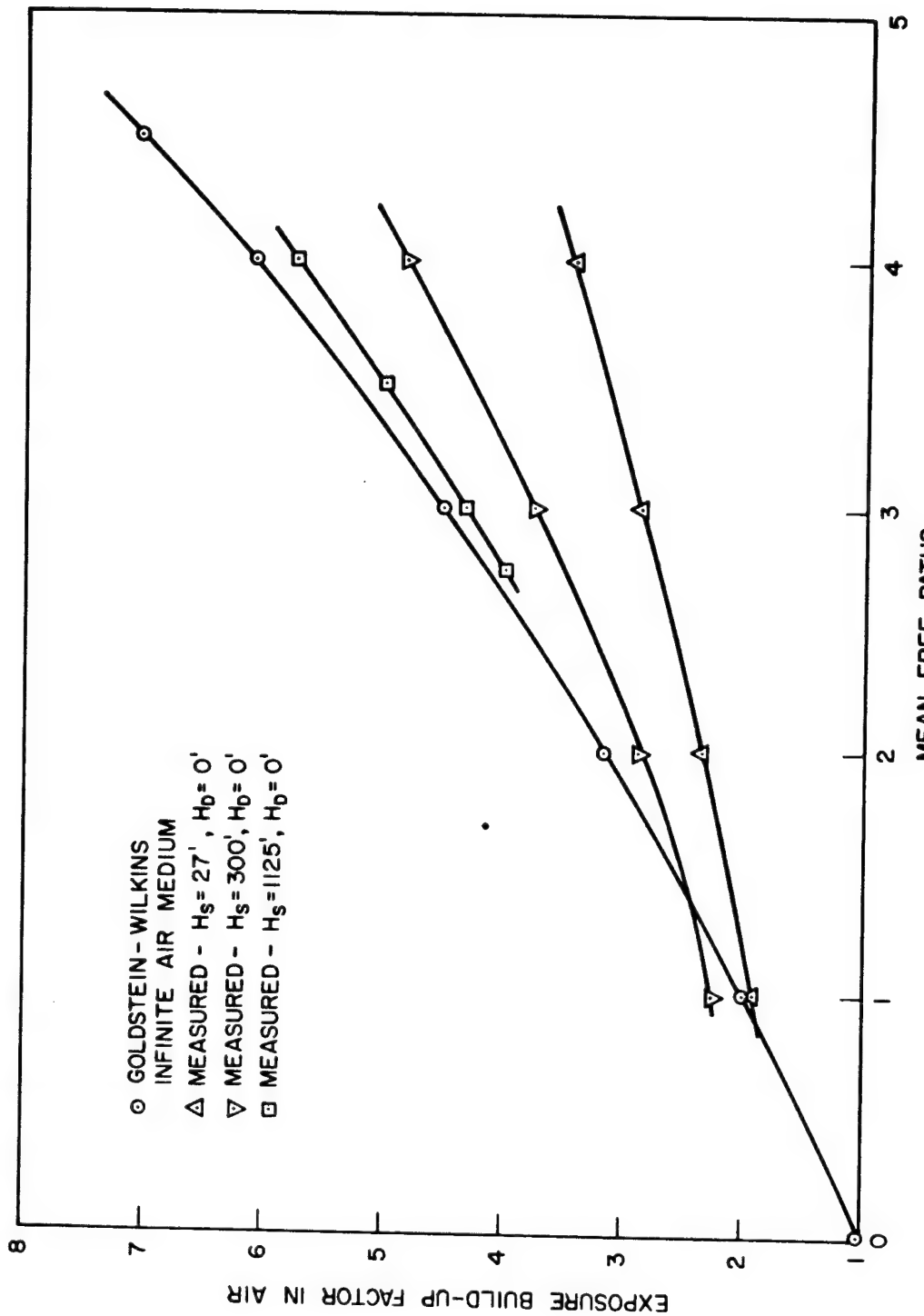

Fig. 30. Exposure Buildup Factor for a Detector Height of 0 Feet as a Function of Mean Free Paths of Air and Height of Co^{60} Source, Compared to Computed Exposure Buildup Factor in an Infinite Air Medium

R = slant range in feet.

μ = total coefficient of absorption.

Values of $D \cdot R^2$ as a function of slant range (R) are presented in Figure 31. The experimental boundary correction factor, K(exp), is the ratio of the exposure rate in the air-over-ground geometry to the exposure rate in the infinite air medium at the same slant range. Values of K(exp) and K are plotted as a function of slant range for several source-detector geometries in Figures 32 through 34. In Figure 32, the curve for K(exp) is seen to be similar in shape to that for K, but the values for K(exp) are approximately 15 to 20 percent greater than K. This is to be expected, considering the data in Figure 28. In Figure 32, K(exp) is for a source height of 27 feet above the interface, and values of K are for the source positioned on the interface. It was shown in Figure 28 that the computed values of exposure rate as a function of slant range (R) for a source on the interface are approximately 15 percent lower than the measured exposure rates as a function of slant range (R) with the source supported 27 feet above the interface. In Figure 33, values of K(exp) for a source height of 300 feet and detector on the interface, and values of K for a source height of 283 feet (0.5 mfp) and detector on the interface, are given as a function of slant range. In Figure 34, the source-detector geometry was altered by placing the detector 100 feet above the interface. The agreement between the curves in these two figures indicates that Monte Carlo techniques may be used in computing the exposure rates from a point Co^{60} source at large slant ranges (greater than one relaxation length), in an air-over-ground geometry.

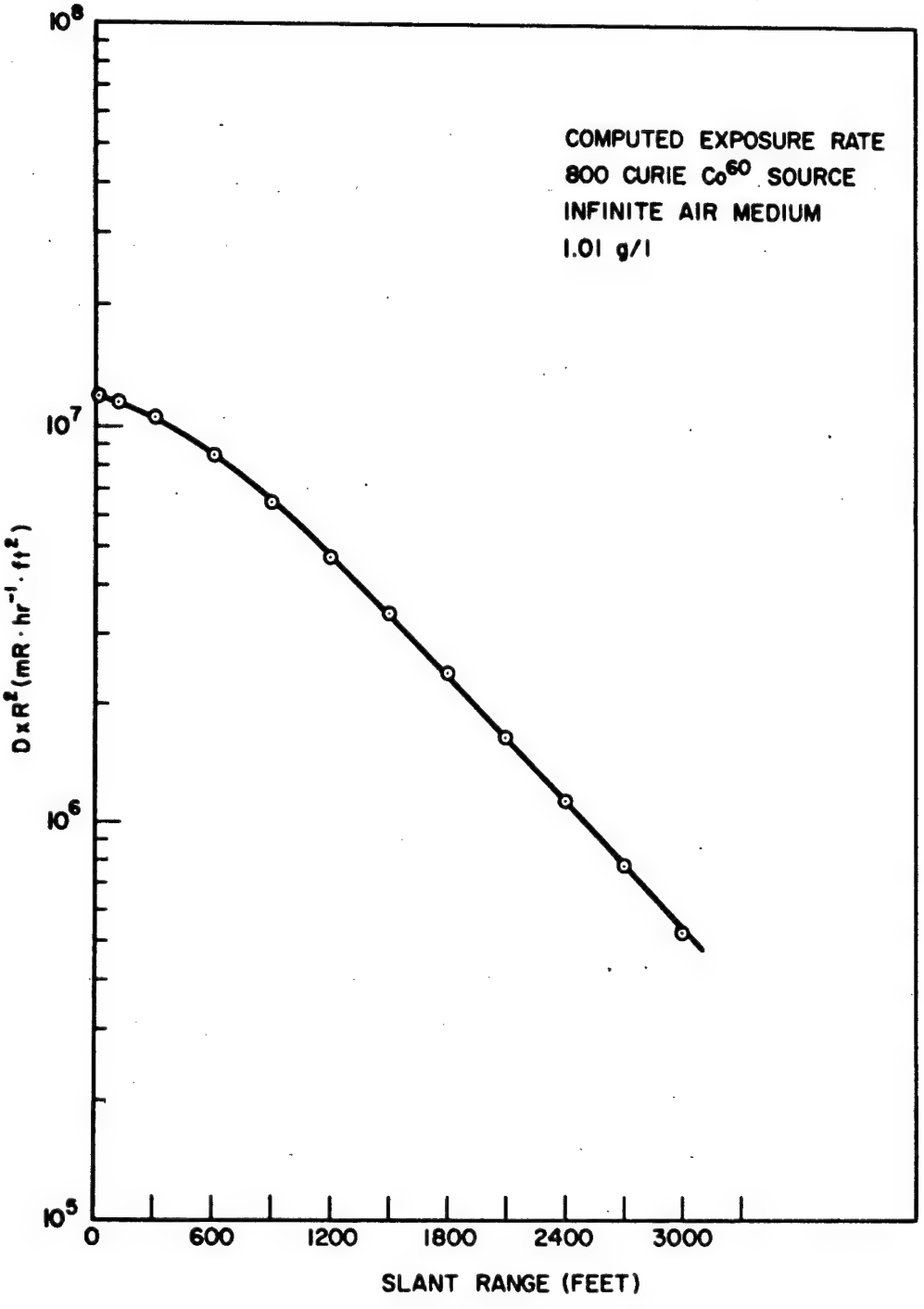

Fig. 31. Computed Co^{60} D x R^2 as a Function of Slant Range (R) in an Infinite Air Medium

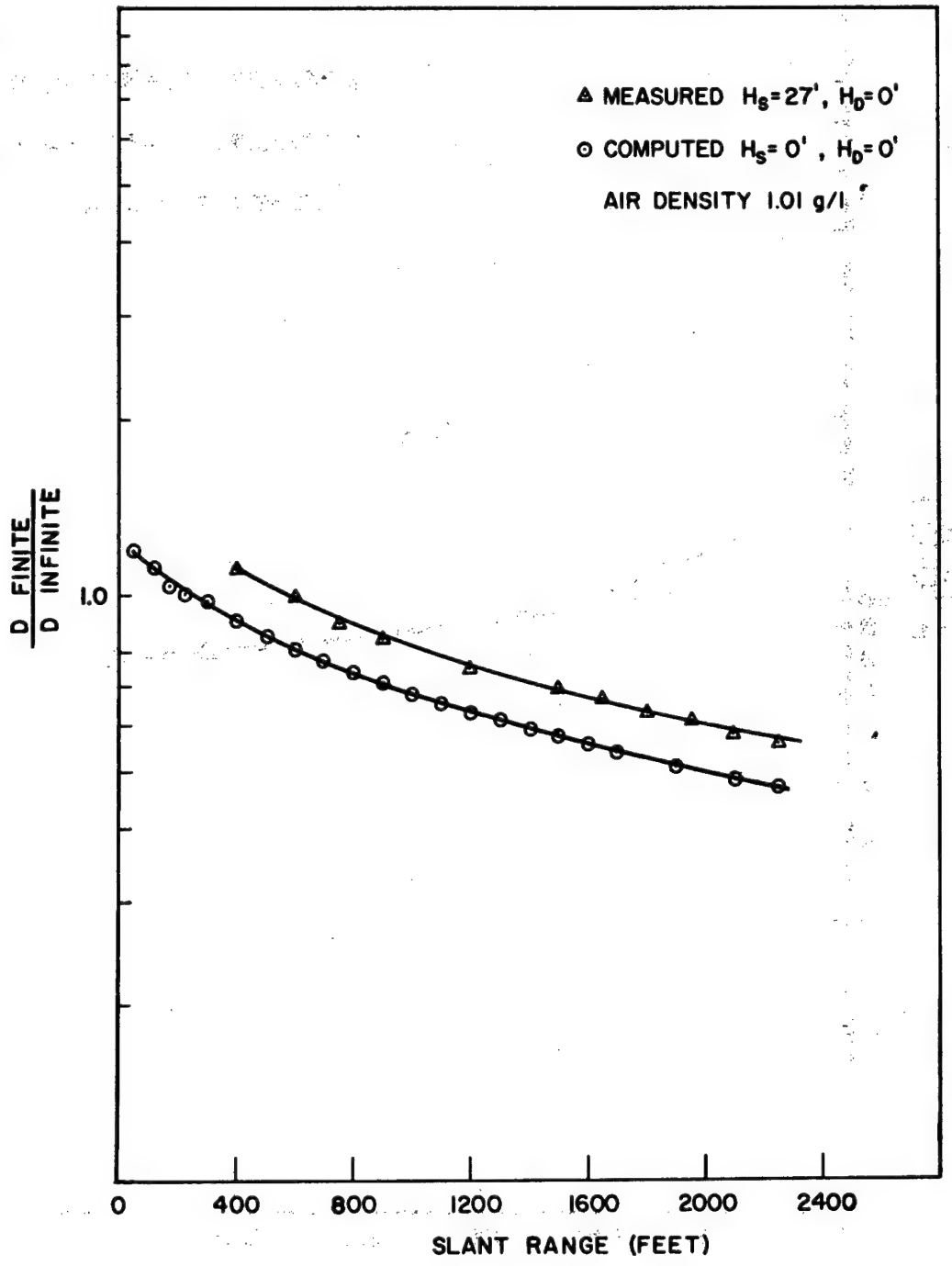

Fig. 32. Comparison of K(exp) for a Co^{60} Source Height of 27 Feet and Detector Height of 0 Feet, to K for a Co^{60} Source Height of 0 Feet and Detector Height of 0 Feet, as a Function of Slant Range (R)

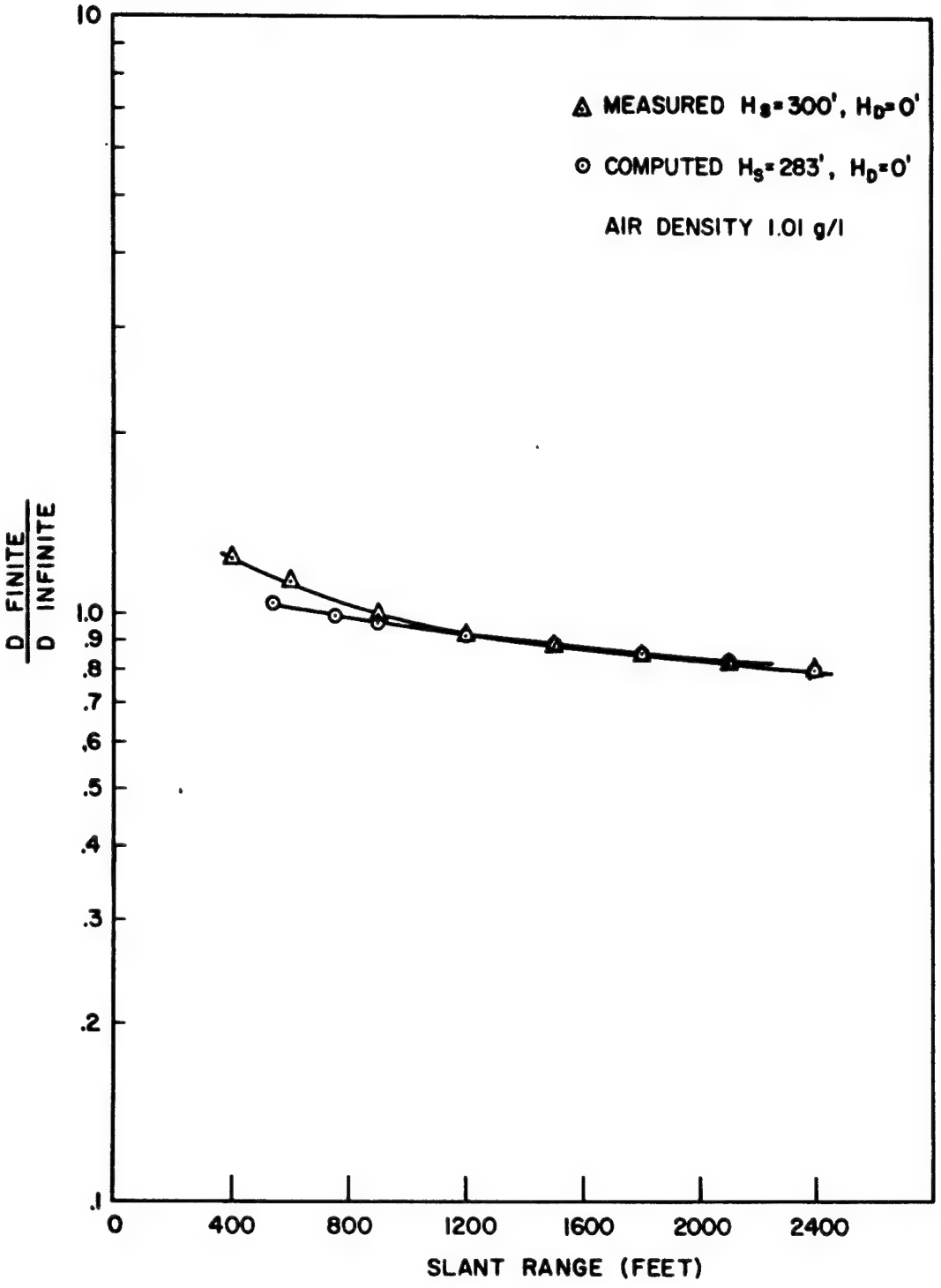

Fig. 33. Comparison of K(exp) for a Co^{60} Source Height of 300 Feet and Detector Height of 0 Feet, to K for a Co^{60} Source Height of 283 Feet and Detector Height of 0 Feet, as a Function of Slant Range (R)

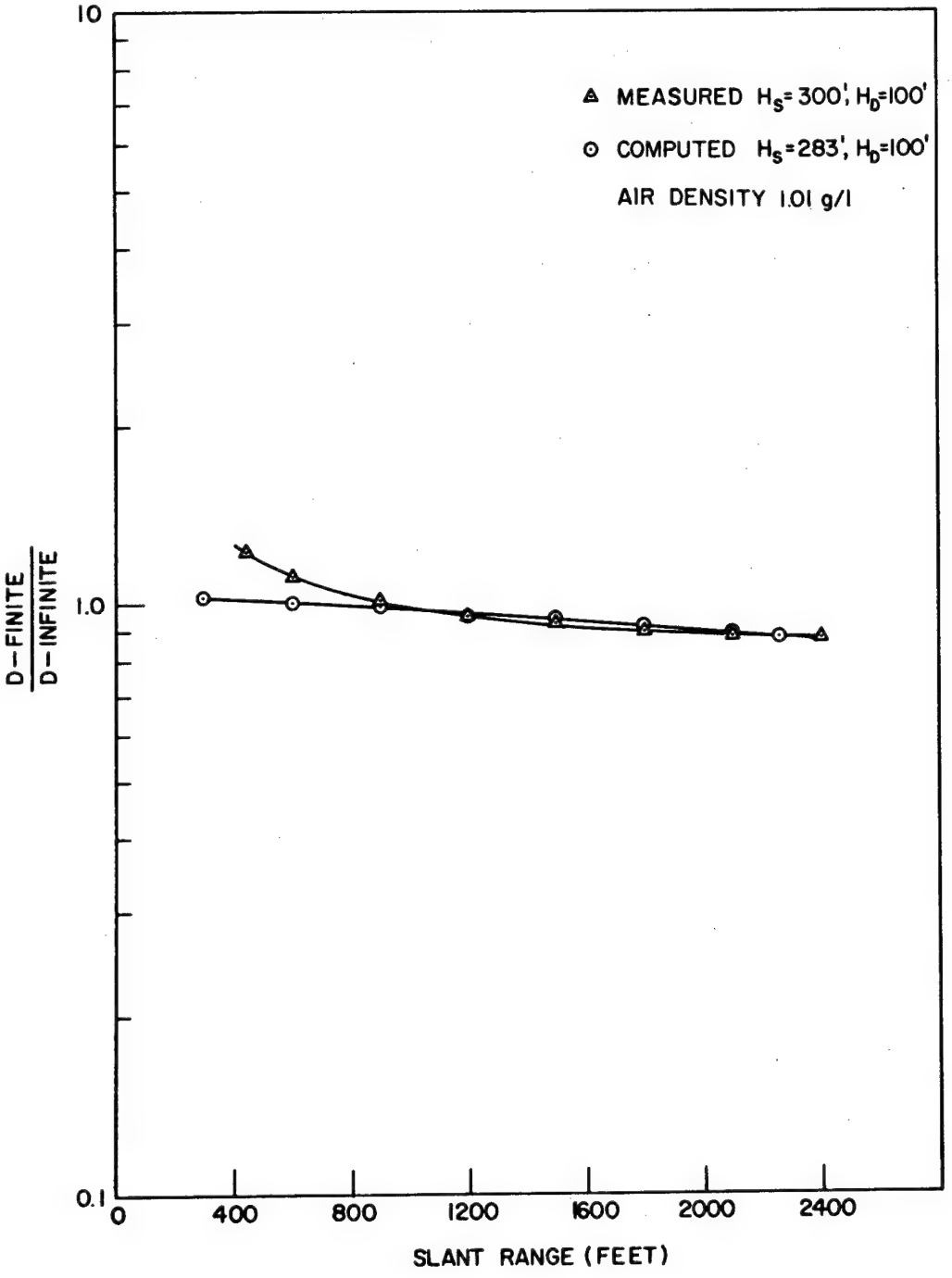

Fig. 34. Comparison of K(exp) for a Co^{60} Source Height of 300 Feet and Detector Height of 100 Feet, to K for a Co^{60} Source Height of 283 Feet and Detector Height of 110 Feet, as a Function of Slant Range (R)

VII. CONCLUSIONS

The experimental study described here was conducted in an effort to expand the present knowledge of the effect of the presence of the air-ground interface on the measurement of neutron first collision tissue dose and gamma-ray exposure in air above the earth's surface. Measurements of neutron dose were made in radiation fields from the Health Physics Research Reactor operating at steady-state power and supported at several heights above the earth's surface. Measurements of gamma-ray exposure were made in radiation fields from the HPRR and from a Co^{60} source supported in a similar geometry.

To substantiate the experimental data, comparisons were made to data which were collected during nuclear weapons tests. Values of relaxation length for neutron dose and gamma-ray exposure were compared in both cases with satisfactory agreement.

Several comparisons of experimental data have been made with computed data. Ritchie has computed boundary correction factors K, for neutrons, for a series of source-detector geometries. In comparing experimentally determined boundary correction factors K(exp), for neutrons, with computed values K, ±10 percent agreement was obtained from a slant range of 100 meters to a slant range of 1000 meters. Ritchie[9] and French[16] have computed the decrease in the infinite medium neutron dose, at large slant ranges, caused by the presence of the air-ground interface. A comparison was made between these values and experimental data (Figure 18), but it was not found to be acceptable. It is recommended that a careful study of this comparison be made when more experimental and theoretical data are available. Experimental values of dose as a function of detector height were compared to French's

computed values (Figure 19) indicating ±2 percent agreement from 10 feet to 100 feet above the interface and ±6 percent at the interface. Berger has computed boundary correction factors K for Co^{60} gamma rays. Experimental determination of K(exp) for Co^{60} are compared to values of K in Figures 32 through 34. In this case, the comparison indicates that Monte Carlo techniques may be used successfully to predict the effect of the presence of the air-ground interface on calculations of exposure at large distances (R > 600 feet) from a point isotropic gamma-ray source, to within ±2 percent.

It was found that for most points in the finite medium, the ratio, neutron dose to gamma-ray exposure is independent of the height of the fission source above the air-ground interface.

It was experimentally determined that, in general, the presence of the air-ground interface enhances the measured radiation at slant ranges close to the source and decreases the measured radiation at large slant ranges. That is to say, for a given source height near the ground, and for a fixed detector height, K(exp) has a value of one for some unique slant range. However, as the height of the source increases, the slant range at which K(exp) = 1 also increases.

BIBLIOGRAPHY

Auxier, J. A., Cheka, J. S., and Sanders, F. W., "Attenuation of Weapons Radiation: Application to Japanese Houses," U. S. Atomic Energy Commission Report WT-1725 (Classified) (1961).

Auxier, J. A., Haywood, F. F., and Gilley, L. W., "General Correlative Studies - Operation BREN," U. S. Atomic Energy Commission Report CEX-62.03 (1963).

Beers, Y., Introduction to the Theory of Error (Addison-Wesley Publishing Co., Inc., Reading, Massachusetts, 1957) p. 48.

Berger, M. J., "Calculation of Energy Dissipation by Gamma Radiation Near the Interface Between Two Media," J. of Appl. Phys. 28, 1502-1508 (1957).

Biggers, W. A., Brown, L. J., Kohr, K. C., "Space, Energy, and Time Distribution of Neutrons at the Ground-Air Interface," Los Alamos Scientific Laboratory Report LA-2390 (1960).

Cheka, J. S., Oak Ridge National Laboratory, private communication.

Clifford, C. E., Carruthers, J. A., and Cunningham, J. R., "γ-Radiation at Air-Ground Interfaces with Distributed Cs Sources," Can. J. Phys. 38, 504-506 (1960).

Cure, J. W., and Hurst, G. S., "Fast-Neutron Scattering: A Correction for Dosimetry," Nucleonics 12, No. 8, 36-38 (1954).

Davis, F. J., and Reinhardt, P. W., "Radiation Measurements Over Simulated Plane Sources," Health Phys. 8, 233-243 (1962).

French, R. L., "A First-Last Collision Model of the Air/Ground Interface Effects on Fission Neutron Distributions," Radiation Research Associates, Inc. Report RRA-M32 (1963).

French, R. L., and Garrett, C. W., "The Angular and Energy Distribution of the Photon Flux from a Co^{60} Point Source Three Feet Above the Air-Ground Interface," talk to be presented at the meeting of the Health Physics Society, Cincinnati, Ohio, June 15-18, 1964.

Glasstone, S., ed., The Effects of Nuclear Weapons (United States Atomic Energy Commission, 1962) pp. 369-413.

Goldstein, H., and Wilkins, J. E., Jr., "Calculations of the Penetration of Gamma Rays," U. S. Atomic Energy Commission Report NYO-3075 (1954).

Hodgman, C. D., ed., Handbook of Chemistry and Physics (Chemical Rubber Publishing Co., Cleveland, Ohio, 1963) pp. 2200, 3204.

Hurst, G. S., "An Absolute Tissue Dosemeter for Fast Neutrons," Brit. J. Radiol. 27, No. 318, 353-357 (1954).

Hurst, G. S., and Ritchie, R. H., "Radiation Dosimetry for Human Exposures," U. S. Atomic Energy Commission Report WT-1504 (Classified) (1958).

Kinney, W. E., "A Monte Carlo Calculation of Scattered Neutron Fluxes at an Air-Ground Interface Due to Point Isotropic Sources on the Interface," Oak Ridge National Laboratory Report ORNL-3287 (1962).

Kleinecke, D. C., "The Effect of an Air-Sand Interface on Gamma-Ray Transport," Shielding Symposium Proceedings (U. S. Naval Radiological Defense Laboratory, San Francisco, California, 1960) pp. 301-307.

Mihalczo, J. T., "Reactivity Calibrations and Fission-Rate Distributions in an Unmoderated, Unreflected Uranium-Molybdenum Alloy Research Reactor," Oak Ridge National Laboratory Report ORNL-TM-189 (1962).

Muckenthaler, F. J., Holland, L. B., and Maerker, R. E., "In-Air Measurements in the Vicinity of the Tower Shielding Reactor II," Oak Ridge National Laboratory Report ORNL-3288 (1963).

O'Brien, K., and McLaughlin, J. E., Jr., "Gamma Radiation at the Air-Ground Interface," U. S. Atomic Energy Commission Report CEX-61.1 (Preliminary) (1963).

Rexroad, R. E., and Schmoke, M. A., "Scattered Radiation and Free-Field Dose Rates from Distributed Cobalt-60 and Cesium-137 Sources," Nuclear Defense Laboratory Report NDL-TR-2, 9 (1960).

Ritchie, R. H., and Hurst, G. S., "Penetration of Weapons Radiation: Application to the Hiroshima-Nagasaki Studies," Health Phys. 1, 390-404 (1959).

Ritchie, R. H., "Health Physics Annual Progress Report for Period Ending July 31, 1961," Oak Ridge National Laboratory Report ORNL-3189, 145-148 (1961).

Sanders, F. W., Haywood, F. F., Lundin, M. I., Gilley, L. W., Cheka, J. S., and Ward, D. R., "Operation Plan and Hazards Report - Operation BREN," U. S. Atomic Energy Commission Report CEX-62.02 (1962).

Soole, B. W., "The Angular Distribution of Multiply-Scattered γ-Radiation," Proc. Roy. Soc. (London) 230, Series A, 343 (1955).

Spielberg, D., "Neutron Fluxes from a Point Fission Source in Air; Moments Method Calculation," Shielding Symposium Proceedings (U. S. Naval Radiological Defense Laboratory, San Francisco, California, 1960) pp. 416-423.

Strickler, T. D., Gilbert, H. E., and Auxier, J. A., "Fast Neutron Scattering from Thick Slabs," Nuc. Sci. and Eng. 3, 11-18 (1957).

Thorngate, J. H., Oak Ridge National Laboratory, private communication.

Thorngate, J. H., Auxier, J. A., Haywood, F. F., and Helf, S., "Energy and Angular Distributions of Neutrons and Gamma Rays - Operation BREN," U. S. Atomic Energy Commission Report CEX-62.12, (to be published).

Titus, F., "Measurement of the Gamma-Ray Dose Near the Interface Between Two Media," Nuc. Sci. and Eng. 3, 609-619 (1958).

Van Dilla, M. A., and Hine, G. J., "Gamma-Ray Diffusion Experiments in Water," Nucleonics 10, No. 7, 54-58 (1962).

Wagner, E. B., and Hurst, G. S., "Advances in the Standard Proportional Counter Method of Fast Neutron Dosimetry," Rev. Sci. Instr. 29, No. 2, 153-158 (1958).

Wagner, E. B., and Hurst, G. S., "Gamma Response and Energy Losses in the Absolute Fast Neutron Dosimeter," Health Phys. 2, 57-61 (1959).

Wagner, E. B., and Hurst, G. S., "A Geiger-Mueller γ-Ray Dosimeter with Low Neutron Sensitivity," Health Phys. 5, 20-26 (1961).

Wells, M. B., "A Comparison of Some Recent Calculations of Neutron Transport in Air," Health Phys. 8, 543-549 (1962).

Wells, M. B., "Angular Distribution of the Air-Scattered Fast-Neutron Dose Rate at the Air-Ground Interface," Radiation Research Associates, Inc. Report RRA-M33 (1963).

CIVIL EFFECTS TEST OPERATIONS REPORT SERIES (CEX)

Through its Division of Biology and Medicine and Civil Effects Test Operations Office, the Atomic Energy Commission conducts certain technical tests, exercises, surveys, and research directed primarily toward practical applications of nuclear effects information and toward encouraging better technical, professional, and public understanding and utilization of the vast body of facts useful in the design of countermeasures against weapons effects. The activities carried out in these studies do not require nuclear detonations.

A complete listing of all the studies now underway is impossible in the space available here. However, the following is a list of all reports available from studies that have been completed. All reports listed are available from the Office of Technical Services, Department of Commerce, Washington 25, D. C., at the prices indicated.

CEX-57.1 ($0.75) The Radiological Assessment and Recovery of Contaminated Areas, Carl F. Miller, September 1960.

CEX-58.1 ($2.75) Experimental Evaluation of the Radiation Protection Afforded by Residential Structures Against Distributed Sources, J. A. Auxier, J. O. Buchanan, C. Eisenhauer, and H. E. Menker, January 1959.

CEX-58.2 ($0.75) The Scattering of Thermal Radiation into Open Underground Shelters, T. P. Davis, N. D. Miller, T. S. Ely, J. A. Basso, and H. E. Pearse, October 1959.

CEX-58.7 ($0.50) AEC Group Shelter, AEC Facilities Division, Holmes & Narver, Inc., June 1960.

CEX-58.8 ($1.00) Comparative Nuclear Effects of Biomedical Interest, Clayton S. White, I. Gerald Bowen, Donald R. Richmond, and Robert L. Corsbie, January 1961.

CEX-58.9 ($1.25) A Model Designed to Predict the Motion of Objects Translated by Classical Blast Waves, I. Gerald Bowen, Ray W. Albright, E. Royce Fletcher, and Clayton S. White, June 1961.

CEX-59.1 ($0.60) An Experimental Evaluation of the Radiation Protection Afforded by a Large Modern Concrete Office Building, J. F. Batter, Jr., A. L. Kaplan, and E. T. Clarke, January 1960.

CEX-59.4 ($1.25) Aerial Radiological Monitoring System. I. Theoretical Analysis, Design, and Operation of a Revised System, R. F. Merian, J. G. Lackey, and J. E. Hand, February 1961.

CEX-59.4 (Pt.II) ($1.50) Aerial Radiological Monitoring System. Part II. Performance, Calibration, and Operational Check-out of the EG&G Arms-II Revised System, J. E. Hand, R. B. Guillou, and H. M. Borella, Oct. 1, 1962.

CEX-59.7C ($0.50) Methods and Techniques of Fallout Studies Using a Particulate Simulant, William Lee and Henry Borella, February 1962.

CEX-59.13 ($0.50) Experimental Evaluation of the Radiation Protection Afforded by Typical Oak Ridge Homes Against Distributed Sources, T. D. Strickler and J. A. Auxier, April 1960.

CEX-59.14 ($1.75) Determinations of Aerodynamic-drag Parameters of Small Irregular Objects by Means of Drop Tests, E. P. Fletcher, R. W. Albright, V. C. Goldizen, and I. G. Bowen, October 1961.

CEX-60.1 ($1.75) Evaluation of the Fallout Protection Afforded by Brookhaven National Laboratory Medical Research Center, H. Borella, Z. Burson, and J. Jacovitch, February 1961.

CEX-60.3 ($1.50) Extended- and Point-source Radiometric Program, F. J. Davis and P. W. Reinhardt, August 1962.

CEX-60.6 ($1.00) Experimental Evaluation of the Radiation Protection Provided by an Earth-covered Shelter, Z. Burson and H. Borella, February 1962.

CEX-61.1 (Prelim.) Gamma Radiation at the Air-Ground Interface, Keran O'Brien and James E. McLaughlin, Jr., May 29, 1963.

CEX-61.4 ($2.25) Experimental Evaluation of the Fallout-radiation Protection Provided by Selected Structures in the Los Angeles Area, Z. G. Burson, Feb. 26, 1963.

CEX-62.01 ($0.50) Technical Concept—Operation Bren, J. A. Auxier, F. W. Sanders, F. F. Haywood, J. H. Thorngate, and J. S. Cheka, January 1962.

CEX-62.02 ($2.25) Operation Plan and Hazards Report—Operation Bren, F. W. Sanders, F. F. Haywood, M. I. Lundin, L. W. Gilley, J. S. Cheka, and D. R. Ward, April 1962.

CEX-62.2 ($1.00) Nuclear Bomb Effects Computer (Including Slide-rule Design and Curve Fits for Weapons Effects), E. Royce Fletcher, Ray W. Albright, Robert F. D. Perret, Mary E. Franklin, I. Gerald Bowen, and Clayton S. White, Feb. 15, 1963.

CEX-62.81 (Prelim.) ($.1.25) Ground Roughness Effects on the Energy and Angular Distribution of Gamma Radiation from Fallout, C. M. Huddleston, Z. G. Burson, R. M. Kinkaid, and Q. G. Klinger, May 22, 1963.

CEX-64.3 ($0.50) Ichiban: The Dosimetry Program for Nuclear Bomb Survivors of Hiroshima and Nagasaki—A Status Report as of April 1, 1964, J. A. Auxier, July 31, 1964.